5

Aerosols, their Direct and Indirect Effects

Co-ordinating Lead Author
J.E. Penner

Lead Authors
M. Andreae, H. Annegarn, L. Barrie, J. Feichter, D. Hegg, A. Jayaraman, R. Leaitch, D. Murphy, J. Nganga, G. Pitari

Contributing Authors
A. Ackerman, P. Adams, P. Austin, R. Boers, O. Boucher, M. Chin, C. Chuang, B. Collins, W. Cooke, P. DeMott, Y. Feng, H. Fischer, I. Fung, S. Ghan, P. Ginoux, S.-L. Gong, A. Guenther, M. Herzog, A. Higurashi, Y. Kaufman, A. Kettle, J. Kiehl, D. Koch, G. Lammel, C. Land, U. Lohmann, S. Madronich, E. Mancini, M. Mishchenko, T. Nakajima, P. Quinn, P. Rasch, D.L. Roberts, D. Savoie, S. Schwartz, J. Seinfeld, B. Soden, D. Tanré, K. Taylor, I. Tegen, X. Tie, G. Vali, R. Van Dingenen, M. van Weele, Y. Zhang

Review Editors
B. Nyenzi, J. Prospero

Contents

Executive Summary

This chapter provides a synopsis of aerosol observations, source inventories, and the theoretical understanding required to enable an assessment of radiative forcing from aerosols and its uncertainty.

• The chemical and physical properties of aerosols are needed to estimate and predict direct and indirect climate forcing.

Aerosols are liquid or solid particles suspended in the air. They have a direct radiative forcing because they scatter and absorb solar and infrared radiation in the atmosphere. Aerosols also alter warm, ice and mixed-phase cloud formation processes by increasing droplet number concentrations and ice particle concentrations. They decrease the precipitation efficiency of warm clouds and thereby cause an indirect radiative forcing associated with these changes in cloud properties. Aerosols have most likely made a significant negative contribution to the overall radiative forcing. An important characteristic of aerosols is that they have short atmospheric lifetimes and therefore cannot be considered simply as a long-term offset to the warming influence of greenhouse gases.

The size distribution of aerosols is critical to all climate influences. Sub-micrometre aerosols scatter more light per unit mass and have a longer atmospheric lifetime than larger aerosols. The number of cloud condensation nuclei per mass of aerosol also depends on the chemical composition of aerosols as a function of size. Therefore, it is essential to understand the processes that determine these properties.

• Since the last IPCC report, there has been a greater appreciation of aerosol species other than sulphate, including sea salt, dust, and carbonaceous material. Regionally resolved emissions have been estimated for these species.

For sulphate, uncertainties in the atmospheric transformation of anthropogenic sulphur dioxide (SO_2) emissions to sulphate are larger than the 20 to 30% uncertainties in the emissions themselves. SO_2 from volcanoes has a disproportionate impact on sulphate aerosols due to the high altitude of the emissions, resulting in low SO_2 losses to dry deposition and a long aerosol lifetime. Modelled dust concentrations are systematically too high in the Southern Hemisphere, indicating that source strengths developed for the Sahara do not accurately predict dust uplift in other arid areas. Owing to a sensitive, non-linear dependence on wind speed of the flux of sea salt from ocean to atmosphere, estimates of global sea salt emissions from two present day estimates of wind speed differed by 55%. The two available inventories of black carbon emissions agree to 25% but the uncertainty is certainly greater than that and is subjectively estimated as a factor of two. The accuracy of source estimates for organic aerosol species has not been assessed, but organic species are believed to contribute significantly to both direct and indirect radiative forcing. Aerosol nitrate is regionally important but its global impact is uncertain.

• There is a great spatial and temporal variability in aerosol concentrations. Global measurements are not available for many aerosol properties, so models must be used to interpolate and extrapolate the available data. Such models now include the types of aerosols most important for climate change.

A model intercomparison was carried out as part of preparation for this assessment. All participating models simulated surface mass concentrations of non-sea-salt sulphate to within 50% of observations at most locations. Whereas sulphate aerosol models are now commonplace and reasonably well-tested, models of both organic and black carbon aerosol species are in early stages of development. They are not well-tested because there are few reliable measurements of black carbon or organic aerosols.

The vertical distribution of aerosol concentrations differs substantially from one model to the next, especially for components other than sulphate. For summertime tropopause conditions the range of model predictions is a factor of five for sulphate. The range of predicted concentrations is even larger for some of the other aerosol species. However, there are insufficient data to evaluate this aspect of the models. It will be important to narrow the uncertainties associated with this aspect of models in order to improve the assessment of aircraft effects, for example.

Although there are quite large spreads between the individual short-term observed and model-predicted concentrations at individual surface stations (in particular for carbonaceous aerosols), the calculated global burdens for most models agree to within a factor of 2.5 for sulphate, organics, and black carbon. The model-calculated range increases to three and to five for dust and sea salt with diameters less than 2 μm, respectively. The range for sea salt increases to a factor of six when different present day surface wind data sets are used.

• An analysis of the contributions of the uncertainties in the different factors needed to estimate direct forcing to the overall uncertainty in the direct forcing estimates can be made. This analysis leads to an overall uncertainty estimate for fossil fuel aerosols of 89% (or a range from –0.1 to –1.0 Wm^{-2}) while that for biomass aerosols is 85% (or a range from –0.1 to –0.5 Wm^{-2}).

For this analysis the central value for the forcing was estimated using the two-stream radiative transfer equation for a simple box model. Central values for all parameters were used and error propagation was handled by a standard Taylor expansion. Estimates of uncertainty associated with each parameter were developed from a combination of literature estimates for emissions, model results for determination of burdens, and atmospheric measurements for determination of mass scattering and absorption coefficients and water uptake effects. While such a simple approach has shortcomings (e.g., it tacitly assumes both horizontal and vertical homogeneity in such quantities as relative humidity, or at least that mean values can well represent the actual distributions), it allows a specific association of parameter uncertainties with their effects on forcing. With this approach, the most important uncertainties for fossil fuel aerosols are the upscatter fraction (or asymmetry parameter), the burden (which includes propagated uncertainties in emissions), and the mass scattering efficiency. The most important uncertainties for

biomass aerosols are the single scattering albedo, the upscatter fraction, and the burden (including the propagated uncertainties in emissions).

- Preliminary estimates of aerosol concentrations have been made for future scenarios.

Several scenarios were explored which included future changes in anthropogenic emissions, temperature, and wind speed. Changes in the biosphere were not considered. Most models using present day meteorology show an approximate linear dependence of aerosol abundance on emissions. Sulphate and black carbon aerosols can respond in a non-linear fashion depending on the chemical parametrization used in the model. Projected changes in emissions may increase the relative importance of nitrate aerosols. If wind speeds increase in a future climate, as predicted by several GCMs, then increased emissions of sea salt aerosols may represent a significant negative climate feedback.

- There is now clear experimental evidence for the existence of a warm cloud aerosol indirect effect.

The radiative forcing of aerosols through their effect on liquid-water clouds consists of two parts: the 1st indirect effect (increase in droplet number associated with increases in aerosols) and the 2nd indirect effect (decrease in precipitation efficiency associated with increases in aerosols). The 1st indirect effect has strong observational support. This includes a recent study that established a link between changes in aerosols, cloud droplet number and cloud albedo (optical depth). There is also clear observational evidence for an effect of aerosols on precipitation efficiency. However, there is only limited support for an effect of changes in precipitation efficiency on cloud albedo. Models which include the second indirect effect find that it increases the overall indirect forcing by a factor of from 1.25 to more than a factor of two. Precipitation changes could be important to climate change even if their net radiative effect is small, but our ability to assess the changes in precipitation patterns due to aerosols is limited.

The response of droplet number concentration to increasing aerosols is largest when aerosol concentrations are small. Therefore, uncertainties in the concentrations of natural aerosols add an additional uncertainty of at least a factor of ±1.5 to calculations of indirect forcing. Because the pre-existing, natural size distribution modulates the size distribution of anthropogenic mass there is further uncertainty associated with estimates of indirect forcing.

A major challenge is to develop and validate, through observations and small-scale modelling, parametrizations for GCMs of the microphysics of clouds and their interactions with aerosols. Projections of a future indirect effect are especially uncertain because empirical relationships between cloud droplet number and aerosol mass may not remain valid for possible future changes in aerosol size distributions. Mechanistic parametrizations have been developed but these are not fully validated.

- An analysis of the contributions of the uncertainties in the different factors needed to estimate indirect forcing of the first kind can be made. This analysis leads to an overall uncertainty estimate for indirect forcing over Northern Hemisphere marine regions by fossil fuel aerosols of 100% (or a range from 0 to $-2.8\ Wm^{-2}$).

For this analysis the central value for the forcing was estimated using the two stream radiative transfer equation for a simple box model. Central values for all parameters were used and error propagation was handled as for the estimate of direct forcing uncertainty. This estimate is less quantitative than that for direct forcing because it is still difficult to estimate many of the parameters and the 2/3 uncertainty ranges are not firm. Moreover, several sources of uncertainty could not be estimated or included in the analysis. With this approach, the most important uncertainties are the determination of cloud liquid-water content and vertical extent. The relationship between sulphate aerosol concentration (with the propagated uncertainties from the burden calculation and emissions) and cloud droplet number concentration is of near equal importance in determining the forcing.

- The indirect radiative effect of aerosols also includes effects on ice and mixed phase clouds, but the magnitude of any indirect effect associated with the ice phase is not known.

It is not possible to estimate the number of anthropogenic ice nuclei at the present time. Except at very low temperatures (<–40°C), the mechanism of ice formation in clouds is not understood. Anthropogenic ice nuclei may have a large (probably positive) impact on forcing.

- There are linkages between policy on national air quality standards and climate change.

Policies and management techniques introduced to protect human health, improve visibility, and reduce acid rain will also affect the concentrations of aerosols relevant to climate.

5.1 Introduction

Aerosols have a direct radiative forcing because they scatter and absorb solar and infrared radiation in the atmosphere. Aerosols also alter the formation and precipitation efficiency of liquid-water, ice and mixed-phase clouds, thereby causing an indirect radiative forcing associated with these changes in cloud properties.

The quantification of aerosol radiative forcing is more complex than the quantification of radiative forcing by greenhouse gases because aerosol mass and particle number concentrations are highly variable in space and time. This variability is largely due to the much shorter atmospheric lifetime of aerosols compared with the important greenhouse gases. Spatially and temporally resolved information on the atmospheric burden and radiative properties of aerosols is needed to estimate radiative forcing. Important parameters are size distribution, change in size with relative humidity, complex refractive index, and solubility of aerosol particles. Estimating radiative forcing also requires an ability to distinguish natural and anthropogenic aerosols.

The quantification of indirect radiative forcing by aerosols is especially difficult. In addition to the variability in aerosol concentrations, some quite complicated aerosol influences on cloud processes must be accurately modelled. The warm (liquid-water) cloud indirect forcing may be divided into two components. The first indirect forcing is associated with the change in droplet concentration caused by increases in aerosol cloud condensation nuclei. The second indirect forcing is associated with the change in precipitation efficiency that results from a change in droplet number concentration. Quantification of the latter forcing necessitates understanding of a change in cloud liquid-water content and cloud amount. In addition to warm clouds, ice clouds may also be affected by aerosols.

5.1.1 Advances since the Second Assessment Report

Considerable progress in understanding the effects of aerosols on radiative balances in the atmosphere has been made since the IPCC WGI Second Assessment Report (IPCC, 1996) (hereafter SAR). A variety of field studies have taken place, providing both process-level understanding and a descriptive understanding of the aerosols in different regions. In addition, a variety of aerosol networks and satellite analyses have provided observations of regional differences in aerosol characteristics. Improved instrumentation is available for measurements of the chemical composition of single particles.

Models of aerosols have significantly improved since the SAR. Because global scale observations are not available for many aerosol properties, models are essential for interpolating and extrapolating available data to the global scale. Although there is a high degree of uncertainty associated with their use, models are presently the only tools with which to study past or future aerosol distributions and properties.

The very simplest models represent the global atmosphere as a single box in steady state for which the burden can be derived if estimates of sources and lifetimes are available. This approach was used in early assessments of the climatic effect of aerosols (e.g., Charlson *et al.*, 1987, 1992; Penner *et al.*, 1992; Andreae, 1995) since the information and modelling tools to provide a spatially- and temporally-resolved analysis were not available at the time. At the time of the SAR, three-dimensional models were only available for sulphate aerosols and soot. Since then, three-dimensional aerosol models have been developed for carbonaceous aerosols from biomass burning and from fossil fuels (Liousse *et al.*, 1996; Cooke and Wilson, 1996; Cooke *et al.*, 1999), dust aerosols (Tegen and Fung, 1994; Tegen *et al.*, 1996), sea salt aerosol (Gong *et al.*, 1998) and nitrate and ammonia in aerosols (Adams *et al.*, 1999, 2001; Penner *et al.*, 1999a). In this report, the focus is on a temporally and spatially resolved analysis of the atmospheric concentrations of aerosols and their radiative properties.

5.1.2 Aerosol Properties Relevant to Radiative Forcing

The radiatively important properties of atmospheric aerosols (both direct and indirect) are determined at the most fundamental level by the aerosol composition and size distribution. However, for purposes of the direct radiative forcing calculation and for assessment of uncertainties, these properties can be subsumed into a small set of parameters. Knowledge of a set of four quantities as a function of wavelength is necessary to translate aerosol burdens into first aerosol optical depths, and then a radiative perturbation: the mass light-scattering efficiency α_{sp}, the functional dependence of light-scattering on relative humidity f(RH), the single-scattering albedo ω_o, and the asymmetry parameter g (cf., Charlson *et al.*, 1992; Penner *et al.*, 1994a).

Light scattering by aerosols is measurable as well as calculable from measured aerosol size and composition. This permits comparisons, called closure studies, of the different measurements for consistency. An example is the comparison of the derived optical depth with directly measured or inferred optical depths from sunphotometers or satellite radiometers. Indeed, various sorts of closure studies have been successfully conducted and lend added credibility to the measurements of the individual quantities (e.g., McMurry *et al.*, 1996; Clarke *et al.*, 1996; Hegg *et al.*, 1997; Quinn and Coffman, 1998; Wenny *et al.*, 1998; Raes *et al.*, 2000). Closure studies can also provide objective estimates of the uncertainty in calculating radiative quantities such as optical depth.

Aerosols in the accumulation mode, i.e., those with dry diameters between 0.1 and 1 μm (Schwartz, 1996) are of most importance. These aerosols can hydrate to diameters between 0.1 and 2 μm where their mass extinction efficiency is largest (see Figure 5.1). Accumulation mode aerosols not only have high scattering efficiency, they also have the longest atmospheric lifetime: smaller particles coagulate more quickly while nucleation to cloud drops or impaction onto the surface removes larger particles efficiently. Accumulation mode aerosols form the majority of cloud condensation nuclei (CCN). Hence, anthropogenic aerosol perturbations such as sulphur emissions have the greatest climate impact when, as is often the case, they produce or affect accumulation mode aerosols (Jones *et al.*, 1994).

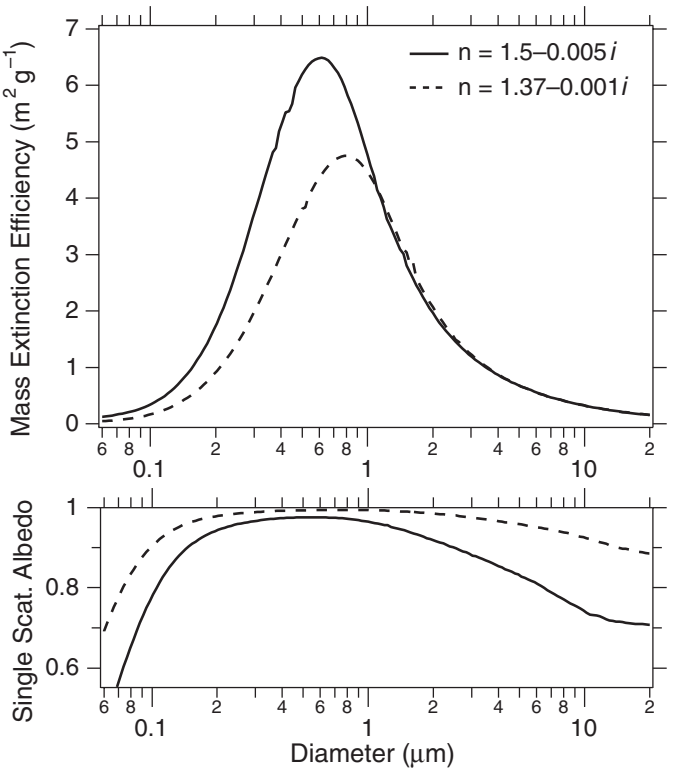

Figure 5.1: Extinction efficiency (per unit total aerosol mass) and single scattering albedo of aerosols. The calculations are integrated over a typical solar spectrum rather than using a single wavelength. Aerosols with diameters between about 0.1 and 2 μm scatter the most light per unit mass. Coarse mode aerosols (i.e., those larger than accumulation mode) have a smaller single scattering albedo even if they are made of the same material (i.e., refractive index) as accumulation mode aerosols. If the refractive index 1.37–0.001*i* is viewed as that of a hydrated aerosol then the curve represents the wet extinction efficiency. The dry extinction efficiency would be larger and shifted to slightly smaller diameters.

The direct radiative effect of aerosols is also very sensitive to the single scattering albedo ω_o. For example, a change in ω_o from 0.9 to 0.8 can often change the sign of the direct effect, depending on the albedo of the underlying surface and the altitude of the aerosols (Hansen *et al.*, 1997). Unfortunately, it is difficult to measure ω_o accurately. The mass of black carbon on a filter can be converted to light absorption, but the conversion depends on the size and mixing state of the black carbon with the rest of the aerosols. The mass measurements are themselves difficult, as discussed in Section 5.2.2.4. Aerosol light absorption can also be measured as the difference in light extinction and scattering. Very careful calibrations are required because the absorption is often a difference between two large numbers. As discussed in Section 5.2.4, it is difficult to retrieve ω_o from satellite data. Well-calibrated sunphotometers can derive ω_o by comparing light scattering measured away from the Sun with direct Sun extinction measurements (Dubovik *et al.*, 1998).

Some encouraging comparisons have been made between different techniques for measurements of ω_o and related quantities. Direct measurements of light absorption near Denver, Colorado using photo-acoustic spectroscopy were highly correlated with a filter technique (Moosmüller *et al.*, 1998). However, these results also pointed to a possible strong wavelength dependence in the light absorption. An airborne comparison of six techniques (extinction cell, three filter techniques, irradiance measurements, and black carbon mass by thermal evolution) in biomass burning plumes and hazes was reported by Reid *et al.* (1998a). Regional averages of ω_o derived from all techniques except thermal evolution agreed within about 0.02 (ω_o is dimensionless), but individual data points were only moderately correlated (regression coefficient values of about 0.6).

Another complication comes from the way in which different chemical species are mixed in aerosols (e.g., Li and Okada, 1999). Radiative properties can change depending on whether different chemicals are in the same particles (internal mixtures) or different particles (external mixtures). Also, combining species may produce different aerosol size distributions than would be the case if the species were assumed to act independently. One example is the interaction of sulphate with sea salt or dust discussed in Section 5.2.2.6.

Fortunately, studies of the effects of mixing different refractive indices have yielded a fairly straightforward message: the type of mixing is usually significant only for absorbing material (Tang, 1996; Abdou *et al.*, 1997; Fassi-Fihri *et al.*, 1997). For non-absorbing aerosols, an average refractive index appropriate to the chemical composition at a given place and time is adequate. On the other hand, black carbon can absorb up to twice as much light when present as inclusions in scattering particles such as ammonium sulphate compared with separate particles (Ackerman and Toon, 1981; Horvath, 1993; Fuller *et al.*, 1999). Models of present day aerosols often implicitly include this effect by using empirically determined light absorption coefficients but future efforts will need to explicitly consider how black carbon is mixed with other aerosols. Uncertainties in the way absorbing aerosols are mixed may introduce a range of a factor of two in the magnitude of forcing by black carbon (Haywood and Shine, 1995; Jacobson, 2000).

To assess uncertainties associated with the basic aerosol parameters, a compilation is given in Table 5.1, stratified by a crude geographic/aerosol type differentiation. The values for the size distribution parameters given in the table were derived from the references to the table. The mass scattering efficiency and upscatter fraction shown in the table are derived from Mie calculations for spherical particles using these size distributions and a constant index of refraction for the accumulation mode. The scattering efficiency dependence on relative humidity (RH) and the single-scattering albedo were derived from the literature review of measurements.

The uncertainties given in the table for the central values of number modal diameter and geometric standard deviation (D_g and σ_g) are based on the ranges of values surveyed in the literature, as are those for f(RH) and ω_o. Those for the derivative quantities α_{sp} and $\bar{\beta}$, however, are based on Mie calculations using the upper and lower uncertainty limits for the central values of the size parameters, i.e., the propagation of errors is based on the functional relationships of Mie theory. The two calculations with coarse modes require some explanation.

Table 5.1: *Variation in dry aerosol optical properties at 550 nm by region/type.*

Aerosol type	D_g (mode) (μm)	Geometric standard dev. σ_g	α_{sp} ($m^2\ g^{-1}$)	Asymmetry parameter g	$\bar{\beta}$	f(RH) (at RH = 80%)	f_b(RH) (at RH = 80%)	Single scattering albedo ω_o (dry)	Single-scattering albedo ω_o (80%)
Pacific marine									
w/single mode	0.19 ± 0.03	1.5 ± 0.15	3.7 ± 1.1	0.616 ± 0.11	0.23 ± 0.05	2.2 ± 0.3		0.99 ± 0.01	1.0 ± 0.01
w/accum & coarse	(0.46)	(2.1)	1.8 ± 0.5	0.661 ± 0.01	0.21 ± 0.003	2.2 ± 0.3		0.99 ± 0.01	1.0 ± 0.01
Atlantic marine	0.15 ± 0.05	1.9 ± 0.6	3.8 ± 1.0	0.664 ± 0.25	0.21 ± 0.11	2.2 ± 0.3		0.97 ± 0.03	1.0 ± 0.03
Fine soil dust	0.10 ± 0.26	2.8 ± 1.2	1.8 ± 0.1	0.682 ± 0.16	0.20 ± 0.07	1.3 ± 0.2		0.82 ± 0.06	0.83 ± 0.06
Polluted continental	0.10 ± 0.08	1.9 ± 0.3	3.5 ± 1.2	0.638 ± 0.28	0.22 ± 0.12	2.0 ± 0.3	0.81 ± 0.08	0.92 ± 0.05	0.95 ± 0.05
Background Continental									
w/single mode	0.08 ± 0.03	1.75 ± 0.34	2.2 ± 0.9	0.537 ± 0.26	0.27 ± 0.11	2.3 ± 0.4		0.97 ± 0.03	1.0 ± 0.03
w/accum. & coarse	(1.02)	(2.2)	1.0 ± 0.08	0.664 ± 0.07	0.21 ± 0.03	2.3 ± 0.4		0.97 ± 0.03	1.0 ± 0.03
Free troposphere	0.072 ± 0.03	2.2 ± 0.7	3.4 ± 0.7	0.649 ± 0.22	0.22 ± 0.10	—		—	
Biomass plumes	0.13 ± 0.02	1.75 ± 0.25	3.6 ± 1.0	0.628 ± 0.12	0.23 ± 0.05	1.1 ± 0.1		0.87 ± 0.06	0.87 ± 0.06
Biomass regional haze	0.16 ± 0.04	1.65 ± 0.25	3.6 ± 1.1	0.631 ± 0.16	0.22 ± 0.07	1.2 ± 0.2	0.81 ± 0.07	0.89 ± 0.05	0.90 ± 0.05

Literature references: Anderson *et al.* (1996); Bodhaine (1995); Carrico *et al.* (1998, 2000); Charlson *et al.* (1984); Clarke *et al.* (1999); Collins *et al.* (2000); Covert *et al.* (1996); Eccleston *et al.* (1974); Eck *et al.* (1999); Einfeld *et al.* (1991); Fitzgerald (1991); Fitzgerald and Hoppel (1982), Frick and Hoppel (1993); Gasso *et al.* (1999); Hegg *et al.* (1993, 1996a,b); Hobbs *et al.* (1997); Jaenicke (1993); Jennings *et al.* (1991); Kaufman (1987); Kotchenruther and Hobbs (1998); Kotchenruther *et al.* (1999); Leaitch and Isaac (1991); Le Canut *et al.* (1992, 1996); Lippman (1980); McInnes *et al.* (1997; 1998); Meszaros (1981); Nyeki *et al.* (1998); O'Dowd and Smith (1993); Quinn and Coffman (1998); Quinn *et al.* (1990; 1993, 1996); Radke *et al.* (1991); Raes *et al.* (1997); Reid and Hobbs (1998); Reid *et al.* (1998b); Remer *et al.* (1997); Saxena *et al.* (1995); Seinfeld and Pandis (1998); Sokolik and Golitsyn (1993); Takeda *et al.* (1987); Tang (1996); Tangren (1982); Torres *et al.* (1998); Waggoner *et al.* (1983); Whitby (1978); Zhang *et al.* (1993).

While the accumulation mode is generally thought to dominate light scattering, recent studies – as discussed below – have suggested that sea salt and dust can play a large role under certain conditions. To include this possibility, a sea salt mode has been added to the Pacific marine accumulation mode. The salt mode extends well into the accumulation size range and is consistent with O'Dowd and Smith (1993). It is optically very important at wind speeds above 7 to 10 ms^{-1}. For the case shown in the table, the sea salt mode accounts for about 50% of the local light scattering and could contribute over a third of the column optical depth, depending on assumptions about the scale height of the salt. Similarly, a soil dust coarse mode based on work by Whitby (1978) was added to the continental background accumulation mode. When present, this mode often dominates light scattering but, except for regions dominated by frequent dust outbreaks, is usually present over so small a vertical depth that its contribution to the column optical depth is generally slight. The importance of these coarse modes points to the importance of using size-resolved salt and dust fluxes such as those given in this report.

5.2 Sources and Production Mechanisms of Atmospheric Aerosols

5.2.1 Introduction

The concept of a "source strength" is much more difficult to define for aerosols than for most greenhouse gases. First, many aerosol species (e.g., sulphates, secondary organics) are not directly emitted, but are formed in the atmosphere from gaseous precursors. Second, some aerosol types (e.g., dust, sea salt) consist of particles whose physical properties, such as size and refractive index, have wide ranges. Since the atmospheric lifetimes and radiative effect of particles strongly depend on these properties, it makes little sense to provide a single value for the source strength of such aerosols. Third, aerosol species often combine to form mixed particles with optical properties and atmospheric lifetimes different from those of their components. Finally, clouds affect aerosols in a very complex way by scavenging aerosols, by adding mass through liquid phase chemistry, and through the formation of new aerosol particles in and near clouds. With regard to aerosol sources, we can report substantial progress over the previous IPCC assessment:

1) There are now better inventories of aerosol precursor emissions for many species (e.g., dimethylsulphide (DMS) and SO_2), including estimates of source fields for future scenarios. The present-day estimates on which this report is based are summarised in Table 5.2, see also Figure 5.2.
2) Emphasis is now on spatiotemporally resolved source and distribution fields.
3) There is now a better understanding of the conversion mechanisms that transform precursors into aerosol particles.
4) There is substantial progress towards the explicit representation of number/size and mass/size distributions and the specification of optical and hydration properties in models.

Table 5.2: *Annual source strength for present day emissions of aerosol precursors (Tg N, S or C /year). The reference year is indicated in parentheses behind individual sources, where applicable.*

	Northern Hemisphere	Southern Hemisphere	Global[a]	Range	Source
NO_x (as TgN/yr)	32	9	41		(see also Chapter 4).
Fossil fuel (1985)	20	1.1	21		Benkovitz *et al*. (1996)
Aircraft (1992)	0.54	0.04	0.58	0.4–0.9	Penner *et al*. (1999b); Daggett *et al*. (1999)
Biomass burning (ca. 1990)	3.3	3.1	6.4	2–12	Liousse *et al*. (1996); Atherton (1996)
Soils (ca. 1990)	3.5	2.0	5.5	3–12	Yienger and Levy (1995)
Agricultural soils			2.2	0–4	"
Natural soils			3.2	3–8	"
Lightning	4.4	2.6	7.0	2–12	Price *et al*. (1997); Lawrence *et al*. (1995)
NH_3 (as TgN/yr)	41	13	54	40–70	Bouwman *et al*. (1997)
Domestic animals (1990)	18	4.1	21.6	10–30	"
Agriculture (1990)	12	1.1	12.6	6–18	"
Human (1990)	2.3	0.3	2.6	1.3–3.9	"
Biomass burning (1990)	3.5	2.2	5.7	3–8	"
Fossil fuel and industry (1990)	0.29	0.01	0.3	0.1–0.5	"
Natural soils (1990)	1.4	1.1	2.4	1–10	"
Wild animals (1990)	0.10	0.02	0.1	0–1	"
Oceans	3.6	4.5	8.2	3–16	"
SO_2 (as TgS/yr)	76	12	88	67–130	
Fossil fuel and industry (1985)	68	8	76	60–100	Benkovitz *et al*. (1996)
Aircraft (1992)	0.06	0.004	0.06	0.03–1.0	Penner *et al*. (1998a); Penner *et al*. (1999b); Fahey *et al*. (1999)
Biomass burning (ca. 1990)	1.2	1.0	2.2	1–6	Spiro *et al*. (1992)
Volcanoes	6.3	3.0	9.3	6–20	Andres and Kasgnoc (1998) (incl. H_2S)
DMS or H_2S (as TgS/yr)	11.6	13.4	25.0	12–42	
Oceans	11	13	24	13–36	Kettle and Andreae (2000)
Land biota and soils	0.6	0.4	1.0	0.4–5.6	Bates *et al*. (1992); Andreae and Jaeschke (1992)
Volatile organic emissions (as TgC/yr)	171	65	236	100–560	
Anthropogenic (1985)	104	5	109	60–160	Piccot *et al.* (1992)
Terpenes (1990)	67	60	127	40–400	Guenther *et al*. (1995)

[a] The global figure may not equal the sum of the N. hemisphere and S. Hemisphere totals due to rounding.

5.2.2 Primary and Secondary Sources of Aerosols

5.2.2.1 Soil dust

Soil dust is a major contributor to aerosol loading and optical thickness, especially in sub-tropical and tropical regions. Estimates of its global source strength range from 1,000 to 5,000 Mt/yr (Duce, 1995; see Table 5.3), with very high spatial and temporal variability. Dust source regions are mainly deserts, dry lake beds, and semi-arid desert fringes, but also areas in drier regions where vegetation has been reduced or soil surfaces have been disturbed by human activities. Major dust sources are found in the desert regions of the Northern Hemisphere, while dust emissions in the Southern Hemisphere are relatively small. Unfortunately, this is not reflected in the source distribution shown in Figure 5.2(f), and represents a probable shortcoming of the dust mobilisation model used. Dust deflation occurs in a source region when the surface wind speed exceeds a threshold velocity, which is a function of surface roughness elements, grain size, and soil moisture. Crusting of soil surfaces and limitation of particle availability can reduce the dust release from a source region (Gillette, 1978). On the other hand, the disturbance of such surfaces by human activities can strongly enhance dust

Table 5.3: *Primary particle emissions for the year 2000 (Tg/yr)*[a].

	Northern Hemisphere	Southern Hemisphere	Global	Low	High	Source
Carbonaceous aerosols						
Organic Matter (0–2 μm)						
Biomass burning	28	26	54	45	80	Liousse *et al*. (1996), Scholes and Andreae (2000)
Fossil fuel	28	0.4	28	10	30	Cook *et al*. (1999), Penner *et al*. (1993)
Biogenic (>1μm)	—	—	56	0	90	Penner (1995)
Black Carbon (0–2 μm)						
Biomass burning	2.9	2.7	5.7	5	9	Liousse *et al*. (1996); Scholes and Andreae (2000)
Fossil fuel	6.5	0.1	6.6	6	8	Cooke *et al*. (1999); Penner *et al*. (1993)
Aircraft	0.005	0.0004	0.006			
Industrial Dust, etc. (> 1 μm)			100	40	130	Wolf and Hidy (1997); Andreae (1995)
Sea Salt						Gong *et al*. (1998)
d< 1 μm	23	31	54	18	100	
d=1–16μm	1,420	1,870	3,290	1,000	6,000	
Total	1,440	1,900	3,340	1,000	6,000	
Mineral (Soil) Dust [b]						
d< 1 μm	90	17	110	—	—	
d=1–2μm	240	50	290	—	—	
d=2–20μm	1,470	282	1,750	—	—	
Total	1,800	349	2,150	1,000	3,000	

[a] Range reflects estimates reported in the literature. The actual range of uncertainty may encompass values larger and smaller than those reported here.
[b] Source inventory prepared by P. Ginoux for the IPCC Model Intercomparison Workshop.

mobilisation. It has been estimated that up to 50% of the current atmospheric dust load originates from disturbed soil surfaces, and should therefore be considered anthropogenic in origin (Tegen and Fung, 1995), but this estimate must be considered highly uncertain. Furthermore, dust deflation can change in response to naturally occurring climate modes. For example, Saharan dust transport to Barbados increases during El Niño years (Prospero and Nees, 1986), and dust export to the Mediterranean and the North Atlantic is correlated with the North Atlantic Oscillation (Moulin *et al.*, 1997). Analysis of dust storm records shows regions with both increases and decreases in dust storm frequency over the last several decades (Goudie and Middleton, 1992).

The atmospheric lifetime of dust depends on particle size; large particles are quickly removed from the atmosphere by gravitational settling, while sub-micron sized particles can have atmospheric lifetimes of several weeks. A number of models of dust mobilisation and transport have been developed for regional to global scales (Marticorena *et al.*, 1997; Miller and Tegen, 1998; Tegen and Miller, 1998).

To estimate the radiative effects of dust aerosol, information is required about particle size, refractive index, and whether the minerals are mixed externally or as aggregates (Tegen *et al.*, 1996; Schulz *et al.*, 1998; Sokolik and Toon, 1999; Jacobson, 2001). Typical volume median diameters of dust particles are of the order of 2 to 4 μm. Refractive indices measured on Saharan dust have often been used to estimate the global dust radiative forcing (Tegen *et al.*, 1996). Since this dust has a single scattering albedo significantly below one, the resulting forcing is small due to partial cancellation of solar and thermal forcing, as well as cancellation of positive and negative forcing over different geographic regions (Tegen and Lacis, 1996). However, different refractive indices of dust from different regions as well as regional differences in surface albedo lead to a large uncertainty in the resulting top-of-atmosphere dust forcing (Sokolik and Toon, 1996; Claquin *et al.*, 1998, 1999).

5.2.2.2 Sea salt

Sea salt aerosols are generated by various physical processes, especially the bursting of entrained air bubbles during whitecap formation (Blanchard, 1983; Monahan *et al.*, 1986), resulting in a strong dependence on wind speed. This aerosol may be the dominant contributor to both light scattering and cloud nuclei in those regions of the marine atmosphere where wind speeds are high and/or other aerosol sources are weak (O'Dowd *et al.*, 1997; Murphy *et al.*, 1998a; Quinn *et al.*, 1998). Sea salt particles are very efficient CCN, and therefore characterisation of their surface production is of major importance for aerosol indirect effects. For example, Feingold *et al.* (1999a) showed that in concentrations of 1 particle per litre, giant salt particles are able to modify stratocumulus drizzle production and cloud albedo significantly.

Sea salt particles cover a wide size range (about 0.05 to 10 μm diameter), and have a correspondingly wide range of atmospheric lifetimes. Thus, as for dust, it is necessary to analyse their emissions and atmospheric distribution in a size-resolved model. A semi-empirical formulation was used by Gong *et al.*

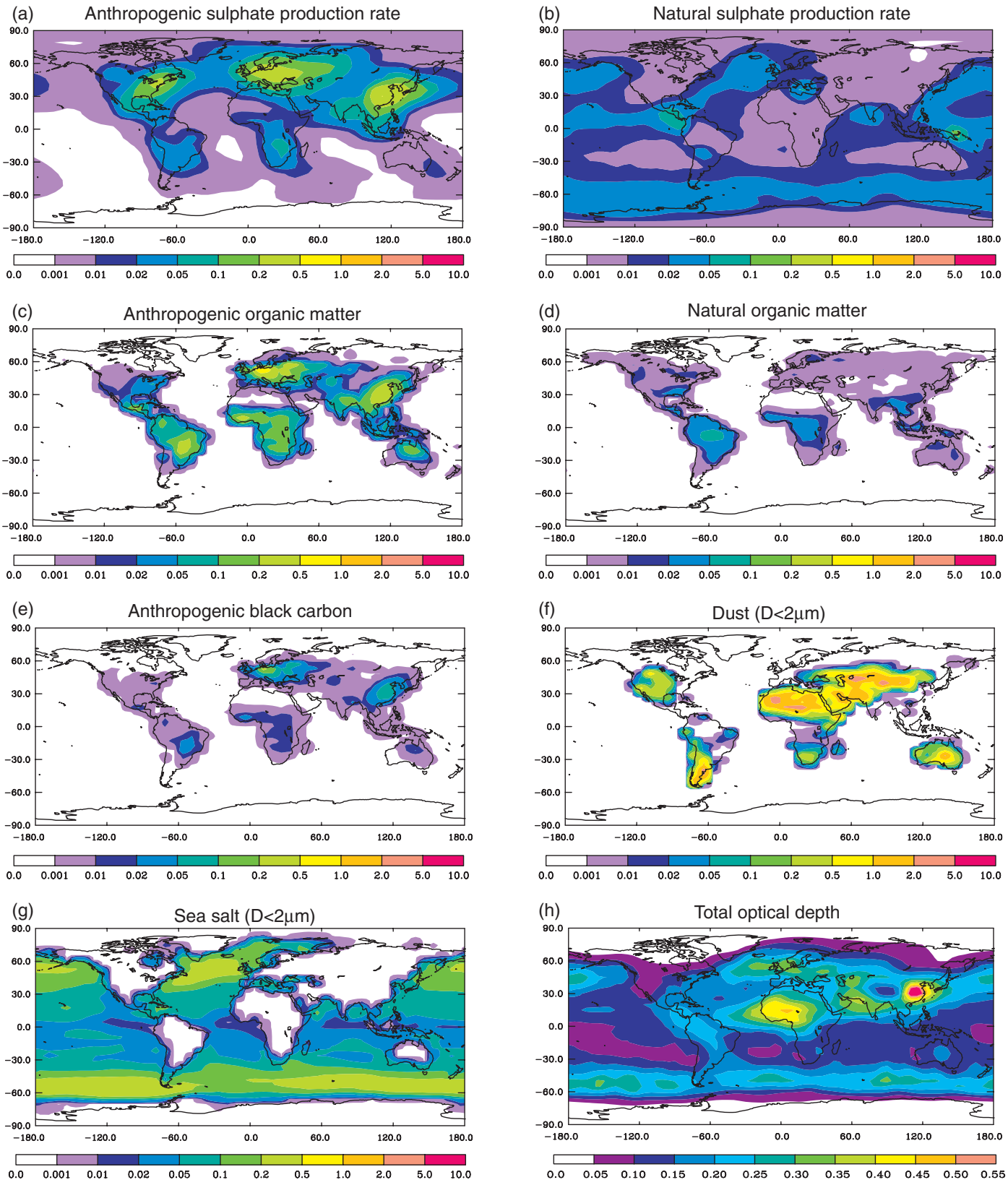

Figure 5.2: Annual average source strength in kg $km^{-2}\,hr^{-1}$ for each of the aerosol types considered here (a to g) with total aerosol optical depth (h). Shown are (a) the column average H_2SO_4 production rate from anthropogenic sources, (b) the column average H_2SO_4 production rate from natural sources (DMS and SO_2 from volcanoes), (c) anthropogenic sources of organic matter, (d) natural sources of organic matter, (e) anthropogenic sources of black carbon, (f) dust sources for dust with diameters less than 2 μm, (g) sea salt sources for sea salt with diameters less than 2 μm, and (h) total optical depth for the sensitivity case ECHAM/GRANTOUR model (see Section 5.4.1.4).

(1998) to relate the size-segregated surface emission rates of sea salt aerosols to the wind field and produce global monthly sea salt fluxes for eight size intervals between 0.06 and 16 μm dry diameter (Figure 5.2g and Table 5.3). For the present-day climate, the total sea salt flux from ocean to atmosphere is estimated to be 3,300 Tg/yr, within the range of previous estimates (1,000 to 3,000 Tg/yr, Erickson and Duce, 1988; 5,900 Tg/yr, Tegen *et al.*, 1997).

5.2.2.3 Industrial dust, primary anthropogenic aerosols

Transportation, coal combustion, cement manufacturing, metallurgy, and waste incineration are among the industrial and technical activities that produce primary aerosol particles. Recent estimates for the current emission of these aerosols range from about 100 Tg/yr (Andreae, 1995) to about 200 Tg/yr (Wolf and Hidy, 1997). These aerosol sources are responsible for the most conspicuous impact of anthropogenic aerosols on environmental quality, and have been widely monitored and regulated. As a result, the emission of industrial dust aerosols has been reduced significantly, particularly in developed countries. Considering the source strength and the fact that much industrial dust is present in a size fraction that is not optically very active (>1 μm diameter), it is probably not of climatic importance at present. On the other hand, growing industrialisation without stringent emission controls, especially in Asia, may lead to increases in this source to values above 300 Tg/yr by 2040 (Wolf and Hidy, 1997).

5.2.2.4 Carbonaceous aerosols (organic and black carbon)

Carbonaceous compounds make up a large but highly variable fraction of the atmospheric aerosol (for definitions see Glossary). Organics are the largest single component of biomass burning aerosols (Andreae *et al.*, 1988; Cachier *et al.*, 1995; Artaxo *et al.*, 1998a). Measurements over the Atlantic in the haze plume from the United States indicated that aerosol organics scattered at least as much light as sulphate (Hegg *et al.*, 1997; Novakov *et al.*, 1997). Organics are also important constituents, perhaps even a majority, of upper-tropospheric aerosols (Murphy *et al.*, 1998b). The presence of polar functional groups, particularly carboxylic and dicarboxylic acids, makes many of the organic compounds in aerosols water-soluble and allows them to participate in cloud droplet nucleation (Saxena *et al.*, 1995; Saxena and Hildemann, 1996; Sempéré and Kawamura, 1996). Recent field measurements have confirmed that organic aerosols may be efficient cloud nuclei and consequently play an important role for the indirect climate effect as well (Rivera-Carpio *et al.*, 1996).

There are significant analytical difficulties in making valid measurements of the various organic carbon species in aerosols. Large artefacts can be produced by both adsorption of organics from the gas phase onto aerosol collection media, as well as evaporation of volatile organics from aerosol samples (Appel *et al.*, 1983; Turpin *et al.*, 1994; McMurry *et al.*, 1996). The magnitude of these artefacts can be comparable to the amount of organic aerosol in unpolluted locations. Progress has been made on minimising and correcting for these artefacts through several techniques: diffusion denuders to remove gas phase organics (Eatough *et al.*, 1996), impactors with relatively inert surfaces and low pressure drops (Saxena *et al.*, 1995), and thermal desorption analysis to improve the accuracy of corrections from back-up filters (Novakov *et al.*, 1997). No rigorous comparisons of different techniques are available to constrain measurement errors.

Of particular importance for the direct effect is the light-absorbing character of some carbonaceous species, such as soot and tarry substances. Modelling studies suggest that the abundance of "black carbon" relative to non-absorbing constituents has a strong influence on the magnitude of the direct effect (e.g., Hansen *et al.*, 1997; Schult *et al.*, 1997; Haywood and Ramaswamy, 1998; Myhre *et al.*, 1998; Penner *et al.*, 1998b).

Given their importance, measurements of black carbon, and the differentiation between black and organic carbon, still require improvement (Heintzenberg *et al.*, 1997). Thermal methods measure the amount of carbon evolved from a filter sample as a function of temperature. Care must be taken to avoid errors due to pyrolysis of organics and interference from other species in the aerosol (Reid *et al.*, 1998a; Martins *et al.*, 1998). Other black carbon measurements use the light absorption of aerosol on a filter measured either in transmission or reflection. However, calibrations for converting the change in absorption to black carbon are not universally applicable (Liousse *et al.*, 1993). In part because of these issues, considerable uncertainties persist regarding the source strengths of light-absorbing aerosols (Bond *et al.*, 1998).

Carbonaceous aerosols from fossil fuel and biomass combustion

The main sources for carbonaceous aerosols are biomass and fossil fuel burning, and the atmospheric oxidation of biogenic and anthropogenic volatile organic compounds (VOC). In this section, we discuss that fraction of the carbonaceous aerosol which originates from biomass or fossil fuel combustion and is present predominantly in the sub-micron size fraction (Echalar *et al.*, 1998; Cooke, *et al.*, 1999). The global emission of organic aerosol from biomass and fossil fuel burning has been estimated at 45 to 80 and 10 to 30 Tg/yr, respectively (Liousse, *et al.*, 1996; Cooke, *et al.*, 1999; Scholes and Andreae, 2000). Combustion processes are the dominant source for black carbon; recent estimates place the global emissions from biomass burning at 6 to 9 Tg/yr and from fossil fuel burning at 6 to 8 Tg/yr (Penner *et al.*, 1993; Cooke and Wilson, 1996; Liousse *et al.*, 1996; Cooke *et al.*, 1999, Scholes and Andreae, 2000; see Table 5.3). A recent study by Bond *et al.* (1998), in which a different technique for the determination of black carbon emissions was used, suggests significantly lower emissions. Not enough measurements are available at the present time, however, to provide an independent estimate based on this technique. The source distributions are shown in Figures 5.2(c) and 5.2(e) for organic and black carbon, respectively.

The relatively close agreement between the current estimates of aerosol emission from biomass burning may underestimate the true uncertainty. Substantial progress has been made in recent years with regard to the emission factors, i.e., the amount of aerosol emitted per amount of biomass burned. In contrast, the estimation of the amounts of biomass combusted per unit area

and time is still based on rather crude assessments and has not yet benefited significantly from the remote sensing tools becoming available. Where comparisons between different approaches to combustion estimates have been made, they have shown differences of almost an order of magnitude for specific regions (Scholes *et al.*, 1996; Scholes and Andreae, 2000). Extra-tropical fires were not included in the analysis by Liousse *et al.* (1996) and domestic biofuel use may have been underrepresented in most of the presently available studies. A recent analysis suggests that up to 3,000 Tg of biofuel may be burned worldwide (Ludwig *et al.*, 2001). This source may increase in the coming decades because it is mainly used in regions that are experiencing rapid population growth.

Organic aerosols from the atmospheric oxidation of hydrocarbons
Atmospheric oxidation of biogenic hydrocarbons yields compounds of low volatility that readily form aerosols. Because it is formed by gas-to-particle conversion, this secondary organic aerosol (SOA) is present in the sub-micron size fraction. Liousse *et al.* (1996) included SOA formation from biogenic precursors in their global study of carbonaceous aerosols; they employed a constant aerosol yield of 5% for all terpenes. Based on smog chamber data and an aerosol-producing VOC emissions rate of 300 to 500 TgC/yr, Andreae and Crutzen (1997) provided an estimate of the global aerosol production from biogenic precursors of 30 to 270 Tg/yr.

Recent analyses based on improved knowledge of reaction pathways and non-methane hydrocarbon source inventories have led to substantial downward revisions of this estimate. The total global emissions of monoterpenes and other reactive volatile organic compounds (ORVOC) have been estimated by ecosystem (Guenther *et al.*, 1995). By determining the predominant plant types associated with these ecosystems and identifying and quantifying the specific monoterpene and ORVOC emissions from these plants, the contributions of individual compounds to emissions of monoterpenes or ORVOC on a global scale can be inferred (Griffin, *et al.*, 1999b; Penner *et al.*, 1999a).

Experiments investigating the aerosol-forming potentials of biogenic compounds have shown that aerosol production yields depend on the oxidation mechanism. In general, oxidation by O_3 or NO_3 individually yields more aerosol than oxidation by OH (Hoffmann, *et al.*, 1997; Griffin, *et al.*, 1999a). However, because of the low concentrations of NO_3 and O_3 outside of polluted areas, on a global scale most VOC oxidation occurs through reaction with OH. The subsequent condensation of organic compounds onto aerosols is a function not only of the vapour pressure of the various molecules and the ambient temperature, but also the presence of other aerosol organics that can absorb products from gas-phase hydrocarbon oxidation (Odum *et al.*, 1996; Hoffmann *et al.*, 1997; Griffin *et al.*, 1999a).

When combined with appropriate transport and reaction mechanisms in global chemistry transport models, these hydrocarbon emissions yield estimated ranges of global biogenically derived SOA of 13 to 24 Tg/yr (Griffin *et al.*, 1999b) and 8 to 40 Tg/yr (Penner *et al.*, 1999a). Figure 5.2(d) shows the global distribution of SOA production from biogenic precursors derived from the terpene sources from Guenther *et al.* (1995) for a total source strength of 14 Tg/yr (see Table 5.3).

It should be noted that while the precursors of this aerosol are indeed of natural origin, the dependence of aerosol yield on the oxidation mechanism implies that aerosol production from biogenic emissions might be influenced by human activities. Anthropogenic emissions, especially of NO_x, are causing an increase in the amounts of O_3 and NO_3, resulting in a possible 3- to 4-fold increase of biogenic organic aerosol production since pre-industrial times (Kanakidou *et al.*, 2000). Recent studies in Amazonia confirm low aerosol yields and little production of new particles from VOC oxidation under unpolluted conditions (Artaxo *et al.*, 1998b; Roberts *et al.*, 1998). Given the vast amount of VOC emitted in the humid tropics, a large increase in SOA production could be expected from increasing development and anthropogenic emissions in this region.

Anthropogenic VOC can also be oxidised to organic particulate matter. Only the oxidation of aromatic compounds, however, yields significant amounts of aerosol, typically about 30 g of particulate matter for 1 kg of aromatic compounds oxidised under urban conditions (Odum *et al.*, 1996). The global emission of anthropogenic VOC has been estimated at 109 ± 27 Tg/yr, of which about 60% is attributable to fossil fuel use and the rest to biomass burning (Piccot *et al.*, 1992). The emission of aromatics amounts to about 19 ± 5 Tg/yr, of which 12 ± 3 Tg/yr is related to fossil fuel use. Using these data, we obtain a very small source strength for this aerosol type, about 0.6 ± 0.3 Tg/yr.

5.2.2.5 Primary biogenic aerosols
Primary biogenic aerosol consists of plant debris (cuticular waxes, leaf fragments, etc.), humic matter, and microbial particles (bacteria, fungi, viruses, algae, pollen, spores, etc.). Unfortunately, little information is available that would allow a reliable estimate of the contribution of primary biogenic particles to the atmospheric aerosol. In an urban, temperate setting, Matthias-Maser and Jaenicke (1995) have found concentrations of 10 to 30% of the total aerosol volume in both the sub-micron and super-micron size fractions. Their contribution in densely vegetated regions, particularly the moist tropics, could be even more significant. This view is supported by analyses of the lipid fraction in Amazonian aerosols (Simoneit *et al.*, 1990).

The presence of humic-like substances makes this aerosol light-absorbing, especially in the UV-B region (Havers *et al.*, 1998), and there is evidence that primary biogenic particles may be able to act both as cloud droplet and ice nuclei (Schnell and Vali, 1976). They may, therefore, be of importance for both direct and indirect climatic effects, but not enough is known at this time to assess their role with any confidence. Since their atmospheric abundance may undergo large changes as a result of land-use change, they deserve more scientific study.

5.2.2.6 Sulphates
Sulphate aerosols are produced by chemical reactions in the atmosphere from gaseous precursors (with the exception of sea salt sulphate and gypsum dust particles). The key controlling variables for the production of sulphate aerosol from its precursors are:

Table 5.4: *Estimates for secondary aerosol sources (in Tg substance/yr[a]).*

	Northern Hemisphere	Southern Hemisphere	Global	Low	High	Source
Sulphate (as NH_4HSO_4)	145	55	200	107	374	from Table 5.5
Anthropogenic	106	15	122	69	214	
Biogenic	25	32	57	28	118	
Volcanic	14	7	21	9	48	
Nitrate (as NO_3^-)[b]						
Anthropogenic	12.4	1.8	14.2	9.6	19.2	
Natural	2.2	1.7	3.9	1.9	7.6	
Organic compounds						
Anthropogenic	0.15	0.45	0.6	0.3	1.8	see text
VOC						
Biogenic VOC	8.2	7.4	16	8	40	Griffin *et al*. (1999b); Penner *et al*. (1999a)

[a] Total sulphate production calculated from data in Table 5.5, disaggregated into anthropogenic, biogenic and volcanic fluxes using the precursor data in Table 5.2 and the ECHAM/GRANTOUR model (see Table 5.8).

[b] Total net chemical tendency for HNO_3 from UCI model (Chapter 4) apportioned as NO_3^- according to the model of Penner *et al.* (1999a). Range corresponds to range from NO_x sources in Table 5.2.

(1) the source strength of the precursor substances,
(2) the fraction of the precursors removed before conversion to sulphate,
(3) the chemical transformation rates along with the gas-phase and aqueous chemical pathways for sulphate formation from SO_2.

The atmospheric burden of the sulphate aerosol is then regulated by the interplay of production, transport and deposition (wet and dry).

The two main sulphate precursors are SO_2 from anthropogenic sources and volcanoes, and DMS from biogenic sources, especially marine plankton (Table 5.2). Since SO_2 emissions are mostly related to fossil fuel burning, the source distribution and magnitude for this trace gas are fairly well-known, and recent estimates differ by no more than about 20 to 30% (Lelieveld *et al.*, 1997). Volcanic emissions will be addressed in Section 5.2.2.8.

Estimating the emission of marine biogenic DMS requires a gridded database on its concentration in surface sea water and a parametrization of the sea/air gas transfer process. A 1°×1° monthly data set of DMS in surface water has been obtained from some 16,000 observations using a heuristic interpolation scheme (Kettle *et al.*, 1999). Estimates for data-sparse regions are generated by assuming similarity to comparable biogeographic regions with adequate data coverage. Consequently, while the global mean surface DMS concentration is quite robust because of the large data set used (error estimate ± 50%), the estimates for specific regions and seasons remain highly uncertain in many ocean regions where sampling has been sparse (error up to factor of 5). These uncertainties are compounded with those resulting from the lack of a generally accepted air/sea flux parametrization. The approach of Liss and Merlivat (1986) and that of Wanninkhof (1992) yield fluxes differing by a factor of two (Kettle and Andreae, 2000). In Table 5.2, we use the mean of these two estimates (24 Tg S(DMS)/yr).

The chemical pathway of conversion of precursors to sulphate is important because it changes the radiative effects. Most SO_2 is converted to sulphate either in the gas phase or in cloud droplets that later evaporate. Model calculations suggest that aqueous phase oxidation is dominant globally (Table 5.5). Both processes produce sulphate mostly in sub-micron aerosols that are efficient light scatterers, but the precise size distribution of sulphate in aerosols is different for gas phase and aqueous production. The size distribution of the sulphate formed in the gas phase process also depends on the interplay between nucleation, condensation and coagulation. Models that describe this interplay are in an early stage of development, and, unfortunately, there are substantial inconsistencies between our theoretical description of nucleation and condensation and the rates of these processes inferred from atmospheric measurements (Eisele and McMurry, 1997; Weber *et al.*, 1999). Thus, most models of sulphate aerosol have simply assumed a size distribution based on present day measurements. Because there is no general reason that this same size should have applied in the past or will in the future, this lends considerable uncertainty to calculations of forcing. Many of the same issues about nucleation and condensation also apply to secondary organic aerosols.

Two types of chemical interaction have recently been recognised that can reduce the radiative impact of sulphate by causing some of it to condense onto larger particles with lower scattering efficiencies and shorter atmospheric lifetimes. The first is heterogeneous reactions of SO_2 on mineral aerosols (Andreae and Crutzen, 1997; Li-Jones and Prospero, 1998; Zhang and Carmichael, 1999). The second is oxidation of SO_2 to sulphate in sea salt-containing cloud droplets and deliquesced sea salt aerosols. This process can result in a substantial fraction of non-sea-salt sulphate to be present on large sea salt particles, especially under conditions where the rate of photochemical H_2SO_4 production is low and the amount of sea salt aerosol surface available is high (Sievering *et al.*, 1992; O'Dowd, *et al.*, 1997; Andreae *et al.*, 1999).

Because the models used to estimate sulphate aerosol production differ in the resolution and representation of physical processes and in the complexity of the chemical schemes, estimates of the amount of sulphate aerosol produced and its

Table 5.5: *Production parameters and burdens of SO_2 and aerosol sulphate as predicted by eleven different models.*

Model	Sulphur source Tg S/yr	Precursor deposition %	Gas phase oxidation %	Aqueous oxidation %	SO_2 burden Tg S	$\tau(SO_2)$ days	Sulphate dry deposition %	Sulphate wet deposition %	SO_4^{2-} burden Tg S	$\tau(SO_4^{2-})$ days	P days
A	94.5	47	8	45	0.30	1.1	16	84	0.77	5.0	2.9
B	122.8	49	5	46	0.20	0.6	27	73	0.80	4.6	2.3
C	100.7	49	17	34	0.43	1.5	13	87	0.63	4.4	2.2
D	80.4	44	16	39	0.56	2.6	20	80	0.73	5.7	3.3
E	106.0	54	6	40	0.36	1.2	11	89	0.55	4.1	1.9
F	90.0	18	18	64	0.61	2.4	22	78	0.96	4.7	3.8
G	82.5	33	12	56	0.40	1.9	7	93	0.57	3.8	2.5
H	95.7	45	13	42	0.54	2.4	18	82	1.03	7.2	3.9
I	125.6	47	9	44	0.63	2.0	16	84	0.74	3.6	2.2
J	90.0	24	15	59	0.60	2.3	25	75	1.10	5.3	4.5
K	92.5	56	15	27	0.43	1.8	13	87	0.63	5.8	2.5
Average	98.2	42	12	45	0.46	1.8	17	83	0.77	4.9	2.9
Standard deviation	14.7	12	5	11	0.14	0.6	6	6	0.19	1.0	0.8

Model/Reference: A MOGUNTIA/Langner and Rodhe, 1991; B: IMAGES/Pham *et al.*, 1996; C: ECHAM3/Feichter *et al.*, 1996; D: Harvard-GISS / Koch *et al.*, 1999; E: CCM1-GRANTOUR/Chuang *et al.*, 1997; F:ECHAM4/Roelofs *et al.*, 1998; G: CCM3/Barth *et al.*, 2000 and Rasch *et al.*, 2000a; H: CCC/Lohmann *et al.*, 1999a.; I: Iversen *et al.*, 2000; J: Lelieveld *et al.*, 1997; K: GOCART/Chin *et al.*, 2000.

atmospheric burden are highly model-dependent. Table 5.4 provides an overall model-based estimate of sulphate production and Table 5.5 emphasises the differences between different models. All the models shown in Table 5.5 include anthropogenic and natural sources and consider at least three species, DMS, SO_2 and SO_4^{2-}, B and D consider more species and have a more detailed representation of the gas-phase chemistry. C, F and G include a more detailed representation of the aqueous phase processes. The calculated residence times of SO_2, defined as the global burden divided by the global emission flux, range between 0.6 and 2.6 days as a result of different deposition parametrizations. Because of losses due to SO_2 deposition, only 46 to 82% of the SO_2 emitted undergoes chemical transformations and forms sulphate. The global turnover time of sulphate is mainly determined by wet removal and is estimated to be between 4 and 7 days. Because of the critical role that precipitation scavenging plays in controlling sulphate lifetime, it is important how well models predict vertical profiles.

The various models start with gaseous sulphur sources ranging from 80 to 130 TgS/yr, and arrive at SO_2 and SO_4^{2-} burdens of 0.2 to 0.6 and 0.6 to 1.1 TgS, respectively. It is noteworthy that there is little correlation between source strength and the resulting burden between models. In fact, the model with the second-highest precursor source (B) has the lowest SO_2 burden, and the model with the highest sulphate burden (J) starts with a much lower precursor source than the model with the lowest sulphate burden (E). Figures 5.2(a) and (b) show the global distribution of sulphate aerosol production from anthropogenic SO_2 and from natural sources (primarily DMS), respectively (see also Table 5.4).

The modelled production efficiency of atmospheric sulphate aerosol burden from a given amount of precursors is expressed as P, the ratio between the global sulphate burden to the global sulphur emissions per day. At the global scale, this parameter varies between the models listed in Table 5.5 by more than a factor of two, from 1.9 to 4.5 days. Within a given model, the potential of a specific sulphur source to contribute to the global sulphate burden varies strongly as a function of where and in what form sulphur is introduced into the atmosphere. SO_2 from volcanoes (P=6.0 days) is injected at higher altitudes, and DMS (P=3.1 days) is not subject to dry deposition and can therefore be converted to SO_2 far enough from the ground to avoid large deposition losses. In contrast, most anthropogenic SO_2 (P=0.8 to 2.9 days) is released near the ground and therefore much of it is lost by deposition before oxidation can occur (Feichter *et al.*, 1997; Graf *et al.*, 1997). Regional differences in the conversion potential of anthropogenic emissions may be caused by the latitude-dependent oxidation capacity and by differences in the precipitation regime. For the same reasons P exhibits a distinct seasonality in mid- and high latitudes.

This comparison indicates that in addition to uncertainties in precursor source strengths, which may be ranging from factors of about 1.3 (SO_2) to 2 (DMS), the estimation of the production and deposition terms of sulphate aerosol introduces an additional uncertainty of at least a factor of 2 into the prediction of the sulphate burden. As the relationship between sulphur sources and resulting sulphate load depends on numerous parameters, the conversion efficiency must be expected to change with changing source patterns and with changing climate.

Sulphate in aerosol particles is present as sulphuric acid, ammonium sulphate, and intermediate compounds, depending on the availability of gaseous ammonia to neutralise the sulphuric acid formed from SO_2. In a recent modelling study, Adams *et al.* (1999) estimate that the global mean NH_4^+/SO_4^{2-} mole ratio is about one, in good agreement with available measurements. This increases the mass of sulphate aerosol by some 17%, but also

changes the hydration behaviour and refractive index of the aerosol. The overall effects are of the order of 10%, relatively minor compared with the uncertainties discussed above (Howell and Huebert, 1998).

5.2.2.7 Nitrates

Aerosol nitrate is closely tied to the relative abundances of ammonium and sulphate. If ammonia is available in excess of the amount required to neutralise sulphuric acid, nitrate can form small, radiatively efficient aerosols. In the presence of accumulation-mode sulphuric acid containing aerosols, however, nitric acid deposits on larger, alkaline mineral or salt particles (Bassett and Seinfeld, 1984; Murphy and Thomson, 1997; Gard *et al.*, 1998). Because coarse mode particles are less efficient per unit mass at scattering light, this process reduces the radiative impact of nitrate (Yang *et al.*, 1994; Li-Jones and Prospero, 1998).

Until recently, nitrate has not been considered in assessments of the radiative effects of aerosols. Andreae (1995) estimated that the global burden of ammonium nitrate aerosol from natural and anthropogenic sources is 0.24 and 0.4 Tg (as NH_4NO_3), respectively, and that anthropogenic nitrates cause only 2% of the total direct forcing. Jacobson (2001) derived similar burdens, and estimated forcing by anthropogenic nitrate to be -0.024 Wm^{-2}. Adams *et al.* (1999) obtained an even lower value of 0.17 Tg (as NO_3^-) for the global nitrate burden. Part of this difference may be due to the fact that the latter model does not include nitrate deposition on sea salt aerosols. Another estimate (van Dorland *et al.*, 1997) suggested that forcing due to ammonium nitrate is about one tenth of the sulphate forcing. The importance of aerosol nitrate could increase substantially over the next century, however. For example, the SRES A2 emissions scenario projects that NO_x emissions will more than triple in that time period while SO_2 emissions decline slightly. Assuming increasing agricultural emissions of ammonia, it is conceivable that direct forcing by ammonium nitrate could become comparable in magnitude to that due to sulphate (Adams *et al.*, 2001).

Forcing due to nitrate aerosol is already important at the regional scale (ten Brink *et al.*, 1996). Observations and model results both show that in regions of elevated NO_x and NH_3 emissions, such as Europe, India, and parts of North America, NH_4NO_3 aerosol concentrations may be quite high and actually exceed those of sulphate. This is particularly evident when aerosol sampling techniques are used that avoid nitrate evaporation from the sampling substrate (Slanina *et al.*, 1999). Substantial amounts of NH_4NO_3 have also been observed in the European plume during ACE-2 (Andreae *et al.*, 2000).

5.2.2.8 Volcanoes

Two components of volcanic emissions are of most significance for aerosols: primary dust and gaseous sulphur. The estimated dust flux reported in Jones *et al.*, (1994a) for the1980s ranges from 4 to 10,000 Tg/yr, with a "best" estimate of 33 Tg/yr (Andreae, 1995). The lower limit represents continuous eruptive activity, and is about two orders of magnitude smaller than soil dust emission. The upper value, on the other hand, is the order of magnitude of volcanic dust mass emitted during large explosive eruptions. However, the stratospheric lifetime of these coarse particles is only about 1 to 2 months (NASA, 1992), due to the efficient removal by settling.

Sulphur emissions occur mainly in the form of SO_2, even though other sulphur species may be present in the volcanic plume, predominantly SO_4^{2-} aerosols and H_2S. Stoiber *et al.* (1987) have estimated that the amount of SO_4^{2-} and H_2S is commonly less than 1% of the total, although it may in some cases reach 10%. Graf *et al.* (1998), on the other hand, have estimated the fraction of H_2S and SO_4^{2-} to be about 20% of the total. Nevertheless, the error made in considering all the emitted sulphur as SO_2 is likely to be a small one, since H_2S oxidises to SO_2 in about 2 days in the troposphere or 10 days in the stratosphere. Estimates of the emission of sulphur containing species from quiescent degassing and eruptions range from 7.2 TgS/yr to 14 ± 6 TgS/yr (Stoiber *et al.*, 1987; Spiro *et al.*, 1992; Graf *et al.*, 1997; Andres and Kasgnoc, 1998). These estimates are highly uncertain because only very few of the potential sources have ever been measured and the variability between sources and between different stages of activity of the sources is considerable.

Volcanic aerosols in the troposphere

Graf *et al.* (1997) suggest that volcanic sources are important to the sulphate aerosol burden in the upper troposphere, where they might contribute to the formation of ice particles and thus represent a potential for a large indirect radiative effect (see Section 5.3.6). Sassen (1992) and Sassen *et al.* (1995) have presented evidence of cirrus cloud formation from volcanic aerosols and Song *et al.* (1996) suggest that the interannual variability of high level clouds is associated with explosive volcanoes.

Calculations using a global climate model (Graf *et al.*, 1997) have reached the "surprising" conclusion that the radiative effect of volcanic sulphate is only slightly smaller than that of anthropogenic sulphate, even though the anthropogenic SO_2 source strength is about five times larger. Table 5.6 shows that the calculated efficiency of volcanic sulphur in producing

Table 5.6: *Global annual mean sulphur budget (from Graf et al., 1997) and top-of-atmosphere forcing in percentage of the total (102 TgS/yr emission, about 1 TgS burden, –0.65 Wm^{-2} forcing). Efficiency is relative sulphate burden divided by relative source strength (i.e. column 3 / column 1).*

Source	Sulphur emission	SO_2 burden	SO_4^{2-} burden	Efficiency	Direct forcing TOA %
Anthropogenic	66	46	37	0.56	40
Biomass burning	2.5	1.2	1.6	0.64	2
DMS	18	18	25	1.39	26
Volcanoes	14	35	36	2.63	33

sulphate aerosols is about 4.5 times larger than that of anthropogenic sulphur. The main reason is that SO_2 released from volcanoes at higher altitudes has a longer residence time, mainly due to lower dry deposition rates than those calculated for surface emissions of SO_2 (cf.B,enkovitz *et al.*, 1994). On the other hand, because different models show major discrepancies in vertical sulphur transport and in upper tropospheric aerosol concentrations, the above result could be very model-dependent.

Volcanic aerosols emitted into the stratosphere

Volcanic emissions sufficiently cataclysmic to penetrate the stratosphere are rare. Nevertheless, the associated transient climatic effects are large and trends in the frequency of volcanic eruptions could lead to important trends in average surface temperature. The well-documented evolution of the Pinatubo plume illustrates the climate effects of a large eruption (Stenchikov *et al.*, 1998).

About three months of post-eruptive aging are needed for chemical and microphysical processes to produce the stratospheric peak of sulphate aerosol mass and optical thickness (Stowe *et al.*, 1992; McCormick *et al.*, 1995). Assuming at this stage a global stratospheric optical depth of the order of 0.1 at 0.55 μm, a total time of about 4 years is needed to return to the background value of 0.003 (WMO/UNEP, 1992; McCormick and Veiga, 1992) using one year as e-folding time for volcanic aerosol decay. This is, of course, important in terms of climate forcing: in the case of Pinatubo, a radiative forcing of about -4 Wm^{-2} was reached at the beginning of 1992, decaying exponentially to about -0.1 Wm^{-2} in a time frame of 4 years (Minnis *et al.*, 1993; McCormick *et al.*, 1995). This direct forcing is augmented by an indirect forcing associated with O_3 depletion that is much smaller than the direct forcing (about -0.1 Wm^{-2}).

The background amount of stratospheric sulphate is mainly produced by UV photolysis of organic carbonyl sulphide forming SO_2, although the direct contribution of tropospheric SO_2 injected in the stratosphere in the tropical tropopause region is significant for particle formation in the lower stratosphere and accounts for about one third of the total stratospheric sulphate mass (Weisenstein *et al.*, 1997). The observed sulphate load in the stratosphere is about 0.15 TgS (Kent and McCormick, 1984) during volcanically quiet periods, and this accounts for about 15% of the total sulphate (i.e., troposphere + stratosphere) (see Table 5.6).

The historical record of SO_2 emissions by erupting volcanoes shows that over 100 Tg of SO_2 can be emitted in a single event, such as the Tambora volcano eruption of 1815 (Stoiber *et al.,* 1987). Such large eruptions have led to strong transient cooling effects (-0.14 to -0.31°C for eruptions in the 19th and 20th centuries), but historical and instrumental observations do not indicate any significant trend in the frequency of highly explosive volcanoes (Robertson *et al.*, 2001). Thus, while variations in volcanic activity may have influenced climate at decadal and shorter scales, it seems unlikely that trends in volcanic emissions could have played any role in establishing a longer-term temperature trend.

5.2.3 Summary of Main Uncertainties Associated with Aerosol Sources and Properties

In the case of primary aerosols, the largest uncertainties often lie in the extrapolation of experimentally determined source strengths to other regions and seasons. This is especially true for dust, for which many of the observations are for a Saharan source. The spatial and temporal distribution of biomass fires also remains uncertain. The non-linear dependence of sea salt aerosol formation on wind speed creates difficulties in parametrizations in large-scale models and the vertical profile of sea salt aerosols needs to be better defined.

Secondary aerosol species have uncertainties both in the sources of the precursor gases and in the atmospheric processes that convert some of those gases to aerosols. For sulphate, the uncertainties in the conversion from SO_2 (factor of 2) are larger than the uncertainties in anthropogenic sources (20 to 30%). For hydrocarbons there are large uncertainties both in the emissions of key precursor gases as a function of space and time as well as the fractional yield of aerosols as those gases are oxidised. Taken at face value, the combined uncertainties can be a factor of three for sulphate and more for organics. On the other hand, the success some models have had in predicting aerosol concentrations at observation sites (see Section 5.4) as well as wet deposition suggests that at least for sulphate the models have more skill than suggested by a worst-case propagation of errors. Nevertheless, we cannot be sure that these models achieve reasonable success for the right reasons.

Besides the problem of predicting the mass of aerosol species produced, there is the more complex issue of adequately describing their physical properties relevant to climate forcing. Here we would like to highlight that the situation is much better for models of present day aerosols, which can rely on empirical data for optical properties, than for predictions of future aerosol effects. Another issue for optical properties is that the quantity and sometimes the quality of observational data on single scattering albedo do not match those available for optical depth. Perhaps the most important uncertainty in aerosol properties is the production of cloud condensation nuclei (Section 5.3.3).

5.2.4 Global Observations and Field Campaigns

Satellite observations (reviewed by King *et al.*, 1999) are naturally suited to the global coverage demanded by regional variations in aerosols. Aerosol optical depth can be retrieved over the ocean in clear-sky conditions from satellite measurements of irradiance and a model of aerosol properties (Mishchenko *et al.*, 1999). These have been retrieved from satellite instruments such as AVHRR (Husar *et al.*, 1997; Higurashi and Nakajima, 1999), METEOSAT (e.g., Jankowiak and Tanré, 1992; Moulin *et al.*, 1997), ATSR (Veefkind *et al.*, 1999), and OCTS (Nakajima *et al.*, 1999). More recently-dedicated instruments such as MODIS and POLDER have been designed to monitor aerosol properties (Deuzé *et al.*, 1999; Tanré *et al.*, 1999; Boucher and Tanré, 2000). Aerosol retrievals over land, especially over low albedo regions, are developing rapidly but are complicated by the spectral and angular dependence of the surface reflectivity (e.g., Leroy *et al.*,

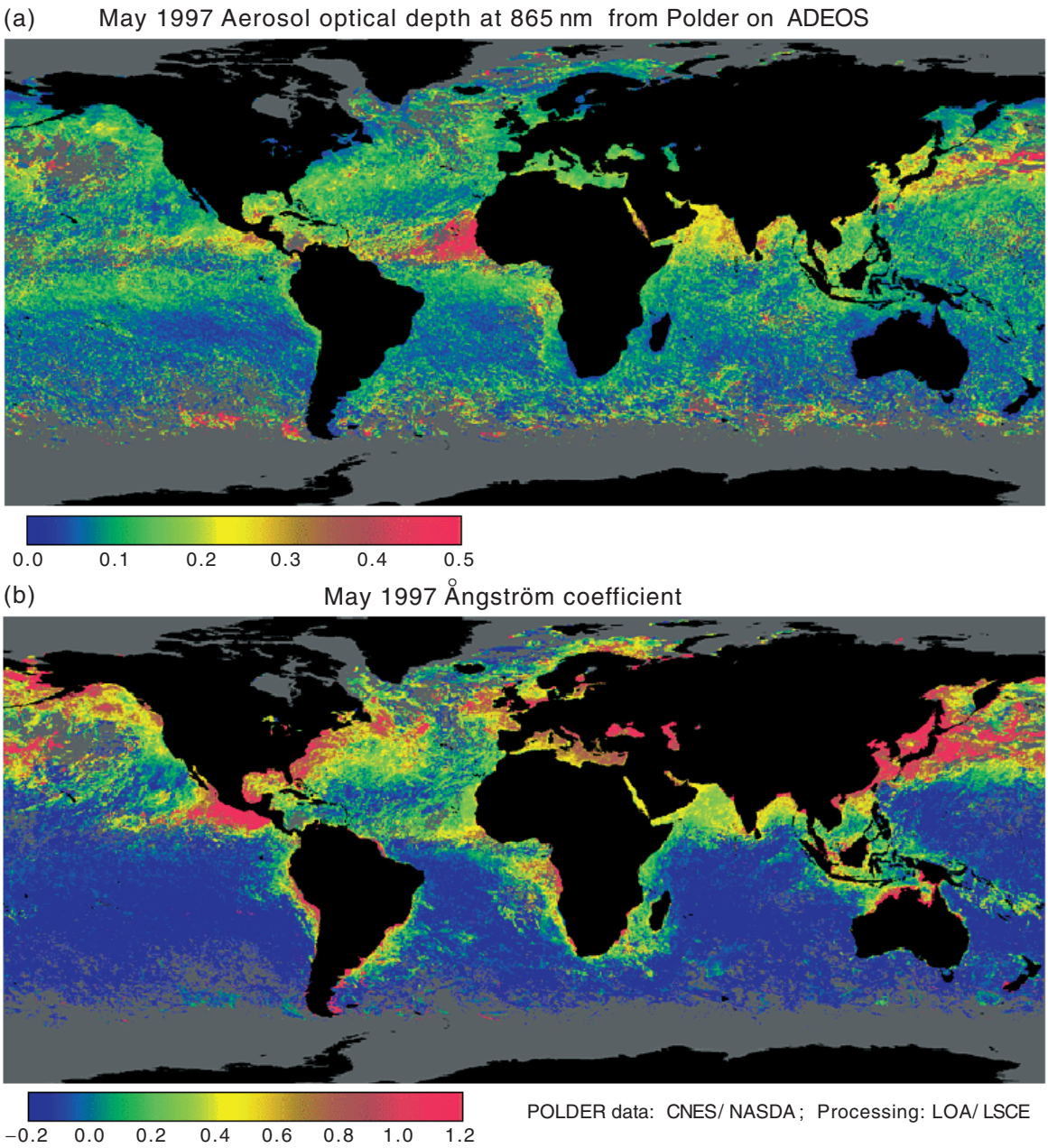

Figure 5.3: (a) Aerosol optical depth and (b) Ångström exponent from POLDER satellite data for May 1997 (Deuzé *et al.*, 1999). The largest optical depths over the Atlantic Ocean are from north African dust. The Ångström exponent expresses the wavelength dependence of scattered light between 670 and 865 nm. The African dust plume has a small Ångström exponent due to the importance of coarse mode aerosols whereas the larger Ångström exponents around the continents show the importance of accumulation mode aerosols in those locations.

1997; Wanner *et al.*, 1997; Soufflet *et al.*, 1997). The TOMS instrument has the capability to detect partially absorbing aerosols over land and ocean but the retrievals are only semi-quantitative (Hsu *et al.*, 1999). Comparisons of ERBE and SCARAB data with radiative transfer models show that aerosols must be included to accurately model the radiation budget (Cusack *et al.*, 1998; Haywood *et al.*, 1999).

There is not enough information content in a single observed quantity (scattered light) to retrieve the aerosol size distribution and the vertical profile in addition to the optical depth. Light scattering can be measured at more than one wavelength, but in most cases no more than two or three independent parameters can be derived even from observations at a large number of wavelengths (Tanré *et al.*, 1996; Kaufman *et al.*, 1997). Observations of the polarisation of backscattered light have the potential to add more information content (Herman *et al.*, 1997), as do observations at multiple angles of the same point in the atmosphere as a satellite moves overhead (Flowerdew and Haigh, 1996; Kahn *et al.*, 1997; Veefkind *et al.*, 1998).

In addition to aerosol optical depth, the vertically averaged Ångström exponent (which is related to aerosol size), can also be retrieved with reasonable agreement when compared to ground-

based sunphotometer data (Goloub *et al.*, 1999; Higurashi and Nakajima, 1999). Vertical profiles of aerosols are available in the upper troposphere and stratosphere from the SAGE instrument but its limb scanning technique cannot be extended downward because of interference from clouds. Active sensing from space shows promise in retrieving vertical profiles of aerosols (Osborn *et al.*, 1998).

The single scattering albedo ω_o, which is important in determining the direct radiative effect, is difficult to retrieve from satellites, especially over oceans (Kaufman *et al.*, 1997). This is due to satellites' viewing geometry, which restricts measurements to light scattering rather than extinction for most tropospheric aerosols. Accurate values of ω_o can be retrieved from satellite data for some special conditions, especially if combined with ground-based data (Fraser and Kaufman, 1985; Nakajima and Higurashi, 1997).

At this time there are no reliable methods for determining from satellite data the fraction of atmospheric aerosols that are anthropogenic. This is a major limitation in determining the radiative forcing in addition to the overall radiative effect of aerosols (Boucher and Tanré, 2000).

Field campaigns such as the Tropospheric Aerosol Radiative Forcing Observational Experiment (TARFOX), the Aerosol Characterisation Experiment (ACE-1, ACE-2), the Indian Ocean Experiment (INDOEX), SCAR-B, and monitoring networks such as AERONET provide essential information about the chemical and physical properties of aerosols (Novakov *et al.*, 1997; Hegg *et al.*, 1997; Hobbs *et al.*, 1997; Ross *et al.*, 1998; Holben *et al.*, 1998). These studies have also shown the importance of mixing and entrainment between the boundary layer and the free troposphere in determining aerosol properties over the oceans (e.g. Bates *et al.*, 1998; Johnson *et al.*, 2000). INDOEX found long-range transport of highly absorbing aerosol. The importance of absorption was shown by a change in irradiance at the surface that was two to three times that at the top of the atmosphere (Satheesh *et al.*, 1999; Podgorny *et al.*, 2000). TARFOX data also show the importance of black carbon in calculating broad-band irradiances, and confirm theoretical calculations that the strongest radiative effect occurred not at noon, but rather when the solar zenith angle was approximately 60 to 70 degrees (Russell *et al.*, 1999; Hignett *et al.*, 1999).

Local closure studies can compare size-resolved aerosol chemistry data with both total mass measurements and light scattering. Both comparisons have been made to within analytical uncertainties of 20 to 40% (Quinn and Coffman, 1998; Neusüß *et al.*, 2000; Putaud *et al.*, 2000). Local closure studies have also successfully compared predicted and measured hygroscopic growth (Carrico *et al.*, 1998; Swietlicki *et al.*, 1999). However, achieving closure between measured aerosol properties and observed cloud nucleation is more difficult (Brenguier *et al.*, 2000).

Column closure studies compare different ways of obtaining a vertically integrated optical property, usually optical depth. Comparisons were made during TARFOX between aerosol optical depths derived from satellites looking down and an aircraft sunphotometer looking up (Veefkind *et al.*, 1998). Optical depths from ATSR-2 retrievals were within 0.03 of sunphotometer data and optical depths from AVHRR were systematically lower but highly correlated with sunphotometer data. Except in some dust layers, aerosol optical depths computed during ACE-2 from *in situ* data, measured from sunphotometers, and retrieved from satellites agreed within about 20% (Collins *et al.*, 2000; Schmid *et al.*, 2000). Optical depths computed from lidar profiles have agreed with sunphotometer measurements within 40% at several sites (Ferrare *et al.*, 1998, 2000; Flamant *et al.*, 2000).

There is considerable common ground between closure studies (Russell and Heintzenberg, 2000). An important uncertainty in both mass closure and hygroscopic growth is often the treatment of organics (e.g. McMurry *et al.*, 1996; Raes *et al.*, 2000). The sampling of coarse aerosols is often a limitation in computing scattering from in-situ data (e.g. Ferrare *et al.*, 1998; Quinn and Coffman, 1998). Black carbon and other light absorbing aerosols are difficult to treat because of difficulties both in measuring them (Section 5.2.2.4) and computing their effects (Section 5.1.2). Layers of dust aerosol pose special problems because they combine coarse particles, uncertainties in optical parameters, non-sphericity, and spatial inhomogeneity (Clarke *et al.*, 1996; Russell and Heintzenberg, 2000). For example, averaged discrepancies during ACE-2 for derived and measured scattering coefficients were less than 20% except in dust layers, where they were about 40% (Collins *et al.*, 2000). There has been a strong consensus from field studies that surface measurements of aerosol properties are rarely sufficient for computations of column properties such as optical depth. Some common reasons are strong vertical gradients in coarse aerosols and the transport of continental aerosols in the free troposphere above a marine boundary layer.

5.2.5 Trends in Aerosols

The regional nature of aerosols makes tropospheric aerosol trends more difficult to determine than trends in long-lived trace gases. Moreover, there are few long-term records of tropospheric aerosols (SAR). Ice cores provide records of species relevant to aerosols at a few locations. As shown in Figure 5.4, ice cores from both Greenland and the Alps display the strong anthropogenic influence of sulphate deposited during this century (Döscher *et al.*, 1995; Fischer *et al.*, 1998). Carbonaceous aerosols also show long-term trends (Lavanchy *et al.*, 1999). Sulphate in Antarctic ice cores shows no such trend (Dai *et al.*, 1995) since its source in the Southern Hemisphere is primarily natural. Aerosols have been measured from balloon sondes at Wyoming since 1971. For the number of aerosols larger than 0.15 μm, decreasing trends of -1.8 ± 1.4%/yr and -1.6 ± 1.8%/yr (90% confidence limits) were found in the 2.5 to 5 and 5 to 10 km altitude ranges, respectively (Hofmann, 1993). The total number of particles increased by 0.7 ± 0.1%/yr at Cape Grim from 1977 to 1991 but the number of particles large enough to nucleate cloud droplets (CCN) decreased by 1.5 ± 0.3%/yr from 1981 to 1991 (Gras, 1995). There are also some long-term data on visibility and turbidity. For example, summertime visibility in the eastern United States was worst in the 1970s, which was also a time of maximum SO_2 emissions (Husar and Wilson, 1993).

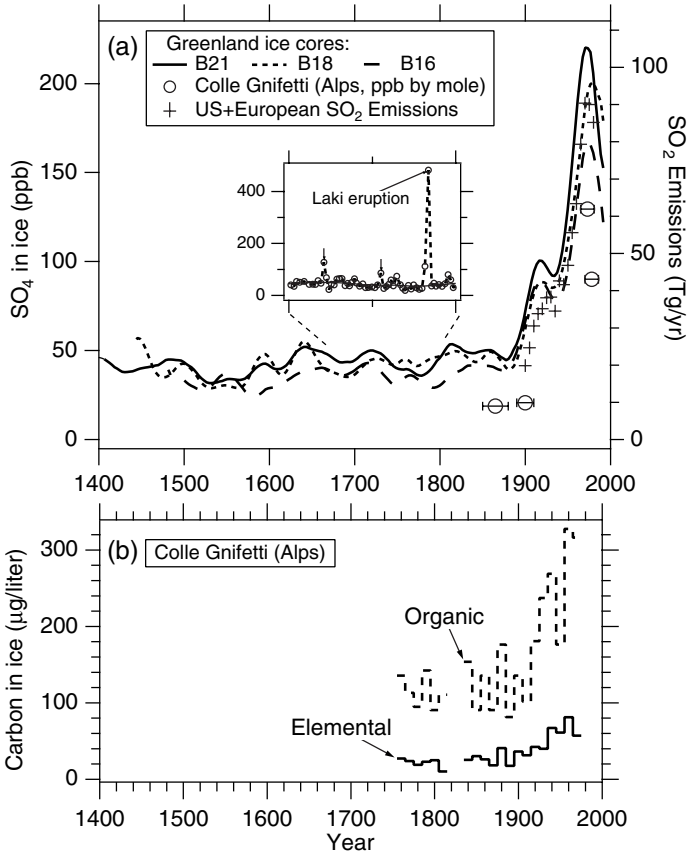

Figure 5.4: (a) Sulphate concentrations in several Greenland ice cores and an Alpine ice core (Fischer *et al.*, 1998; Döscher *et al.*, 1995). Also shown are the total SO_2 emissions from sources from the US and Europe (Gschwandtner *et al.*, 1986; Mylona, 1996). The inset shows how peaks due to major volcanic eruptions have been removed by a robust running median method followed by singular spectrum analysis. (b) Black carbon and organic carbon concentrations in alpine ice cores (Lavanchy *et al.*, 1999).

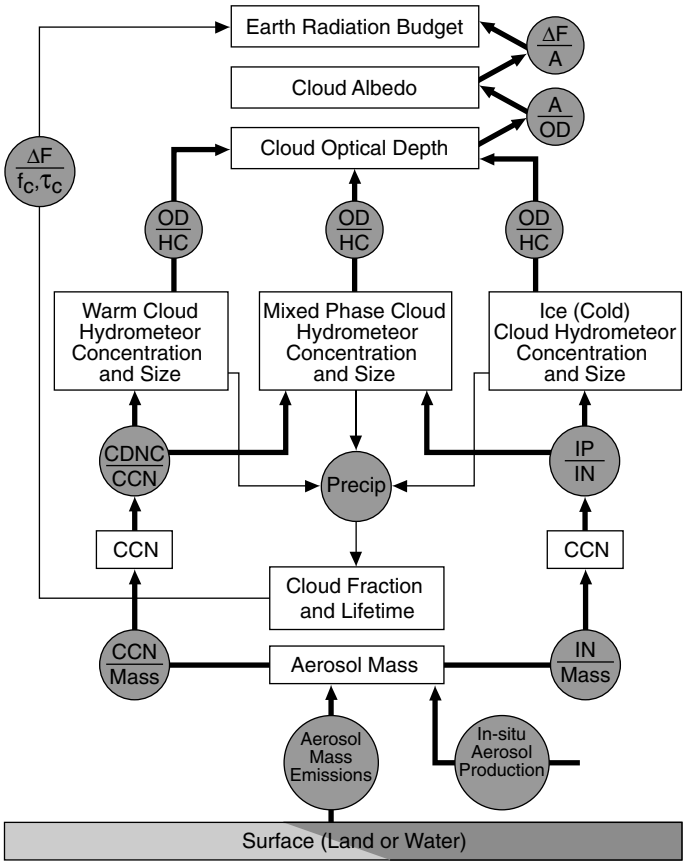

Figure 5.5: Flow chart showing the processes linking aerosol emissions or production with changes in cloud optical depth and radiative forcing. Bars indicate functional dependence of the quantity on top of the bar to that under the bar. Symbols: CCN (Cloud condensation nuclei); CDNC (Cloud droplet number concentration); IN (Ice nuclei); IP (Ice particles); OD (Optical depth); HC (Hydrometeor concentration); A (Albedo); f_c (Cloud fraction); τ_c (Cloud optical depth); ΔF (Radiative forcing).

5.3 Indirect Forcing Associated with Aerosols

5.3.1 Introduction

Indirect forcing by aerosols is broadly defined as the overall process by which aerosols perturb the Earth-atmosphere radiation balance by modulation of cloud albedo and cloud amount. It can be viewed as a series of processes linking various intermediate variables such as aerosol mass, cloud condensation nuclei (CCN) concentration, ice nuclei (IN) concentration, water phase partitioning, cloud optical depth, etc., which connect emissions of aerosols (or their precursors) to the top of the atmosphere radiative forcing due to clouds. A schematic of the processes involved in indirect forcing from this perspective is shown in Figure 5.5. Rather than attempt to discuss fully all of the processes shown in Figure 5.5, we concentrate here on a selected suite of linkages, selected either because significant progress towards quantification has been made in the last five years, or because they are vitally important. However, before delving into these relationships, we present a brief review of the observational evidence for indirect forcing.

5.3.2 Observational Support for Indirect Forcing

Observational support for indirect forcing by aerosols derives from several sources. Considering first remote sensing, satellite studies of clouds near regions of high SO_2 emissions have shown that polluted clouds have higher reflectivity on average than background clouds (Kuang and Yung, 2000). A study by Han *et al.* (1998a) has shown that satellite-retrieved column cloud drop concentrations in low-level clouds increase substantially from marine to continental clouds. They are also high in tropical areas where biomass burning is prevalent. Wetzel and Stowe (1999) showed that there is a statistically significant correlation of aerosol optical depth with cloud drop effective radius(r_{eff}) (negative correlation) and of aerosol optical depth with cloud optical depths (positive correlation) for clouds with optical depths less than 15. Han *et al.* (1998b), analysing ISCCP data, found an expected increase in cloud albedo with decreasing droplet size for all optically thick clouds but an unexpected decrease in albedo with decreasing droplet size in optically thinner clouds (τ_c<15) over marine locations. This latter relationship may arise because of the modulation of the

liquid-water path by cloud dynamics associated with absorption of solar radiation (Boers and Mitchell, 1994) but may also arise from the generally large spatial scale of some satellite retrievals which can yield misleading correlations. For example, Szczodrak *et al.* (2001), using 1 km resolution AVHRR data, do not see the increase in liquid-water path (LWP) with increasing effective radius for all clouds seen by Han *et al.* (1998b), who utilised 4 km resolution pixels. In any case, a relationship similar to that found by Han *et al.* (1998b) was found in the model of Lohmann *et al.* (1999b,c) and that model supports the finding of a significant indirect forcing with increases in aerosol concentrations (Lohmann *et al.*, 2000). Further evidence for an indirect forcing associated with increases in aerosol concentrations comes from the study by Nakajima *et al.* (2001). They found increases in cloud albedo, decreases in cloud droplet r_{eff}, and increases in cloud droplet number associated with increases in aerosol column number concentration.

In-situ measurement programmes have found linkages between CCN concentrations and both drizzle and cloud droplet r_{eff} in marine stratocumulus (cf., Hudson and Yum, 1997; Yum and Hudson, 1998). Moreover, several studies have contrasted the microstructure of polluted and clean clouds in the same airshed (e.g., Twohy *et al.*, 1995; Garrett and Hobbs, 1995) while others have linked seasonal variations in drop concentrations and r_{eff} with seasonal variations in CCN (Boers *et al.*, 1998). Indeed, recent studies by Rosenfeld (1999, 2000) show a dramatic impact of aerosols on cloud precipitation efficiency. Until recently, evidence of the impact of aerosols on cloud albedo itself has been confined primarily to studies of ship tracks (e.g., Coakley *et al.*, 1987; Ferek *et al.*, 1998; Ackerman *et al.*, 2000) although some other types of studies have indeed been done (e.g., Boers *et al.*, 1998). However, new analyses have not only identified changes in cloud microstructure due to aerosols but have associated these changes with increases in cloud albedo as well. An example of this, from Brenguier *et al.* (2000), can be seen in Figure 5.6, which displays measured cloud reflectances at two wavelengths for clean and polluted clouds examined during ACE-2. Thus, our understanding has advanced appreciably since the time of the SAR and these studies leave little doubt that anthropogenic aerosols have a non-zero impact on warm cloud radiative forcing. An estimate of the forcing over oceans (from satellite studies) ranged from –0.7 to –1.7 Wm^{-2} (Nakajima *et al.*, 2001).

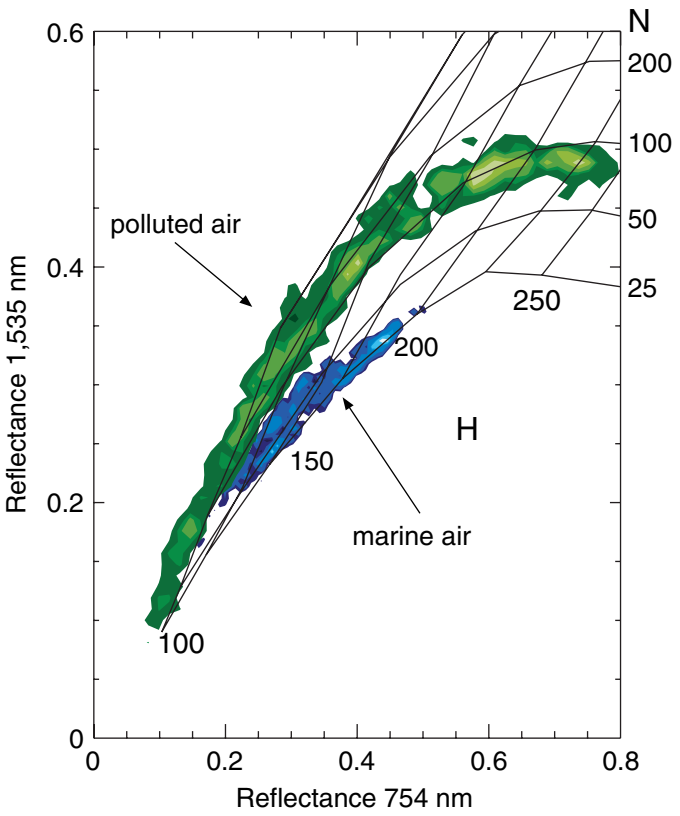

Figure 5.6: Frequency distributions of the reflectances at 1,535 nm versus reflectances at 754 nm determined during the ACE-2 experiment. Isolines of geometrical thickness (H) and droplet number concentration (N) demonstrate the higher reflectance in polluted cloud if normalised by a similar geometrical thickness (Brenguier *et al.* 2000).

For cirrus clouds, much of both the observational and theoretical support for indirect forcing by anthropogenic aerosols has been recently summarised in the report on the impact of aviation-derived aerosols on clouds (Fahey *et al.*, 1999). There is a remarkably consistent upward trend in cirrus fractional cloudiness in areas of high air traffic over the last two decades observable, in at least broad outline, in both ground-based and satellite databases (Fahey *et al*., 1999). The suggested increase in cirrus cloud cover of about 4% since 1971 is much larger than can be attributed to linear-shaped contrails, with the resulting implication that aviation emissions are perturbing high altitude cloud amount. While purely meteorological trends (i.e., increasing upper atmospheric water vapour, changing circulation patterns) and/or increases associated with surface-based emissions cannot be excluded as a possible cause for these trends, these observations are very suggestive of a perturbation from aviation emissions.

5.3.3 Factors Controlling Cloud Condensation Nuclei

The effectiveness of an aerosol particle as a CCN depends on its size and response to water. Atmospheric aerosol particles are either hydrophobic (i.e. will not activate in cloud under any circumstances), water-insoluble but possess hydrophyllic sites that allow the particles to wet and activate at higher supersaturations, or have some water-soluble component and will activate at lower supersaturations given sufficient time to achieve their critical radius. Only particles with some water-soluble species are significant for the indirect forcing (e.g., Kulmala *et al.*, 1996; Eichel *et al.*, 1996). However, there are many water-soluble compounds in the atmospheric aerosol with widely varying degrees of solubility.

Sulphates, sodium chloride, and other water-soluble salts and inorganic acids are common to the atmospheric aerosol (Section 5.2) and to CCN (e.g., Hudson and Da, 1996). The abilities of these species to serve as CCN are relatively well

known, whereas our understanding of the ability of organic species to act as CCN is relatively poor. This is a critical area of uncertainty for the global-scale modelling of cloud droplet nucleation.

The water-soluble fraction of organic species in aerosols can be high relative to sulphate (e.g., Li *et al.*, 1996; Zappoli *et al.*, 1999), and organics may be important sources of CCN in at least some circumstances (Novakov and Penner, 1993; Rivera-Carpio *et al.*, 1996). Aerosols from biomass burning are primarily composed of organics and may act as CCN, but some of their CCN activity may actually be due to co-resident inorganic constituents (Van-Dinh *et al.* 1994; Novakov and Corrigan, 1996; Leaitch *et al.*, 1996a). Measurements from a forested area suggest that some of the products of terpene oxidation may serve as CCN (Leaitch *et al.*, 1999), and Virkkula *et al.* (1999) found that particles from pinene oxidation absorbed some water at an RH of about 84%. Cruz and Pandis (1997) examined the CCN activity of particles of adipic acid and of glutaric acid (products of alkene oxidation) and found reasonable agreement with Köhler theory, whereas Corrigan and Novakov (1999) measured much higher activation diameters than predicted by theory. Volatile organic acids (formic, acetic, pyruvic, oxalic) may also contribute to the formation of CCN in areas covered with vegetation and in plumes from biomass burning (Yu, 2000). Pösfai *et al.* (1998) suggest that organic films can be responsible for relatively large water uptake at low RH.

The wide range of solubilities of the organic species may help to explain why observations do not always provide a consistent picture of the uptake of water. The water solubility of the oxygenated organic species tends to decrease with increasing the carbon number (Saxena and Hildemann, 1996). Shulman *et al.* (1996) showed that the cloud activation of organic species with lower solubilties might be delayed due to the increased time required for dissolution, and delays of 1–3 seconds have been observed (Shantz *et al.*, 1999). For a mixture of an inorganic salt or acid with an organic that is at least slightly soluble, the presence of the organic may contribute to some reduction in the critical supersaturation for activation (Corrigan and Novakov, 1999) especially if the organics reduce the surface tension (Shulman *et al.* 1996) as demonstrated in natural cloud water (Facchini *et al.*, 1999).

Historically, much of the interest in organics has focused on the inhibition of CCN activation in cloud by surface-active organics. Recently, Hansson *et al.* (1998) found that thick coatings of either of two insoluble high molecular weight organics (50 to 100% by mass of tetracosane or of lauric acid) reduced the hygroscopic growth factor for particles of NaCl. On the other hand, studies by Shulman *et al.* (1996), Cruz and Pandis (1998), and Virkkula *et al.* (1999) suggest that coatings of organic acids do not necessarily inhibit the effect of the other species on the condensation of water. The ability of the hydrophobic coating to form a complete barrier to the water vapour is a critical aspect of this issue. It is unlikely that such coatings are common in the atmosphere.

Although the CCN activities of inorganic components of the aerosol are well known, there are other aspects to the water activity of these species that need to be considered. Highly soluble gases, such as HNO_3, can dissolve into a growing solution droplet prior to activation in cloud. The addition of this inorganic substance to the solution can decrease the critical supersaturation for activation (Kulmula *et al.*, 1993; Laaksonen *et al.*, 1998). The result is an increase in cloud droplet number but this is tempered somewhat by an enhanced condensation rate that contributes to a slight reduction in the cloud supersaturation. The importance of this effect will depend on the mixing ratio of such gases relative to the CCN solute concentrations and this has not been properly evaluated. An important consideration for the development of the CCN spectrum is the in-cloud oxidation of SO_2. Current models indicate that the fraction of secondary sulphate that is due to SO_2 oxidation in cloud can be in the range of 60 to 80% (Table 5.5). While the uncertainty in this estimate does not greatly impact the model sulphur budgets, it has significant consequences for the magnitude of the predicted indirect forcing (Chuang *et al.*, 1997; Zhang *et al.*, 1999).

Large-scale models must be able to represent several factors related to CCN in order to better assess the indirect effect: the size distribution of the mass of water-soluble species, the degree of solubility of the represented species, and the amount of mixing of individual species within a given size fraction. The most critical species are sulphates, organics, sea salt and nitrates.

5.3.4 Determination of Cloud Droplet Number Concentration

The impact of CCN on the cloud droplet number concentration (N_d) can be non-linear. One consequence of this is that the number of natural CCN can strongly influence the way that CCN from anthropogenic emissions affect the indirect radiative forcing. For example, Ghan *et al.* (1998) have shown that the presence of relatively high concentrations of sea salt particles can lead to increased N_d at lower sulphate concentrations and higher updraught speeds. Conversely, the N_d are lowered by high salt concentrations if sulphate concentrations are higher and updraught speeds are weaker (see also O'Dowd *et al.* (1999)). However, it is not clear whether these processes significantly affect the radiative forcing.

There are two general methods that have been used to relate changes in N_d to changes in aerosol concentrations. The first and simplest approach uses an empirical relationship that directly connects some aerosol quantity to N_d. Two such empirical treatments have been derived. Jones *et al.* (1994b) used a relationship between N_d and the number concentration of aerosol particles (N_a) above a certain size. This method is appropriate for the particles that serve as nuclei for cloud droplets in stratiform cloud, but it can be ambiguous for cumuliform cloud because of the activation of particles smaller than the threshold of the N_a (Isaac *et al.*, 1990; Gillani *et al.*, 1995). Boucher and Lohmann (1995) used observations of N_d and of CCN versus particulate or cloudwater sulphate to devise relationships between N_d and particulate sulphate. This approach has the advantage that it circumvents the assumptions required in deriving the aerosol number concentration N_a from sulphate mass. The use of sulphate as a surrogate for N_d implicitly accounts for other particulate species in the aerosol, but only as long as relationships are used that take into account the potential regional and seasonal

differences in the chemical mixture of the aerosol (e.g., Van Dingenen *et al.*, 1995; Menon and Saxena, 1998). Thus, the empirical relationships derived for regions with high industrial sulphate loading may not be appropriate for biomass aerosols. A new empirical approach relates N_d to the particle mass concentration and mean volume diameter in the accumulation mode aerosol. It is based on mass scavenging efficiencies of the accumulation-mode aerosol by stratiform clouds (Glantz and Noone, 2000). When deriving empirical relationships, it is important to be aware of the effects of the averaging scale (Gultepe and Isaac, 1998). An advantage of the empirical methods is that they may account for the effects on N_d that are associated with cloud dynamics in an average sense. Variance in the cloud updraught velocities is one of the main reasons for the large scatter in the observations from which these empirical relationships are derived (Leaitch *et al.*, 1996b; Feingold *et al.*, 1999b).

The second method that has been used to relate changes in N_d to changes in aerosol concentrations is based on a prognostic parametrization of the cloud droplet formation process (Ghan *et al.*, 1993, 1995, 1997; Chuang and Penner, 1995; Abdul-Razzak *et al.,* 1998; Abdul-Razzak and Ghan, 2000). This type of approach requires a representation of the CCN activity of the particles and a representation of the dynamic and thermodynamic properties of the cloud. At present, some of the aerosol properties necessary to describe the CCN spectrum must be assumed in order to apply this approach.

A comparison of the empirical and prognostic methods currently in use for determining the N_d is shown in Figure 5.7. The empirical relationships are taken from Jones *et al.* (1994b) and Boucher and Lohmann (1995) and represent stratiform cloud. The curves labelled PROG follow the prognostic parametrization used by Chuang and Penner (1995). There is some relative general agreement between the empirical curves and the prognostic curves for low updraught velocity. The prognostic curves for the higher updraught velocity, i.e. more convective cloud, give much higher N_d than the empirical results for stratiform cloud. The relatively close agreement of the 10 cms^{-1} updraught curve with the empirical scheme for the ocean is somewhat fortuitous. Further work comparing both the empirical and prognostic schemes with observations is needed, especially for the climatologically important marine stratocumulus, to better understand the reasons for the agreements and differences in Figure 5.7.

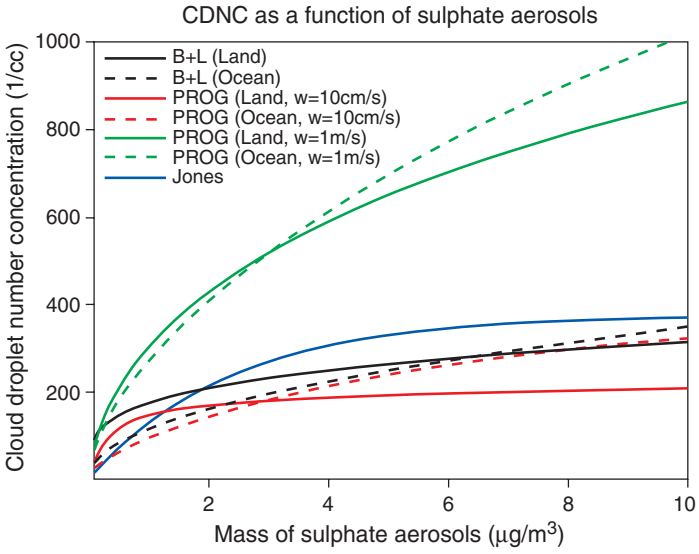

Figure 5.7. Droplet concentration as a function of sulphate concentration for 3 different treatments: the empirical treatment of Jones *et al.* (1994b), the empirical treatment of Boucher and Lohmann (1995) (denoted B+L), and the mechanistic treatment of Chuang and Penner (1995) (denoted PROG).

There are also atmospheric dynamic factors that affect the prediction of N_d. Trajectories of air parcels through stratocumulus are highly variable (e.g., Feingold *et al.*, 1998). For the prognostic methods with their explicit representation of the updraught velocity, there is a need to understand not just the probability distribution function (PDF) of updraughts in these clouds, but the PDF of those that actually nucleate droplets. No satisfactory method of parametrizing the local updraught has yet been devised. The prognostic methods also produce an adiabatic N_d, which leads to the problem of how to represent the mean N_d in the cloud in the presence of the entrainment of dry air. Entrainment can even result from changes in N_d (Boers and Mitchell, 1994). These issues are critical for the prognostic prediction of N_d and deserve continued study to determine how best to take their effects into account.

5.3.5 Aerosol Impact on Liquid-Water Content and Cloud Amount

The indirect effect of aerosols on clouds is determined not only by the instantaneous mean droplet concentration change (i.e., the first indirect or Twomey effect; Twomey, 1977) but is also strongly associated with the development of precipitation and thus the cloud liquid-water path, lifetime of individual clouds and the consequent geographic extent of cloudiness (second indirect effect). These processes are well illustrated by marine stratiform clouds.

The longevity of marine stratiform clouds, a key cloud type for climate forcing in the lower troposphere, is dictated by a delicate balance between a number of source and sink terms for condensed water, including turbulent latent and sensible heat fluxes from the ocean surface, radiative cooling and heating rates, entrainment of dry air from above the cloud top inversion, and the precipitation flux out of the cloud. Unfortunately, changes to cloud extent induced by plausible changes in cloud droplet number concentration due to aerosol modulation can be slight and difficult to characterise (cf., Hignett, 1991). For example, Pincus and Baker (1994) point out that changes in short-wave absorption induced by changes in drop number act primarily to change cloud thickness – and cloud thickness is also strongly modulated by non-radiative processes. Depending on the cloud type, feedbacks involving cloud thickness can substantially reduce or enhance changes in cloud albedo due to change in droplet concentration (Boers and Mitchell 1994; Pincus and Baker, 1994). Feingold *et al.* (1997) have more recently examined the impact of drizzle modulation by aerosol on cloud optical depth.

Nevertheless, precipitation processes are extremely important to marine cloud fraction, with varying precipitation efficiency leading to varying fractional cloudiness and liquid water content (Albrecht, 1989). The postulated mechanism is as follows. The activation of a larger number of aerosol particles limits the size to which drops can grow for an available cooling rate. Hence, the number of drops which grow large enough to initiate the collision-coalescence process (the dominant precipitation process in warm clouds) is decreased and precipitation rates are attenuated. With precipitation attenuated, a major sink for cloud drops is removed and cloud lifetime is enhanced. Liou and Cheng (1989) first estimated the potential global significance of this process. Further studies with more sophisticated models have supported the significance of the modulation of precipitation by aerosols and led to the consideration of several different processes that contribute to the effects of aerosols on clouds.

One such process is the modulation of cloud optical depth by precipitation. Pincus and Baker (1994) showed, using a simple mixed-layer model, that the cloud optical depth in marine stratiform clouds was a strong function of the initial aerosol concentration upon which the cloud formed, the dependence being close to exponential. Boers (1995) subsequently demonstrated, through modelling calculations coupled with field observations, that a substantial part of the seasonal cycle in cloud albedo at Cape Grim could be due to the modulation of cloud optical depth by aerosols and their effects on the efficiency of precipitation.

A second important process which may be affected by onset of precipitation is that of decoupling of the cloud layer from the surface. Precipitation may sometimes produce a sub-cloud stable layer that cuts off the moisture flux to the cloud. However, decoupling is not an inevitable consequence of precipitation formation and, under some circumstances, a balance between the moisture flux from the surface and precipitation sinks determine the cloud extent. Pincus *et al.* (1997) observed no difference between precipitating and non-precipitating stratocumulus with respect to cloud fraction and both Austin *et al.* (1995) and Stevens *et al.* (1998) found that observed stratocumulus seemed able to maintain themselves despite a considerable precipitation rate.

While the effect of precipitation modulation on cloud amount is supported by a number of studies, several others have argued that external thermodynamic factors such as sea surface temperature (SST) are the main factors determining the formation and dissipation of marine stratocumulus (cf., Wyant *et al.*, 1997). Such an analysis is also supported by the relationship of satellite-derived aerosol number concentration with cloud droplet number concentration and with liquid-water path. The former shows a positive correlation while the latter shows no particular relationship (Nakajima *et al.*, 2001). Thus, the climatological significance of this aspect of the indirect effect needs a great deal more investigation.

Finally, it is important to note that the impact of anthropogenic aerosols on precipitation modulation will be dependent on both the natural and anthropogenic aerosol size distributions. For example, a number of studies have suggested that both natural (e.g., Feingold *et al.*, 1999a) and anthropogenic (Eagen *et al.*, 1974) giant CCN have a great impact on precipitation and will influence the effect of smaller, anthropogenic CCN on precipitation.

5.3.6 Ice Formation and Indirect Forcing

Formation of ice in the atmosphere has long been recognised to be a topic of great importance due to its key role in the precipitation process. However, progress in elucidating this role has been plagued by a host of complex issues such as the precise mode of action of ice nuclei (IN) (e.g., Cooper, 1980), *in situ* modification of IN activity by various substrate coatings, including residual ice (Borys, 1989; Curry *et al.*, 1990; Rosinski and Morgan, 1991; Beard, 1992; Vali, 1992), secondary ice production (e.g., Beard, 1992) and a lack of consistency in measurement techniques (cf., Bigg, 1990; Vali, 1991; Rogers, 1993; Pruppacher and Klett, 1997).

Because of these issues, it is premature to quantitatively assess the impact of ice formation on indirect forcing. Instead, the potential importance of such formation is given a preliminary assessment by addressing a set of four fundamental and serial questions whose answers would, in principle, yield the desired assessment. A summary of what is known with respect to these questions is given below.

Does ice formation have an impact on radiative forcing?
In principle the phase partitioning of water in clouds should have a substantial impact on cloud radiative forcing, first because the ice hydrometeors will tend to be much larger than cloud drops and thus increase precipitation, and second because the size of hydrometeors (determined by both ice/vapour and ice/liquid partitioning) can have a significant impact on radiative balances. Several GCM sensitivity studies have supported these expectations (e.g., Senior and Mitchell, 1993; Fowler and Randall, 1996) by demonstrating that the fraction of supercooled water in the models which is converted to ice has a significant impact on the global radiative balance. A simple sensitivity study with the ECHAM model (cf., Lohmann and Feichter, 1997) conducted for this assessment revealed a very large difference in globally averaged cloud forcing of +16.9 Wm^{-2} induced by allowing only ice in clouds with temperatures below 0°C as compared with allowing only water in clouds with temperatures above –35°C. The liquid-water path change in these experiments (160 gm^{-2} to 54.9 gm^{-2}) was larger than the 60% uncertainty in this quantity from measurements (Greenwald *et al.*, 1993; Weng and Grody, 1994). However, this certainly demonstrates that even small changes in ice formation could have a significant impact on the indirect climate forcing due to aerosols.

Is formation of the ice phase modulated by aerosols?
The relative roles of different types of ice nucleation in cirrus clouds is very complex (e.g., Sassen and Dodd, 1988; Heymsfield and Miloshevich, 1993, 1995; DeMott *et al.*, 1997, 1998; Strom *et al.*, 1997; Xu *et al.*, 1998; Martin, 1998; Koop *et al.*, 1999). Presumably there is a temperature-dependent transition from predominantly heterogeneous nucleation (i.e., initiated at a phase boundary with a substrate – the heterogeneous nucleus) to homogeneous nucleation (i.e., within the liquid phase alone – no substrate required) that depends on the chemistry and size of the precursor haze drops of the homogeneous process as well as on the chemistry and concentration of the heterogeneous nuclei.

Supersaturations with respect to ice in excess of 40 to 50% are necessary to freeze sulphate haze drops, even at quite low temperatures. Far lower supersaturations will be adequate if heterogeneous IN are present. There is thus a large supersaturation range in which heterogeneous IN could have a significant impact (Fahey *et al.*, 1999). However, in both heterogeneous and homogeneous cases, aerosols play an important role in glaciation.

For lower level, warmer (though still supercooled) clouds, in principle the answer to our query is necessarily positive. In this vast, liquid-water reservoir, temperatures are simply too warm for homogeneous freezing of cloud drops to occur and aerosol surfaces of some sort must provide the substrate for ice initiation. However, prolific secondary ice formation due to such processes as the Hallett-Mossop mechanism renders the establishment of a clear relationship between measured IN concentrations and ice particle concentrations quite difficult (cf., Beard, 1992; Rangno and Hobbs, 1994). Nevertheless, in some instances relationships between IN concentrations and ice formation in lower-tropospheric clouds have been found (e.g., Stith *et al.*, 1994; DeMott *et al.*, 1996). This lends credibility to the view that the actual ice initiation process must be modulated by aerosols.

For both upper and lower level clouds in the troposphere, it seems clear that the ice initiation process is dependent on aerosols, though the nucleation process can proceed via different pathways and from a variety of different nucleating chemical species.

Are a significant fraction of ice nucleating aerosols anthropogenic?

For cirrus cloud formed by homogeneous nucleation on haze particles, there are clearly solid grounds for asserting that there is a substantive anthropogenic component to the associated IN. Most chemical transport models (e.g., Penner *et al.*, 1994b; Feichter *et al.*, 1996; Graf *et al.*, 1997; Koch *et al.*, 1999; Rasch *et al.*, 2000a) as well as sulphur isotope studies (e.g., Norman *et al.*, 1999) suggest that a substantial fraction of the upper-tropospheric sulphate burden (and thus the sulphate haze droplets involved in homogeneous nucleation) is anthropogenic although quantitative estimates vary from model to model. Furthermore, for wintertime polar clouds, a special case of low-level cirrus, there are observations and modelling results to indicate that, through suppression of the freezing point, the acidic aerosols of Arctic haze favour the formation of large ice crystals rather than the smaller particles in unpolluted ice fog during the Arctic airmass cooling process. The larger particles increase the sedimentation flux and deplete water vapor from the atmosphere, providing a negative forcing (Blanchet and Girard, 1995). There are also grounds for asserting that changes in the sulphate abundance will lead to increases in ice nucleation (cf., Jensen and Toon, 1992, 1994; Kärcher *et al.*, 1998; Lin *et al.*, 1998; Fahey *et al.* 1999) so that a positive forcing is plausible. In any case, anthropogenic modulation of ice particles should certainly be considered.

For cirrus clouds in the upper troposphere formed on insoluble, heterogeneous IN, the situation is much less clear. Recent observations of heterogeneous IN in both the upper and lower troposphere are suggestive of a large role for crustally derived aerosols (e.g., Kumai, 1976; Hagen *et al.*, 1995; Heintzenberg *et al.*, 1996; Kriedenweis *et al.*, 1998). On the other hand, there is some evidence of a carbonaceous component as well (Kärcher *et al.*, 1996), quite likely coming from aircraft exhaust (Jensen and Toon, 1997; Chen *et al.*, 1998; Strom and Ohlsson, 1998; Petzold *et al.*, 1998). Hence, while the precise partitioning of heterogeneous IN amount between anthropogenic and natural is not currently feasible, a significant fraction might be anthropogenic.

For ice formation in other lower-tropospheric clouds, the situation is also unclear. All of the IN must necessarily be heterogeneous nuclei, with all of the ambiguities as to source that this implies. Natural ice nuclei are certainly not lacking. In addition to the soil source alluded to above, biogenic IN have been measured at significant levels, in both laboratory and field studies (cf., Schnell and Vali, 1976; Levin and Yankofsky, 1983). Much of this work has been recently reviewed in Szyrmer and Zawadzki (1997).

Numerous aerosol species of anthropogenic origin have been identified, both in the laboratory and in the field, as effective ice initiators (e.g., Hogan, 1967; Langer *et al.*, 1967; Van Valin *et al.*, 1976). However, measurement of enhanced IN concentrations from industrial sources has produced contradictory results. In some cases (e.g., Hobbs and Locatelli, 1970; Al-Naime and Saunders, 1985), above background IN concentrations have been found in urban plumes while in other instances below background levels have been found (e.g., Braham and Spyers-Duran, 1974; Perez *et al.*, 1985). Some of the discrepancies may be attributable to differing measurement techniques (Szyrmer and Zawadzki, 1997). However, it is possible that a good deal of it is due to differing degrees of deactivation of IN by pollutants such as sulphate, which readily forms in the atmosphere and can coat IN surfaces thereby deactivating them (particularly if the mechanism for ice formation involves deposition from the gas phase). Indeed, Bigg (1990) has presented evidence, albeit inconclusive, of a long-term decrease in IN associated with increasing pollution, perhaps acting through such a mechanism. There is also the possibility that secondary aerosol constituents such as aliphatic alcohols or dicarboxylic acids could coat inactive particles and thus transform them into efficient IN. If so, an incubation period after primary emission would be necessary and measurements could differ depending on time from emission. Although variability in natural heterogeneous IN sources may produce frequent circumstances where natural IN sources exceed anthropogenic IN in importance, it is difficult to see how the anthropogenic impact, both positive and negative, can be neglected.

How might the anthropogenic IN component vary with time?

This is the least tractable question of all, with all of the uncertainties in the answers to the previous questions propagating into any proposed answer. For homogeneous nucleation in upper-level, cirriform clouds, an assertion that the number of ice forming particles will be related to sulphur emissions is at least tenable. However, for the lower troposphere, little can be said at present. The impact of anthropogenic emissions could be negative, due to "poisoning" of natural IN; positive, due perhaps, to increased organic and inorganic carbon compared to inorganic non-carbon pollution emissions; or simply have little impact due to a small net source strength compared to those of natural IN.

5.4 Global Models and Calculation of Direct and Indirect Climate Forcing

5.4.1 Summary of Current Model Capabilities

In the past, many climate models used prescribed climatologies (Tanré *et al.*, 1984: d'Almeida, 1991) or precalculated monthly or annual mean column aerosol to describe the geographical distribution of aerosols and aerosol types. Optical properties were calculated offline by Mie-calculations assuming a uniform particle size, density and particle composition for each of the aerosol components (Shettle and Fenn, 1976; Krekov, 1993).

Most current GCMs are beginning to incorporate the calculation of aerosol mass interactively, taking account of the effect of aerosols on meteorology (Taylor and Penner, 1994; Roeckner *et al.*, 1999). In addition, models (GCMs and Chemistry Transport Models) are now available which directly use information on cloud formation and removal from the GCMs to account for the complex interactions between cloud processes, heterogeneous chemistry and wet removal (e.g. Feichter *et al.*, 1997; Roelofs *et al.*, 1998; Koch *et al.*, 1999; Rasch *et al.*, 2000a). These models are able to represent the high temporal and spatial variability of the aerosol particle mass distribution but must assume a size distribution for the aerosol to calculate their radiative effects.

The number and size of primary aerosols depend on the initial size distribution attributed to their source profiles together with the main growth and removal process. Models which represent number concentration have been developed for mineral dust studies (Tegen *et al.*, 1996; Schulz *et al.*, 1998) and for sea salt aerosols (Gong *et al.*, 1998). Representation of aerosol number is far more difficult for sulphate and secondary organics because the size distributions of condensing species depend on the size distribution of aerosols which are present before condensation and on cloud processes, but attempts to include these processes have been intiated (Herzog *et al.*, 2000; Ghan *et al.*, 2001a,b,c).

Because the processes for treating aerosol removal associated with precipitation and deposition and in-cloud conversion of SO_2 to sulphate are represented in climate models as sub-grid scale processes, there are significant variations in the efficiency of these processes between different models (see Section 5.2.2.6). In the past, model intercomparisons sponsored by the World Climate Research Programme (WCRP) have focussed on ^{222}Rn, ^{210}Pb, SO_2, and SO_4^{2-} (Jacob *et al.*, 1997; Rasch *et al.*, 2000b; Barrie *et al.*, 2001). These comparisons provide a "snapshot" in time of the relative performance of a major fraction of available large-scale sulphur models. They have shown that most of the models are able to simulate monthly average concentrations of species near the surface over continental sites to within a factor of two. Models are less sensitive to changes in removal rates near source regions, and they tend to agree more closely with observations over source regions than over remote regions. Comparison of models with observations at remote receptor sites can indicate whether transport and wet removal is well simulated but, for sulphate, may also be an indication of whether local source strengths are correctly estimated. The WCRP-sponsored model intercomparison in 1995 showed that model simulations differed significantly in the upper troposphere for species undergoing wet scavenging processes (Rasch *et al.*, 2000b) and the IPCC workshop (Section 5.4.1.2) demonstrated a similar sensitivity. Unfortunately, observations to characterise particle concentrations in remote regions and in the upper troposphere are limited. The vertical particle distribution affects aerosol forcing because scattering particles exhibit a greater forcing when they are located in the lower part of the troposphere, due to the effects of humidity on their size. Also, absorbing aerosols yield a greater forcing when the underlying surface albedo is high or when the aerosol mass is above low clouds (Haywood and Ramaswamy, 1998).

5.4.1.1 Comparison of large-scale sulphate models (COSAM)

One measure of our knowledge comes from the convergence in predictions made by a variety of models. Difficulties in the analysis and evaluation of such comparisons can result from models employing different emissions, meteorological fields etc. A set of standardised input was provided for the Comparison of Large Scale Sulphate Aerosol Models (COSAM) workshop which took place in 1998 and 1999 (see Barrie *et al.,* 2001). Ten models participated in this comparison. As noted above in Section 5.2.2.6, the simulation of the processes determining the sulphate concentration differed considerably between models. The fraction of sulphur removed by precipitation ranged from 50 to 80% of the total source of sulphur. The fraction of total chemical production of sulphate from SO_2 that took place in clear air (in contrast to in-cloud) ranged from 10 to 50%. This latter variability points to important uncertainties in current model capability to predict the indirect forcing by anthropogenic sulphate, because the mechanism of sulphate production determines the number of CCN produced (Section 5.3.3).

The ability of the models to predict the vertical distributions of aerosols was examined by comparing model predictions of the vertical distribution of SO_4^{2-}, SO_2 and related parameters such as ozone, hydrogen peroxide and cloud liquid-water content to mean profiles taken during aircraft campaigns at North Bay, a remote forested location (in southern Nova Scotia) 500 km north of the city of Toronto (Lohmann *et al.*, 2001). For SO_4^{2-}, the models were within a factor of 2 of the observed mean profiles (which were averages of 64 and 46 profiles for North Bay and Novia Scotia, respectively) but there was a tendency for the models to be higher than observations. The sulphur dioxide concentration was generally within a factor of two of the observations. Those models that overpredicted SO_4^{2-} also underpredicted SO_2, demonstrating that the model treatment for the chemical transformation of SO_2 to SO_4^{2-} is a source of uncertainty in the prediction of the vertical distribution of SO_4^{2-}.

A comparison of modelled and observed ground level sulphate at 25 remote sites showed that on average, most models predict surface level seasonal mean SO_4^{2-} aerosol mixing ratios to within 20%, but that surface SO_2 was overestimated by 100% or more. A high resolution limited area model performed best by matching both parameters within 20%. This was consistent with the large variation in the ability of models to transport and disperse sulphur in the vertical.

Both regional source budget analyses (Roelofs *et al.*, 2001) as well as long-range transport model tests (Barrie *et al.*, 2001)

suggest that the dominant cause of model-to-model differences is the representation of cloud processes (e.g. aqueous-phase sulphate production rates, wet deposition efficiency and vertical transport efficiencies) and horizontal advection to remote regions.

In summary, the COSAM model comparison showed that both convective transport and oxidation of sulphur dioxide to sulphate are processes that are not well simulated in large-scale models. In addition, the treatment of dry and wet deposition of aerosols and aerosol precursors continues to lead to important variations among the models. These variations lead to uncertainties in atmospheric sulphate concentrations of up to a factor of 2. The uncertainties in SO_2 are larger than those for SO_4^{2-}.

5.4.1.2 The IPCC model comparison workshop: sulphate, organic carbon, black carbon, dust, and sea salt

Comparisons of models with observations for sulphate aerosols and other sulphur compounds are particularly relevant for assessing model capabilities because the emissions of sulphur bearing compounds are better known than the emissions of other aerosol compounds (Section 5.2). Thus, comparison can focus on the capabilities of the models to treat transport and oxidation processes. Recent field studies, however, have pointed out the importance of organic aerosol compounds (Hegg *et al.*, 1997), dust aerosols (Li-Jones and Prospero, 1998; Prospero, 1999), and sea salt aerosols (Murphy *et al.*, 1998a). Also, soot is important because it decreases the reflection and increases the absorption of solar radiation (Haywood and Shine, 1995). Furthermore, the magnitude of the indirect effect is sensitive to the abundance of natural aerosols (Penner *et al.* 1996; O'Dowd *et al.*, 1999; Chuang *et al.*, 2000). Therefore, an examination of model capability to represent this entire suite of aerosol components was undertaken as part of this report.

Emissions for this model comparison were specified by the most recently available emissions inventories for each component (see Tables 5.2, 5.3, Section 5.2 and Table 5.7). Eleven aerosol models participated in the model intercomparison of sulphate, and of these, nine treated black carbon, eight treated organic carbon, seven treated dust, and six treated sea salt. Eight scenarios were defined (see Table 5.7). The first, SC1, was selected to provide good estimates of present day aerosol emissions. SC2 was defined to simulate aerosol concentrations in 2030 according to preliminary estimates from the IPCC SRES A2 scenario (Nakićenović, *et al.*, 2000). SC3 was defined to simulate the draft A2 scenario in 2100 and SC4 to simulate the draft B1 scenario in 2100. SC1-SC4 used present day chemistry and natural emissions. In addition, we estimated possible future changes in emissions of the natural components DMS, terpenes, dust and sea salt in 2100 in SC5 for the A2 scenario and in SC8 for the B1 scenario. Scenario SC6 also estimated changes in emissions of other gas phase components associated with the production of sulphate in the A2 scenario in 2100 (see Chapter 4) and SC7 estimated changes in climate (temperature, winds and precipitation patterns) as well. Table 5.7 also shows the estimates of anthropogenic emissions in 2100 associated with the IS92a scenario. Some of the participants also provided estimates of direct and indirect forcing. These estimates, together with the range of predicted concentrations among the models, help to define the uncertainty due to different model approaches in aerosol forcing for future scenarios. The models, participants, scenarios they provided, and the aerosol components treated are summarised in Table 5.8.

5.4.1.3 Comparison of modelled and observed aerosol concentrations

Like previous model intercomparisons, the IPCC comparison showed large differences (factor of 2) in model predictions of the vertical distribution of aerosols. The model simulations of surface sulphate concentrations (Figure 5.8) indicate that much of the difference in sulphate radiative forcing reported in the literature is most likely to be associated with either variations in the vertical distribution or with the response of sulphate aerosols to variations in relative humidity (Penner *et al.*, 1998b).

The IPCC comparison showed that the capability of models to simulate other aerosol components is inferior to their capability to simulate sulphate aerosol. For example, sea salt in the North and South Pacific shows poorer agreement, with an average absoute error of 8 μgm^{-3} (Figure 5.9) than the corresponding sulphate comparison which is less than 1 μgm^{-3} (Figure 5.8) (see Table 5.9 also).

For dust the model-observation comparison showed a better agreement with surface observations in the Northern than in the Southern Hemisphere. For example, the average absolute error in the Northern Pacific was 179%, while it was 268% in the Southern Pacific. In the Southern Hemisphere, almost all models predict concentrations higher than the observations at all stations poleward of 22°S. Thus, it appears that dust mobilisation estimates may be too high, particularly those for Australia and South America. The paucity of dust from these regions relative to other arid dust source areas has been noted previously (Prospero *et al.*, 1989; Tegen and Fung, 1994; Rea, 1994), and may reflect the relative tectonic stability, low weathering rates, duration of land-surface exposure, and low human impacts in this area.

The interpretation of the comparison of observed and model-predicted concentrations for both organic carbon and black carbon is more difficult because of both inaccuracies in the observations (Section 5.1.2) and the fact that most measured concentrations are only available on a campaign basis. In addition, the source strength and atmospheric removal processes of carbonaceous aerosols are poorly known. Most models were able to reproduce the observed concentrations of BC to within a factor of 10 (see Figure 5.10) and some models were consistently better than this. Both modelled and observed concentrations varied by a factor of about 1,000 between different sites, so agreement to within a factor of 10 demonstrates predictive capability. However, there are still large uncertainties remaining in modelling carbonaceous aerosols.

Table 5.9 presents an overview of the comparison between observed and calculated surface mixing ratios. Table 5.9a gives the comparison in terms of absolute mass concentrations while Table 5.9b gives the comparison in terms of average differences of percents. The average absolute error for sulphate surface concentrations is 26% (eleven models) and the agreement

Table 5.7: *Global emissions specified for the IPCC model intercomparison workshop.*

	SC1	SC2	SC3	SC4	SC5	
		A2	A2	B1	A2	IS92a
Year	2000	2030	2100	2100	2100+ natural	2100
Sulphur (as Tg S)[a]						
Anthropogenic SO_2	69.0	111.9	60.3	28.6	60.3	147.0
Ocean DMS	25.3	25.3	25.3	25.3	27.0	
Volcanic SO_2	9.6	9.6	9.6	9.6	9.6	
Organic Carbon (as OM)[b]						
Anthropogenic	81.4	108.6	189.5	75.6	189.5	126.5
Natural	14.4	14.4	14.4	14.4	20.7	
Black Carbon[b]						
Anthropogenic	12.4	16.2	28.8	12.0	28.8	19.3
Dust (<2 μm diameter)[c]	400	400	400	400	418.3	
Dust (>2 μm diameter)[c]	1,750	1,750	1,750	1,750	1,898	
Sea Salt (as Na) (<2 μm diameter)[d]	88.5	88.5	88.5	88.5	155.0	
Sea Salt (as Na) (>2 μm diameter)[d]	1,066	1,066	1,066	1,066	1,866	

[a] Anthropogenic SO_2 emissions were the preliminary emissions from Nakicenovic *et al.* (2000). DMS emissions were the average of the emissions based on Wanninkhof (1992) and those based on Liss and Merlivat (1986) using methods described in Kettle *et al.* (1999). Volcanic SO_2 emissions were those available from the IGAC Global Emissions Inventory Activity (http://www.geiacenter.org) described by Andres and Kasgnoc (1998).

[b] Organic carbon is given as Tg of organic matter (OM) while black carbon is Tg C. For anthropogenic organic matter, the black carbon inventory of Liousse *et al.* (1996) was scaled up by a factor of 4. This scaling approximately accounts for the production of secondary organic aerosols consistent with the analysis of Cooke *et al.* (1999). For 2030 and 2100, the ratio of the source strengths for CO in 2030 and 2100 to that in 2000 was used to scale the source of organic carbon and black carbon at each grid location. For natural organic aerosols, the terpene emissions from Guenther *et al.* (1995) were assumed to rapidly undergo oxidation yielding a source of aerosol organic matter of 11% by mass per unit C of the emitted terpenes.

[c] The dust emission inventory was prepared by P. Ginoux.

[d] The sea salt emissions were those developed by Gong *et al.* (1997a,b) based on the Canadian Climate Model winds.

Table 5.8: *Aerosol models participating in IPCC model intercomparison workshop.*[a]

Code	Model	Contributor	Aerosol components treated	Scenarios	Forcing provided
1	ULAQ	Pitari	Sulphate, OC, BC, dust, sea salt	SC1, SC2, SC3, SC4, SC5, SC7	
2	GISS	Koch, Tegen	Sulphate, OC, BC, dust, sea salt	SC1, SC2, SC3, SC4, SC8	Direct, Indirect
3	Georgia Tech./GSFC GOCART	Chin, Ginoux	Sulphate, OC, BC, dust, sea salt	SC1, SC2, SC3, SC4, SC5	
4	Hadley Center, UK Met Office	Roberts, Woodage, Woodward, Robinson	Sulphate, BC, dust	SC1, SC2, SC3, SC4, SC5	Direct
5	LLNL/U. Mich. (CCM1/ GRANTOUR)	Chuang Penner Zhang	Sulphate, OC, BC, dust, sea salt	SC1, SC2, SC3, SC4, SC5, SC8	Indirect
6	Max Planck/ Dalhousie U. (ECHAM4.0)	Feichter Land Lohmann	Sulphate, OC, BC	SC1, SC2, SC3	Indirect
7	U. Michigan (ECHAM3.6/ GRANTOUR)	Herzog, Penner Zhang	Sulphate, OC, BC, dust, sea salt	SC1, SC2, SC3, SC4, SC5, SC8	Direct
8	UKMO/Stochem	Collins	Sulphate	SC1,SC3	
9	NCAR/Mozart	Tie	Sulphate, BC	SC1	
10	KNMI/TM3	van Weele	Sulphate	SC1	
11	PNNL	Ghan, Easter	Sulphate, OC, BC, dust, sea salt	SC1, SC3	Direct, indirect

[a] References to the models: (1) Pitari *et al.*, (2001); Pitari and Mancini (2001); (2) Koch *et al.* (1999); Tegen and Miller (1998); (3) Chin *et al.* (2000); (4) Jones *et al.* (1994b); (5) Chuang *et al.* (2000); (6) Feichter *et al.* (1996); Lohmann *et al.* (1999b); (7) This model is similar to those described by Chuang *et al.* (1997) and Chuang *et al.* (2001), but with updated cloud scavenging and convective processes; (8) Stevenson *et al.* (1998); (9) Brasseur *et al.* (1998); (10) Houweling *et al.* (1998); Jeuken *et al.* (2001); (11) Ghan *et al.* (2001a,b,c).

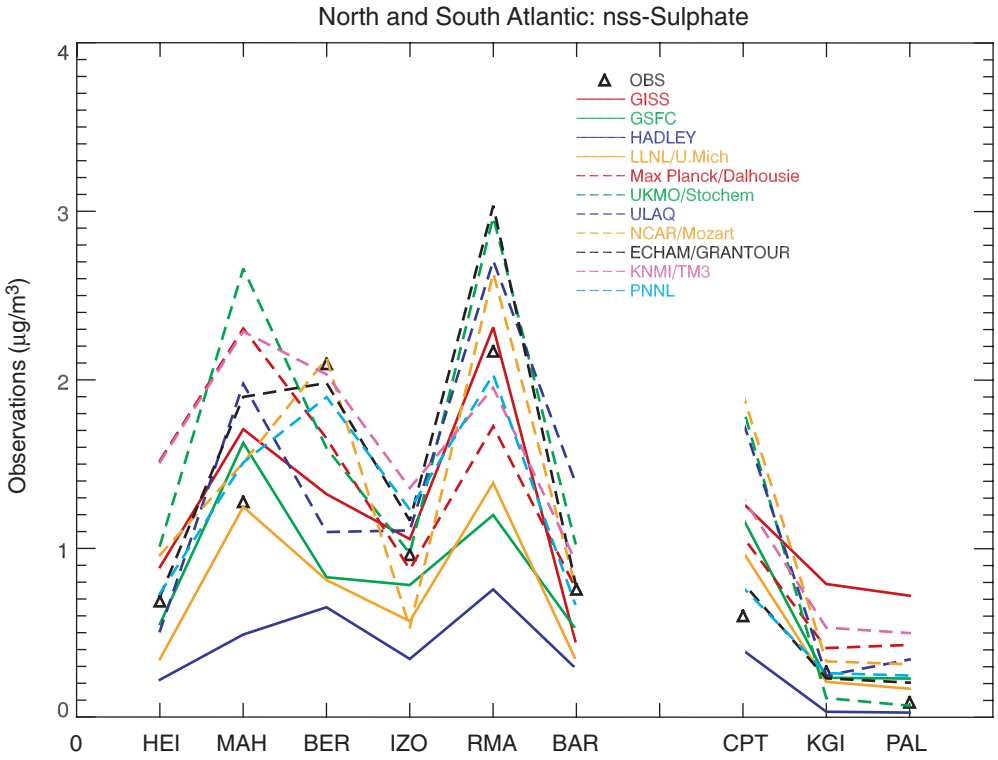

Figure 5.8: Observed and model-predicted annual average concentrations of non-sea salt sulphate (in µg m^{-3}) at a series of stations in the North and South Atlantic. The models are listed in Table 5.8. Data were provided by D. Savoie and J. Prospero (University of Miami). Stations refer to: Heimaey, Iceland (HEI); Mace Head, Ireland (MAH); Bermuda (BER); Izania (IZO); Miami, Florida (RMA); Ragged Point, Barbados (BAR); Cape Point, South Africa (CPT); King George Island (KGI); and Palmer Station, Antarctica (PAL).

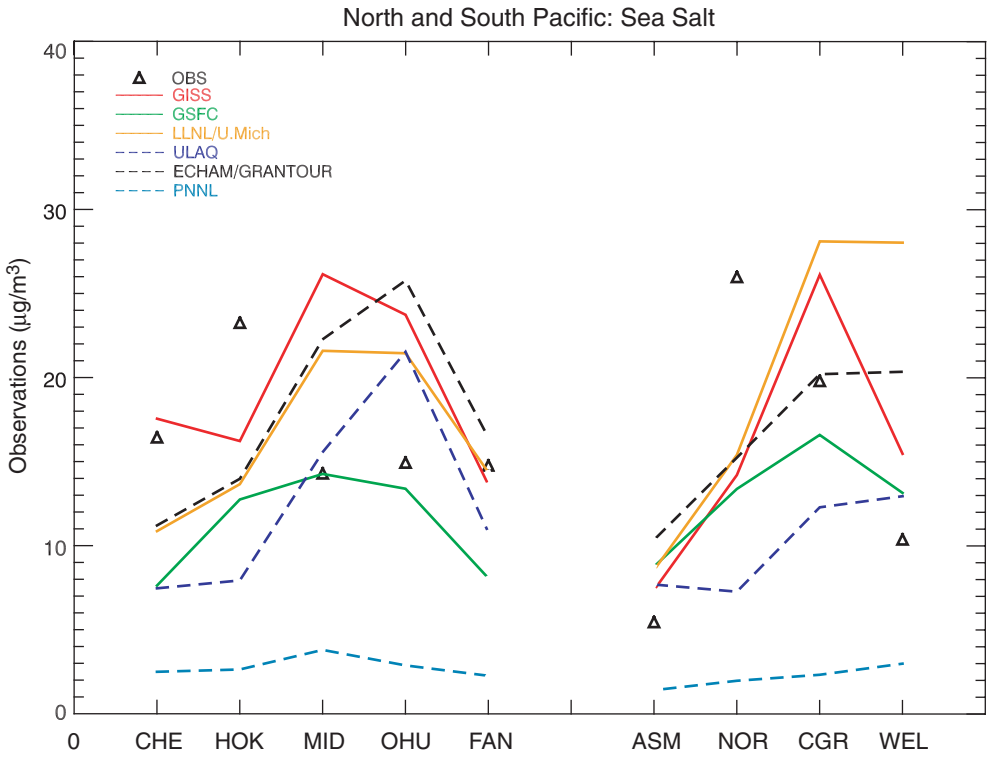

Figure 5.9: Observed and model-predicted annual average concentrations of sea salt (as Na) (in µgm^{-3}) at a series of stations in the North and South Pacific. The models are listed in Table 5.8. Data were provided by D. Savoie and J. Prospero (University of Miami). Stations refer to: Cheju, Korea (CHE); Hedo, Okinawa, Japan (HOK); Midway Island (MID); Oahu, Hawaii (OHU); Fanning Island (FAN); American Samoa (ASM); Norfolk Island (NOR); Cape Grim, Tasmania (CGR); and Wellington/Baring Head, New Zealand (WEL).

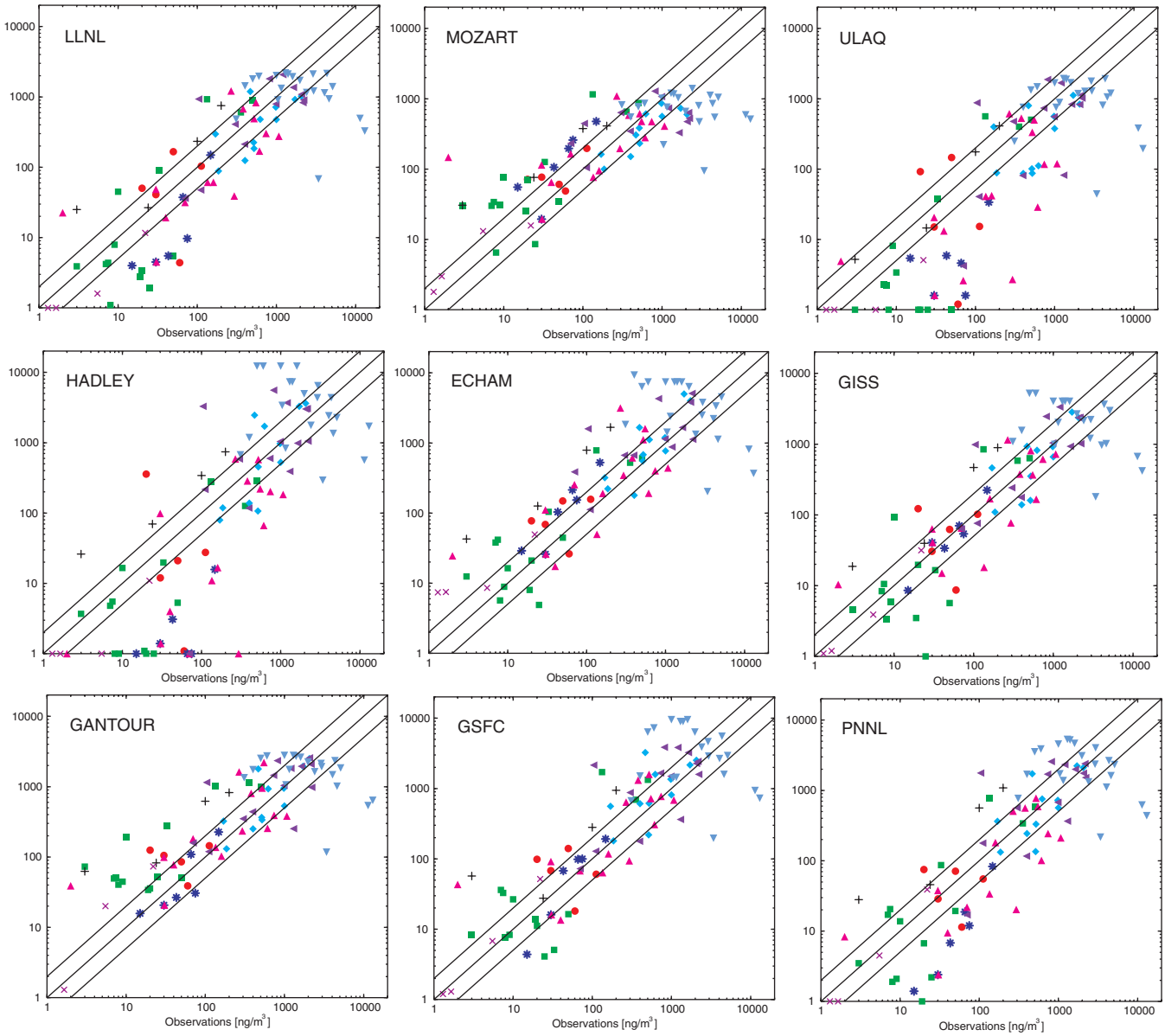

Figure 5.10: Observed and model-predicted concentrations of black carbon (in ng C m^{-3}) at a number of locations. The models are listed in Table 5.8. Observations refer to those summarised by Liousse *et al.* (1996) and Cooke *et al.* (1999). Symbols refer to: circle, Liousse Atlantic; square, Liousse Pacific; diamond, Liousse Northern Hemisphere rural; plus, Liousse Southern Hemisphere rural; asterisk, Liousse Northern Hemisphere remote; cross, Liousse Southern Hemisphere remote; upward triangle, Cooke remote; left triangle, Cooke rural; downward triangle, Cooke urban.

between modelled concentrations and observations is better for sulphate than for any other species. The largest difference with observed values is that of carbonaceous aerosols with an average absolute error (BC: nine models, OC: eight models) of about 179%. This may be partly due to the large uncertainties in the estimated strength of biomass burning and biogenic sources. The average absolute error for the dust (six models) and sea salt (five models) simulations is 70 and 46%, respectively.

In addition to the model comparison with observations, an analysis of the variation in aerosol burden among the models was considered. After throwing out the burdens from models that were outliers in terms of their comparison with observations, the model results still differed by a factor of 2.2 for sulphate, by a factor of 2.2 for organic carbon (seven models), and by a factor of 2.5 for black carbon (eight models). In contrast, the range of total burdens for dust was a factor of 2.8 and 4.5 for aerosols with diameter less than and greater than 2 μm, respectively, while that for sea salt was a factor of 4.9 and 5.3, respectively. The range for sea salt with D<2 μm increases to 6 if the GSFC Gocart model is considered (with its higher sea salt flux). These differences were also evident in comparing concentrations in the upper troposphere. For example, in the upper troposphere (8 to 12 km) between 30 and 60°N, the range of predicted concentrations of sulphate, organic carbon and black carbon was about a factor of 5 to 10. This range increased to as much as a factor of 20 or more in the case of sea salt and dust.

Table 5.9a: *Comparison of models and observations of aerosol species at selected surface locations (μg/m³)[a,b].*

Model	Sulphate		Black carbon		Organic carbon		Dust		Sea salt	
	Average bias (μg/m³)	Average absolute error (μg/m³)	Average bias (μg/m³)	Average absolute error (μg/m³)	Average bias (μg/m³)	Average absolute error (μg/m³)	Average bias (μg/m³)	Average absolute error (μg/m³)	Average bias (μg/m³)	Average absolute error (μg/m³)
GISS	0.15	0.33	0.16	0.61	0.69	1.52	5.37	5.37	3.90	11.94
GSFC	–0.10	0.28	0.71	1.00	0.71	1.57	–0.5	1.98	–3.02	9.23
Hadley	–0.54	0.55	0.74	1.18			–2.47	3.48		
CCM/Grantour	–0.31	0.40	–0.18	0.50	–0.84	1.20	1.77	2.99	5.26	14.48
ECHAM	0.09	0.42	0.74	1.07	1.52	2.09				
Stochem	0.34	0.40								
ULAQ	0.18	0.34	–0.30	0.48	–0.47	1.43	1.82	3.69	0.81	12.57
Mozart	0.05	0.39	–0.34	0.51						
ECHAM/Grantour	0.26	0.28	0.07	0.55	–0.57	1.40	5.2	5.27	2.07	10.55
TM3	0.27	0.47								
PNNL	–0.04	0.28	0.16	0.64	0.79	1.50	–2.48	2.64	–13.46	13.74
Average of all models	0.03	0.38	0.20	0.73	0.26	1.53	2.73	3.86	–0.74	12.09

[a] Aerosol sulphate, dust and sea salt were compared to observations at a selection of marine locations. The observations for organic carbon and black carbon were those compiled by Liousse *et al.* (1996) and Cooke *et al.* (1999).

[b] The average bias and the average absolute error is the average differences between each model result and the observations over all stations.

Table 5.9b: *Comparison of models and observations of aerosol species at selected surface locations (%)[a,b].*

Model	Sulphate		Black carbon		Organic carbon		Dust		Sea salt	
	Average bias (%)	Average absolute error (%)	Average bias (%)	Average absolute error (%)	Average bias (%)	Average absolute error (%)	Average bias (%)	Average absolute error (%)	Average bias (%)	Average absolute error (%)
GISS	26	31	85	127	91	121	121	121	37	40
GSFC	7	15	189	219	109	134	39	42	21	30
Hadley	–11	16	140	220						
CCM/Grantour	1	15	43	111	13	85	78	80	63	68
ECHAM	32	35	253	276	273	285				
Stochem	30	34								
ULAQ	10	17	–10	84	23	100	21	35	81	88
Mozart	28	31	164	211						
ECHAM/Grantour	31	31	204	230	88	135	70	70	29	33
TM3	43	46								
PNNL	17	21	75	133	189	220			–12	16
Average of all models	19	26	127	179	112	154	66	70	36	46

[a] Aerosol sulphate, dust and sea salt were compared to observations at a selection of marine locations. The observations for organic carbon and black carbon were those compiled by Liousse *et al.* (1996) and Cooke *et al.* (1999).

[b] The average bias and the average absolute error is the average percentage difference between each model result and the observations over all stations.

Based on this model comparison study, the ability of the global models to reproduce the aerosol mixing ratios at the surface can be described as acceptable for sulphate. However, improvement is needed for the other aerosol species. The large differences in predicted atmospheric aerosol burden which is the relevant parameter in determining the forcing, impede an accurate estimate of the aerosol climate effect. Improvement of the assessment of aerosol burden requires more measurements within the free troposphere.

5.4.1.4 Comparison of modelled and satellite-derived aerosol optical depth

Comparison of model results with remote surface observations of the major components making up the composition of the atmospheric aerosol provide a test of whether the models treat transport and removal of individual species adequately. But as noted above, the difference between the vertical distribution of species among the models is significant (i.e. a difference of more

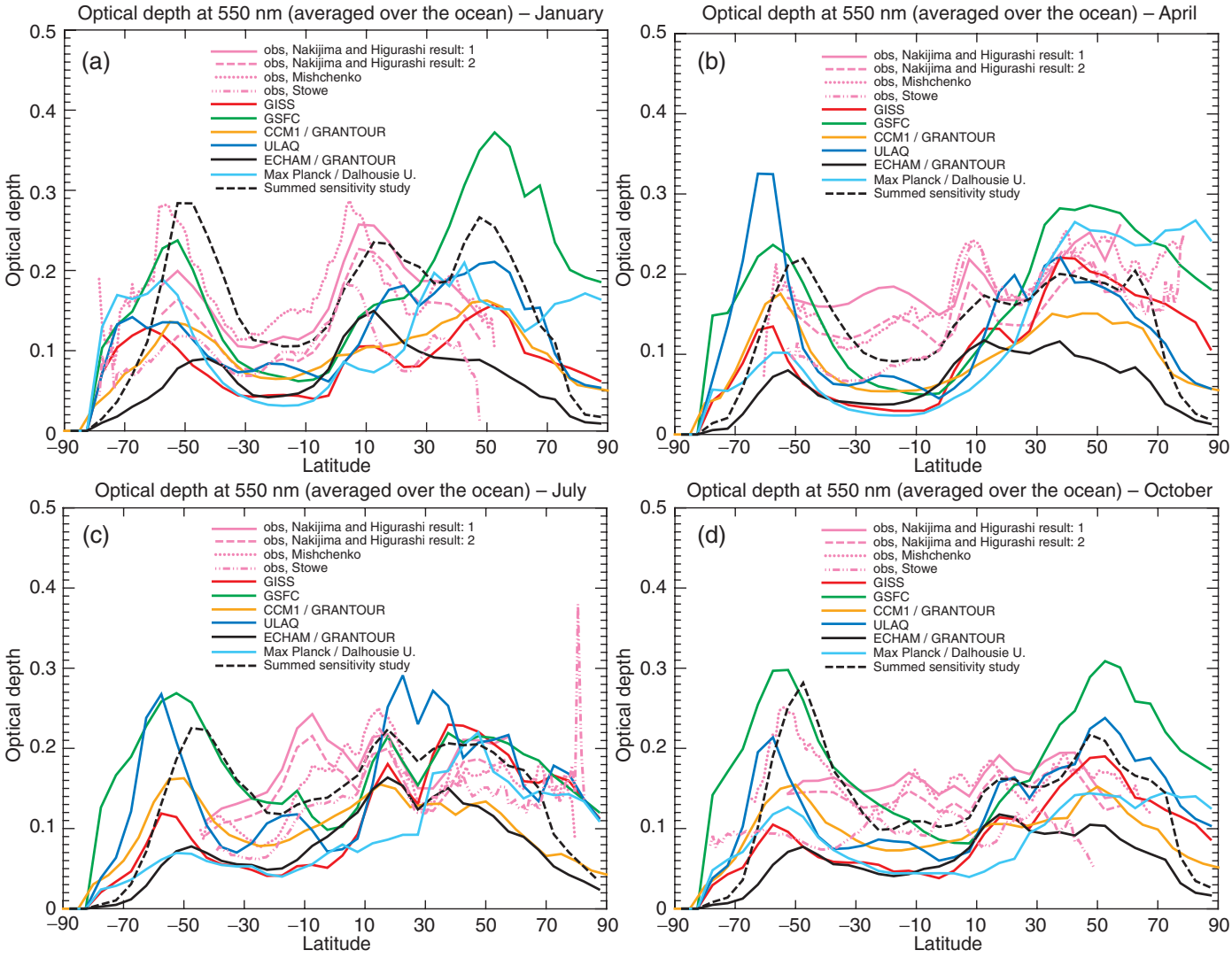

Figure 5.11: Aerosol optical depth derived from AVHRR satellite analysis following Nakajima *et al.* (1999) (labelled result: 1 and result: 2), Mishchenko *et al.* (1999) and Stowe *et al.* (1997) for January, April, July and October. The results from Nakajima refer to 1990, while those from Mishchenko and Stowe refer to an average over the years 1985 to 1988. The results derived from the models which participated in the IPCC-sponsored workshop are also shown (see Table 5.8). The case labelled "summed sensitivity study" shows the derived optical depth for the ECHAM/GRANTOUR model using a factor of two increase in the DMS flux and the monthly average sea salt fluxes derived using the SSM/I wind fields.

than a factor of 2 in the upper troposphere) and the global average abundance of individual components varies significantly (more than a factor of 2) between the models, especially for components such as dust and sea salt. Two methods have been used to try to understand whether the models adequately treat the total aerosol abundance. The first, comparison of total optical depth with satellite measurements, was employed by Tegen *et al.* (1997), while the second, comparison of total reflected short-wave radiation with satellite observations, was employed by Haywood *et al.* (1999). We examined both measures in an effort to understand whether the model-predicted forcing associated with aerosols is adequate.

Figure 5.11 shows the zonal average optical depth deduced from AVHRR data for 1990 by Nakajima and Higurashi (Nakajima *et al.*, 1999) and for an average of the time period February 1985 to October 1988 by Mishchenko *et al.* (1999) and by Stowe *et al.* (1997). The two results from Nakajima *et al.* (1999) demonstrate the sensitivity of the retrieved optical depth to the assumed particle size distribution. Results from the models which participated in the intercomparison workshop are also included. Because the GISS, CCM1, ECHAM/GRANTOUR and ULAQ models all used the same sources, the differences between these models are due to model parametrization procedures. The GOCART (GSFC) model used a source distribution for sea salt that was derived from daily varying special sensor microwave imager (SSM/I; Atlas *et al.*, 1996) winds for 1990 and was, on average, 55% larger than the baseline sea salt source specified for the model workshop. The MPI/Dalhousie model used monthly average dust and sea salt distributions from prior CCM1 model simulations (cf., Lohmann *et al.*, 1999b,c).

Workshop participants were asked to report their derived optical depths. However, these varied widely and were often much smaller than that derived here. Therefore, we constructed the optical depths shown in Figure 5.11 from the frequency distribution of relative humidity from the T21 version of the ECHAM 3.6 general circulation model, together with the reported monthly average distributions of aerosol mixing ratios. The model optical depths were derived using extinction coefficients at 0.55 μm for dry sea salt of 3.45 m^2g^{-1}, 0.69 m^2g^{-1}, and 0.20 m^2g^{-1} for diameters in the size range from 0.2 to 2 μm, 2.0 to 8 μm and 8 to 20 μm, respectively, and an extinction coefficient of 9.94 m^2g^{-1} for sulphate. The humidity dependence of the extinction for sea salt and dust was determined using the model described in Penner *et al.* (1999a). The dust extinction coefficients were from Tegen *et al.* (1997) and organic and black carbon extinction coefficients for 80% relative humidity were from Haywood *et al.* (1999). We also examined the sensitivity of the modelled optical depths to a factor of two increase in the DMS flux and to the use of monthly average sea salt fluxes derived using the SSM/I wind fields. The OC and BC extinction coefficients were also varied, adding the humidity dependence determined by Penner *et al.* (1998b). Finally, the extinction coefficient for sulphate was altered to that calculated for an assumed ratio of total NH_3 and HNO_3 to H_2SO_4 of four. The line in the graph labelled "summed sensitivity study" shows the results for the ECHAM/GRANTOUR model when these parameters were varied. Most of the difference between the summed sensitivity case and that for the baseline ECHAM/GRANTOUR model is due to the use of larger DMS and sea salt fluxes.

The satellite-derived optical depths from Stowe *et al.* (1997) are lower on average by 0.05 and by 0.03 than those from Mischenko *et al.* (1999) and result 2 from Nakajima *et al.* (1999), respectively. The latter two retrievals make use of a two-wavelength technique which is thought to be more accurate than the one-wavelenth technique of Stowe *et al.* (1997). However, it is worth bearing in mind that most of the difference in retrieved aerosol optical depth may be related to cloud screening techniques (Mishchenko *et al.*, 1999) or to assumed size distribution (Nakajima *et al.*, 1999).

Modelled optical depths north of 30°N are sometimes higher and sometimes lower than those of the retrieved AVHRR optical depths. For example, there is an average difference of 0.13 in July for the ULAQ model in comparison with result 2 for Nakajima *et al.* (1999) while the average difference is –0.09 in January for the ECHAM/GRANTOUR model in comparison with the retrieved optical depths from Mishchenko *et al.* (1999). The modelled optical depths in the latitude band from 30°N and 40°N are systematically too high in July. For example, the average of the modelled optical depths is larger than the satellite-derived optical depth of Nakajima, Mishchenko, and Stowe on average by 0.06, 0.05 and 0.04, respectively. We note that sulphate and dust provide the largest components of optical depth in this region with sea salt providing the third most important component. Since the sources represent the year 2000, while the measured optical depths refer to an average of the years 1985 to 1988, some of the overprediction of optical depth may be associated with higher sources than the time period of the measurements. The black dashed line shows the estimated optical depths from the ECHAM/GRANTOUR model with the larger sea salt fluxes deduced from the SSM/I winds, with doubled DMS flux, and with optical properties for an assumed ratio of total NO_3 to H_2SO_4 of 4:1. Comparison of these results with those of the retrieved optical depths shows that the uncertainties in these parameters lead to changes in optical depth that are of the order of 0.05 or more.

Modelled aerosol optical depths near 10°N are dominated by dust with some contribution from organic carbon and sulphate (especially in January and April). They are systematically lower (by, on average, 0.08) than the average retrieved optical depth. The discrepancy between modelled and retrieved optical depths in this region, however, would be reduced if the sea salt fluxes derived from SSM/I winds and larger DMS fluxes had been used.

The modelled aerosol optical depths from 10°S to 30°S are due to a combination of different aerosol types. They are systematically lower than the average of the retrieved optical depths by an average of 0.06 with biases ranging from –0.14 to 0.01 in January, from –0.12 to –0.02 in April, from –0.13 to 0.07 in July and from –0.11 to 0.06 in October. As shown by the sensitivity study, much of the difference between the modelled and retrieved zonal average optical depths could be removed by using higher sea salt and DMS fluxes. However, the spatial character of the differences reveals that the cause of the discrepancies probably cannot be attributed to any single source. For example, Figure 5.12 shows the difference between the base case and sensitivity case for the ECHAM/GRANTOUR model and the optical depths retrieved by Mishchenko *et al.* (1999). In January the differences are largest in the central Pacific Ocean. In April the differences appear largest in the Pacific Ocean and in the Indian Ocean west of Australia. In July and October the differences are mainly to the west and east of the African continent and also in the mid-Pacific Ocean and west of South America in October. We note that the large overprediction of optical depth in both the base case and the sensitivity case off the coast of Asia in July may be due to the difference in simulated year and the year of the optical depth retrievals. The model simulations used anthropogenic sulphate emissions appropriate to 2000 while the retrievals refer to an average of 1985 to 1988 data.

Modelled aerosol optical depths near 60°S are dominated by sea salt. This component appears to be reasonably well represented by the models, especially for the optical depths predicted using the SSM/I sea salt fluxes. However, if some of the other models had used the higher fluxes used in the GSFC model, the optical depths would be overpredicted in this region.

Haywood *et al.* (1999) found a large and significant difference between modelled and observed reflectivity at northern latitudes when higher sea salt fluxes based on the algorithm used here were used together with the SSM/I-derived winds. The use of this algorithm corrected a significant underprediction of reflected radiation in mid-ocean regions when the sea salt parametrization of Lovett (1978) was used. We used the aerosol burdens from the models in the IPCC intercomparison to scale the optical depths in the Haywood *et al.* study in order to compare the average reflected radiation from each of the models in the intercomparison with that from the ERBE satellite. For the GSFC model which also used winds derived from the SSM/I, results similar to those reported by Haywood *et al.* (1999) were found (i.e. an overpredicted flux at

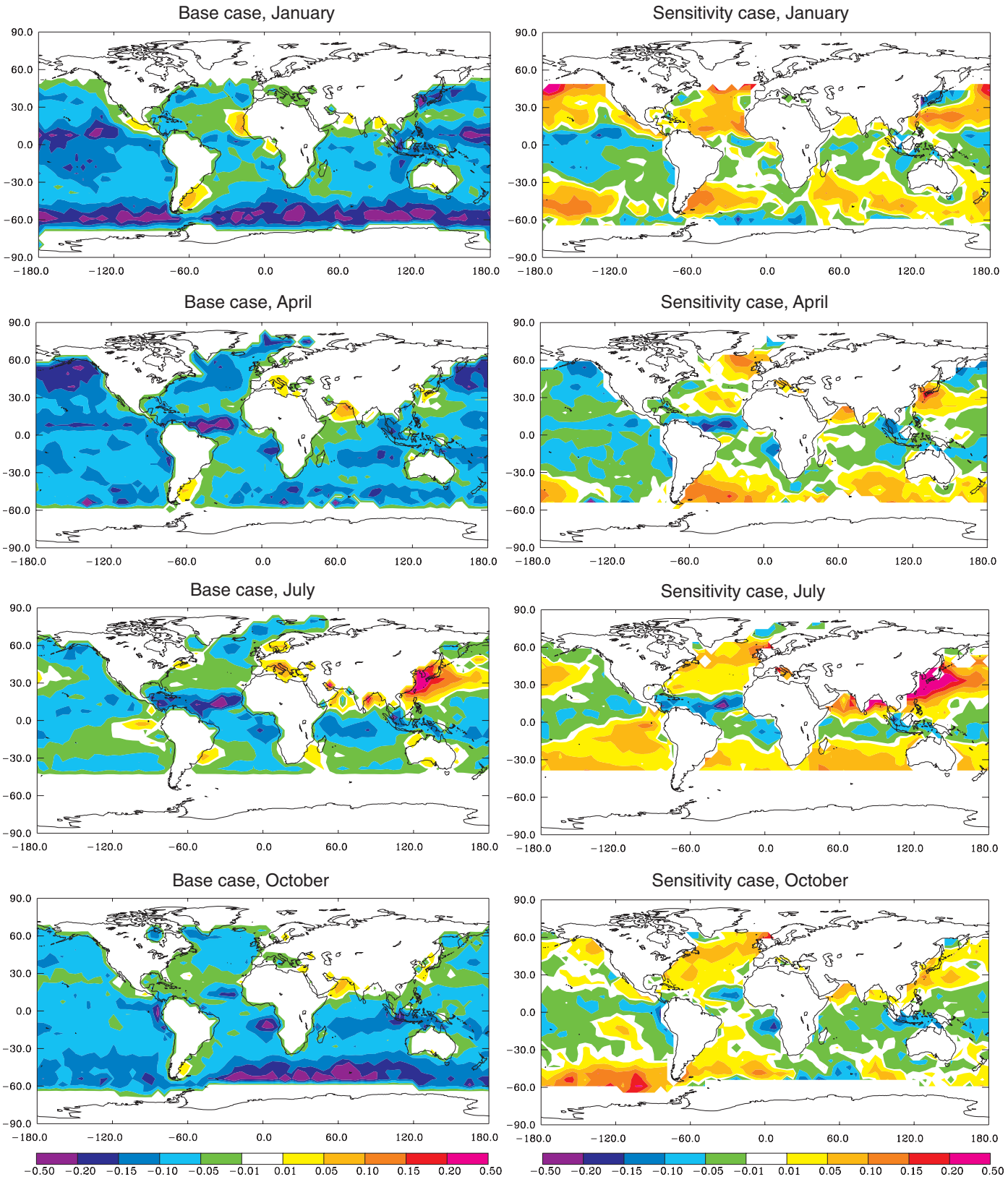

Figure 5.12: Difference between the ECHAM/GRANTOUR computation of optical depth and the satellite-retrieved optical depths from Mishchenko *et al.* (1999). The left column shows the optical depths derived for the standard set of sources, while the right panel shows the derived optical depths for the sensitivity study using a factor of two increase in the DMS flux and the monthly average sea salt fluxes derived using the SSM/I wind fields (see text). Note that the anthropogenic sulphate sources were for the year 2000 while the satellite analysis covers the time period 1985 to 1988. This may explain the systematic overestimate of optical depth off the coast of Asia in July.

northern latitudes, but no large biases elsewhere). For the other models, the reflected radiation in mid-ocean regions was underpredicted relative to ERBE, but the area of underprediction was not as large as the area of underprediction for the GFDL model with the low sea salt option. For these models, the predicted reflected radiation for the region north of 30°N was sometimes higher than that from the ERBE satellite, but this was not consistent across all models. In general, this analysis showed that the comparison of model results with the reflected radiation from ERBE is broadly consistent with that developed above for the comparison between modelled and AVHRR-retrieved aerosol optical depth.

In summary, analysis of the AVHRR comparisons indicates that significant uncertainties remain in both our ability to retrieve aerosol optical thickness from satellites and in our ability to model aerosol effects on the radiation budget. For example, there is a global average difference between the optical depth retrieved by Mishchenko *et al.* (1999) and that retrieved by Stowe *et al.* (1997) of 0.05 and a difference between Nakajima *et al.* (1999) and Stowe *et al.* (1997) of 0.03. The global average difference between the average optical depth from the models and the average optical depth from the satellite retrieval is of the same magnitude, namely –0.04. In the region 10°S to 30°S, the analysis indicates that modelled optical depths are consistently too low. Such a model underestimate might indicate that the retrieved optical depth from satellites is too high, for example, because the cloud screening algorithm is not adequate in this region. Alternatively, there may be a need for a larger source of aerosols in this region or for smaller modelled removal rates.

5.4.2 Overall Uncertainty in Direct Forcing Estimates

To illustrate how the uncertainty associated with each of the factors determining aerosol direct forcing contribute to the overall uncertainty in forcing, we adopt a simple box-model of the overall change in planetary albedo. This approach follows that presented in Penner *et al.* (1994a), but is updated in several respects. For this model, the change in global average planetary albedo associated with anthropogenic aerosols is described as (Chylek and Wong, 1995):

$$\Delta\alpha_p = [T_a^2(1-A_c)][2(1-R_s)^2\bar{\beta}f_b M\alpha_s f(RH) - 4R_s M\alpha_s f(RH)((1-\omega_0)/\omega_0)]$$

where,

T_a = atmospheric transmissivity above the main aerosol layer
A_c = global cloud fraction
R_s = global average surface albedo
$\bar{\beta}$ = upscatter fraction for isotropic incoming radiation
f_b = hygroscopic growth factor for upscatter fraction
M = global mean column burden for aerosol constituent, (gm^{-2})
α_s = aerosol mass scattering efficiency, (m^2g^{-1})
f(RH) = hygroscopic growth factor for total particle scattering
ω_0 = single scattering albedo at ambient RH (assumed to be 80% for this analysis).

The key quantities that enter into the calculation of uncertainties are listed in Table 5.10, together with estimates of their 2/3 uncertainty range. Given these central values and uncertainties, the variance (and thus uncertainty) associated with the planetary albedo change ($\Delta\alpha_p$) is determined by standard Taylor expansion of the function around the central values for the change in planetary albedo. Thus, with variances given by S_{xi}^2:

$$S_{\Delta\alpha p}^2 = \left[\frac{\partial\Delta\alpha_p}{\partial x_i}\right]^2 S_{xi}^2 + \mathrm{cov}(x_i, x_j)\left[\frac{\partial\Delta\alpha_p}{\partial x_i}\right]\left[\frac{\partial\Delta\alpha_p}{\partial x_j}\right]$$

where the function $\mathrm{cov}(x_i,x_j)$ is the covariance of the variables in the argument and a variable subscript (i.e., i or j) implicitly requires summation from 1 to n where n is the number of variables. Significant covariances are found between $\bar{\beta}$ and α_s, $\bar{\beta}$ and f_b, α_s and f(RH), and ω_0 and f(RH). For these variable pairs, Bravais-Pearson (linear) correlation coefficients were found to be –0.9, –0.9, 0.9 and 0.9, respectively. These were determined by sampling the probability distribution associated with each pair of variables to generate a large set of corresponding pairs of values. Linear regression analysis was then performed on these corresponding pairs to determine the linear correlation coefficient between the paired variables. The burden estimates in Table 5.10 are based on model calculations from the IPCC workshop. The uncertainty range was taken from the range in burdens from the models (assumed here to be a 2/3 uncertainty range) which may be a reasonable estimate for some of the "structural uncertainty" associated with different parametrization choices in the models (Pan *et al.*, 1997). It includes both "chemical" quantities such as the fraction of emitted SO_2 that is converted to sulphate aerosol and the mean residence time of the aerosol. The central emissions estimates are those specified in the model workshop (except where noted) and the uncertainties are those estimated in Section 5.2. The uncertainty range for the burden, M, used in evaluating the change in planetary albedo was calculated from the uncertainty in emissions together with the uncertainty in burden utilising the geometric concatenation procedure of Penner *et al.* (1994a).

The resulting overall uncertainty in the forcing by aerosols associated with fossil fuels and other industrial emissions is ± 0.42 Wm^{-2}; that is, if the global mean forcing is evaluated as –0.6 Wm^{-2} (the row value calculated by using the central values in the forcing equation), then the range of estimated global mean forcing is –0.1 to –1.0 Wm^{-2}. This range encompasses values for recent evaluations of the forcing for the individual components comprising the industrial aerosols (see Chapter 6). The main uncertainties are those for the upscatter fraction, the burden (which includes the propagated uncertainties in emissions), and the mass scattering efficiency, in that order. If the mode of mixing of black carbon were assumed to be external, instead of internal as used here, then the uncertainty range would be similar, but the central value for fossil fuel aerosols might be –0.7 Wm^{-2} instead of –0.6 Wm^{-2}.

The overall uncertainty in the forcing by biomass aerosols is ± 0.24 Wm^{-2}; thus, if the global mean forcing is –0.3 Wm^{-2}, then the 2/3 uncertainty range of estimated global mean forcing is –0.1 to –0.5 Wm^{-2}. The main uncertainties are the single scattering albedo, the upscatter fraction, and the burden.

Several assumptions are implicit in the above approach. First, there is a specific assumption concerning the determination of the single scattering albedo at 80% RH since most measure-

Table 5.10a: *Factors contributing to uncertainties in the estimates of the direct forcing by aerosols associated with fossil fuels and other industrial processes and their estimated range. Note that optical parameters are for a wavelength of 550 nm and are for dry aerosol.*

Quantity	Central Value	2/3 Uncertainty Range
Total emission of anthropogenic OC from fossil fuel burning (Tg/yr) [a]	20	10 to 30
Atmospheric burden of OC from fossil fuels (Tg)[b]	0.48	0.33 to 0.70
Total emission of anthropogenic BC from fossil fuel burning (Tg/yr)	7	4.67 to 10.5
Atmospheric burden of BC from fossil fuel burning (Tg)[b]	0.133	0.11 to 0.16
Total emission of anthropogenic sulfate from fossil fuel burning (Tg/yr)	69	57.5 to 82.8
Atmospheric burden of sulphate from fossil fuel burning (Tg S)	0.525	0.35 to 0.79
Fraction of light scattered into upward hemisphere, $\bar{\beta}$ [c]	0.23	0.17 to 0.29
Aerosol mass scattering efficiency (m^2g^{-1}), α_s^c	3.5	2.3 to 4.7
Aerosol single scattering albedo (dry), ω_0^c	0.92	0.85 to 0.97
T_a, atmospheric transmittance above aerosol layer [d]	0.87	0.72 to 1.00
Fractional increase in aerosol scattering efficiency due to hygroscopic growth at RH=80%	2.0	1.7 to 2.3
Fraction of Earth not covered by cloud [d]	0.39	0.35 to 0.43
Mean surface albedo[d]	0.15	0.08 to 0.22
Result: If central value is –0.6 Wm^{-2} the 2/3 uncertainty range is from –0.1 to –1.0 Wm^{-2}		

[a] The central value estimated here was taken from Table 5.3, while the value used in intercomparison was 29.

[b] The burden was estimated from the model intercomparison for total anthropogenic carbon taking the fraction associated with fossil fuels from the fraction of emissions associated with fossil fuels.

[c] The central estimate and uncertainty range were calculated from the size distribution for polluted continental aerosols in Table 5.1.

[d] Central estimate and uncertainty range adapted from values used by Penner *et al.* (1994a).

Table 5.10b: *Factors contributing to uncertainties in the estimates of the direct forcing by biomass burning aerosols and their estimated range. Note that optical parameters are for a wavelength of 550 nm and are for dry aerosol.*

Quantity	Central Value	2/3 Uncertainty Range
Total emission of anthropogenic OC from biomass burning (Tg/yr)	62.5	45 to 80
Atmospheric burden of OC from smoke (Tg)[a]	1.04	0.75 to 1.51
Total emission of anthropogenic BC from biomass burning (Tg/yr)	7	5.0 to 9.8
Atmospheric burden of BC from biomass burning (Tg)[a]	0.133	0.11 to 0.16
Fraction of light scattered into upward hemisphere, $\bar{\beta}$ [b]	0.23	0.17 to 0.29
Aerosol mass scattering efficiency (m^2g^{-1}), α_s^b	3.6	2.5 to 4.7
Aerosol single scattering albedo (dry), ω_0^b	0.89	0.83 to 0.95
T_a, atmospheric transmittance above aerosol layer [c]	0.87	0.72 to 1.00
Fractional increase in aerosol scattering efficiency due to hygroscopic growth at RH=80%	1.2	1.0 to 1.4
Fraction of Earth not covered by cloud [c]	0.39	0.35 to 0.43
Mean surface albedo[c]	0.15	0.08 to 0.22
Result: If central value is –0.3 Wm^{-2} the range is from –0.1 to –0.5 Wm^{-2}		

[a] The burden was estimated from the model intercomparison for total anthropogenic carbon taking the fraction associated with biomass aerosols from the fraction of emissions associated with biomass aerosols.

[b] The central estimate and uncertainty range were calculated from the size distribution for biomass regional haze in Table 5.1.

[c] Central estimate and uncertainty range adapted from values used by Penner *et al.* (1994a).

ments of this parameter are for low (dry) RH. Second, it was assumed that the specific aerosol absorption did not change with humidification while that of light scattering followed f(RH). While reasonable at this time, this issue needs further investigation. Another assumption implicit in the formula for planetary albedo change is that both absorption and scattering by aerosols are not significant compared to cloud effects when clouds are present. As Haywood and Ramaswamy (1998) have pointed out, this assumption is reasonable for scattering aerosols but not for strongly absorbing aerosols. The overall effect of including the effects of absorbing aerosols in the presence of clouds would be to reduce the net forcing relative to that calculated here. Turning to other issues, only second order terms were used in the Taylor expansion. While certainly valid for cases in which the uncertainties in the independent parameters do not exceed 20% of the central values, this neglect becomes somewhat problematic for larger uncertainties. Since there are several variables whose uncertainties are of the order of 50%, an assessment was made of possible underestimation of error by full functional evaluation, i.e., a population of values for the forcing function was generated from the population of the most uncertain variables (all other variables held constant) and the variance in the forcing function generated in this way compared with that derived from Taylor expansion. It was found that the error in variance propagation was second order (<10%) and has therefore been neglected here. Finally, there is an implicit assumption that all of the variables are normally distributed.

There are, of course, several sources of uncertainty that can not be evaluated using this approach. For example, uncertainties associated with the vertical distribution of the aerosol and with potential correlations between clouds and aerosol abundances are not evaluated. Furthermore, uncertainties associated with the radiative transfer treatment (which might be of order 20% (Boucher *et al.*, 1998)) are neglected. A further caveat is that the uncertainty estimates of Table 5.9 depend on the assumption that the data chosen for the size distribution are representative throughout those areas where these aerosol types contribute to forcing. Because we used observations from continental polluted regions for fossil fuel aerosols and from regional measurements for biomass aerosols, they may not encompass the full set of size distributions that may occur in regions outside of those where these measurements are valid.

5.4.3 Modelling the Indirect Effect of Aerosols on Global Climate Forcing

Published estimates of the indirect forcing by anthropogenic aerosols are summarised in Table 5.11. The results in Table 5.11a are for the assumption that changes in initial droplet concentrations do not lead to any changes in cloud properties. These results, therefore, did not include any feedbacks to liquid-water content or cloud amount as a result of changes to precipitation efficiency. The results in Table 5.11b include a calculation of the decrease in precipitation efficiency that results from an increase in N_d. Therefore, these results do include feedbacks to changes in liquid-water and cloud amount from changes in cloud microphysics.

The forcing calculations estimated from the models described by Boucher and Lohmann (1995), Jones and Slingo (1996), Feichter *et al.* (1997), Kiehl *et al.* (2000) and Rotstayn (1999) were performed as the difference between two simulations with fixed sea surface temperatures. These calculations, therefore, allow some feedback of the perturbation in the cloud albedo to both the dynamic fields and to water vapour and cloud amount. By definition, these GCM forcing estimates are therefore not strict radiative forcings, however, Rotstayn and Penner (2001) have shown that for the first indirect effect the inclusion of the feedback changes their forcing estimate by only about 10%. The other results are from chemical transport models/GCMs that do not include any feedbacks.

All models in Table 5.11a explicitly consider only sulphate, except those of Chuang *et al.* (1997, 2000) and Iversen *et al.* (2000). Five of the models in 5.11a use an empirical method to relate N_d to sulphate mass concentration, which implicitly includes some effect of other industrial aerosol components (e.g., OC), and their forcing estimates range from –0.4 to –1.8 Wm^{-2} with a median of –0.9 Wm^{-2}. Chuang *et al.* (2000) and Iversen *et al.* (2000) use mechanistic parametrizations to calculate N_d. Chuang *et al.* (2000) consider organic carbon, black carbon, sea salt and dust as well as sulphate. The estimate of indirect forcing from Chuang *et al.* (1997) is for sulphate only and that from Iversen *et al.* (2000) is for sulphate and BC. The range of the forcing estimates for industrial aerosols from the models using the mechanistic approaches for N_d (–0.82 to –1.36 Wm^{-2}) is similar to that of the empirical methods. The inclusion of forcing by biomass aerosols increases the total forcing to –1.85 Wm^{-2} in the model of Chuang *et al.* (2000).

The estimates of indirect forcing that include feedback to the liquid-water path and cloud amount from changes in cloud microphysics and precipitation efficiency range from –1.1 Wm^{-2} to –4.8 Wm^{-2} (Table 5.11b). Due to the nature of the calculation, these are not strict estimates of radiative forcing, but as noted above, Rotstayn and Penner (2001) have shown that the feedback effects are probably not significant so that these may be viewed as estimates of forcing. The largest absolute value, that obtained by Lohmann and Feichter (1997) using the Xu and Randall and the Beheng parametrization schemes, is considered less realistic because the comparison of the short- and long-wave cloud radiative fluxes with those from the Earth Radiation Budget Experiment (ERBE) was relatively poor. The next highest value (–3.2 Wm^{-2} from Ghan *et al.*, 2001b) was obtained with a model using a very simple cloud cover parametrization (full coverage if saturated and no coverage if unsaturated). Thus, based on the present modelling, a more likely range for the combination of the first and second indirect effects is –1.1 to –2.2 Wm^{-2}. However, this range only includes one model estimate for the effects of aerosols from biomass burning as well as industrial aerosols (i.e. –1.1 to –1.9 from Lohmann *et al.*, 2000) and the assessment of carbon aerosol forcing from this model (–0.9 Wm^{-2}) is less than that for carbon aerosols from the first indirect effect from the Chuang *et al.* (2000a) model in Table 5.11a (i.e. –1.51 Wm^{-2}). In view of this, the range of forcing estimates for the combination of first and second indirect effects is –1.1 to –3.7 Wm^{-2}. Clearly, the

uncertainty is relatively large, and considerable effort will be required to improve indirect forcing estimates.

A few of the factors that may contribute to this uncertainty are:

- The pre-industrial sulphate used in these studies varies by a factor of just over two, and the anthropogenic indirect forcing is calculated from the difference between the pre-industrial and industrial scenarios. Considering the non-linearities in the parametrizations of N_d, the pre-industrial sulphate concentration can be a significant factor.
- The variance in the industrial sulphate concentrations is about 50%.
- The parametrizations or methods of relating droplet number concentrations to aerosol concentrations have been discussed in Section 5.3.4. Using Figure 5.7, we can estimate the range of uncertainty attached to simply the differences in the parametrizations shown in the figure. For stratiform cloud, assuming a mean sulphate concentration of 0.5 $\mu g\ m^{-3}$ over the oceans and 2.0 $\mu g\ m^{-3}$ over the land, the differences among the parametrizations in Figure 5.7 amount to about 30%. Neglecting that there is a serious question about the ability of the empirical methods to represent the global aerosol, this is a reasonable approximation based on current knowledge. As a couple of footnotes, Rotstayn (1999) compared the forcings using the Boucher and Lohmann (1995) parametrization with a similar parametrization from Roelofs *et al.* (1998), and found the result with the Roelofs *et al.* method was 25% higher. And the relatively close agreement of the Boucher and Lohmann (1995) method with the prognostic method (Figure 5.7) has also been seen in the simulated results from MIRAGE model (Ghan *et al.*, 2001a).
- Changes in the vertical distribution of the aerosol will affect the indirect forcing because of changes in its spatial relationship to cloud. Rotstayn (1999) found a 24% change in the radiative forcing depending on whether the aerosol concentration decreased exponentially or was uniform with height through the lower 10 km. Jones and Slingo (1996) distributed the aerosol mass uniformly, half in the lower 2 km, and half above, compared with Jones *et al.* (1994b) who confined half the aerosol mass to the lower 1.5 km. Jones and Slingo (1996) obtained an indirect forcing 15% higher than Jones *et al.* (1994b).

It is important to draw attention to some other factors concerning the comparison of the forcing estimates from the various models.

- Boucher and Lohmann (1995) found very little difference between the LMD (French) and ECHAM (German) models. Jones and Slingo (1996) found that the Hadley (UK Met Office) model produced a lower forcing in the Northern Hemisphere relative to the Boucher and Lohmann results, however, this may have been due to differences in the distribution of sulphate mass as well as the GCM.
- The effect of horizontal resolution of the GCM was considered by Ghan *et al.* (2001b). They found an increase in the indirect forcing of about 40% when the horizontal resolution was degraded from 2.8°×2.8° to 4.5°×7.5°.
- There have been no studies that have explicitly considered the effect of the cloud cover parametrization on the first indirect effect alone. Lohmann and Feichter (1997) examined the effect of two different cloud cover parametrizations (Sundquist *et al.*, 1989 and Xu and Randall, 1996) on the combined first and second indirect effects, which gave a difference of more than a factor of 3 in the indirect forcing. Indeed, the effect of uncertainties in the GCM predictions of cloud cover (which are known to be inaccurate) is not known.
- The autoconversion parametrization is a critical step in the simulation of the second indirect effect. Lohmann and Feichter (1997) compared two such parametrizations and found a difference in the total indirect forcing of a factor of two. Ghan *et al.* (2001b) compared two other methods for autoconversion and found a difference of about 30%. Rotstayn (1999) performed a sensitivity experiment in which the droplet size threshold for autoconversion was increased. This resulted in a reduction of the second indirect effect, but there was a slightly compensating increase in the first indirect effect. This is an area of high sensitivity and uncertainty.

5.4.4 Model Validation of Indirect Effects

Validation of the simulations from global models is an essential component of estimating and reducing the uncertainties in the indirect forcing. Comparisons of observations and modelled concentrations of chemical species have been discussed in Section 5.4.1.3 while comparisons of modelled and satellite-derived aerosol optical depths were discussed in Section 5.4.1.4. Here, comparisons with observations of several other model products important for indirect forcing are examined. Unfortunately, there is only a very small set of observations of the physical, chemical, and radiative properties of clouds from *in situ* methods available. Thus, validations with these types of datasets are left to limited temporal and spatial scales and to comparing relationships among various quantities. Lohmann *et al.* (2001), for example, compared prognostic simulations with observations of the relationships between particulate sulphate and total particle mass, between particle number concentration and sulphate mass, and between N_d and sulphate mass. The relationships between sulphate mass and total particle number concentrations was larger than observations in the case of internal mixtures but was smaller than observations in the case of external mixtures. Ghan *et al.* (2001a) found that the results of their determination of N_d using their mechanistic parametrization were comparable to the results using the empirical parametrization of Boucher and Lohmann (1995). Such tests are important for large-scale model parametrizations because comparisons of absolute concentrations on the scale of the model grid size are difficult.

Satellites offer observations over large temporal and spatial scales; however, for the derived parameters of interest, they are much less accurate than *in situ* observations. Han *et al.* (1994) retrieved an r_{eff} for liquid-water clouds from ISCCP satellite data that showed a significant land/sea contrast. Smaller droplets were found over the continents, and there was a systematic difference between the two Hemispheres with larger droplets in the Southern Hemisphere clouds. The r_{eff} calculated by different models and the observations from Han *et al.* are shown in Table 5.12. Since the r_{eff} tends to increase with increasing height above

Table 5.11a: *Comparison of model-predicted indirect forcing without cloud amount and liquid-water path feedback.*

Model	Pre-industrial aerosol (Tg)	Industrial aerosol (Tg)	N_d parametrization	Cloud cover parametrization	Forcing (Wm^{-2})
B&L (1995)	0.34 Tg S	Sulphate: 0.44 Tg S	Various empirical results	Le Treut and Li (1991); Roeckner *et al.* (1991)	–0.5 to –1.4; –0.5 to –1.5
Jones and Slingo (1996)	0.16 Tg S	Sulphate: 0.3 Tg S	Jones *et al*. (1994b); Hegg (1994); B&L (1995)	Smith (1990)	–1.5; –0.5; –0.6
Chuang *et al.* (1997)	Sulphate: 0.25 Tg S, Carbon aerosols: 1.72 Tg	Sulphate: 0.30 Tg S	Chuang and Penner (1995)	NCAR-CCM1	–0.62 to –1.24 (internal mix); –1.64 (external mix)
Feichter *et al.* (1997)	Sulphate 0.3 Tg S	Sulphate: 0.38 Tg	B&L (1995)	Sundqvist *et al.* (1989)	–0.76
Lohmann and Feichter (1997)			B&L (1995)	Sundqvist *et al.* (1989)	–1.0
Chuang *et al.* (2000)	Sea salt: 0.79Tg, Dust: 4.93 Tg, Sulphate: 0.25 TgS, Organic matter: 0.12 Tg	Sulphate: 0.30 TgS, Organic matter: 1.4 Tg BC: 0.19 Tg	Chuang and Penner (1995)		−1.85 (all aerosols) −1.51 (all carbon aerosols) −1.16 (biomass aerosols only); − 0.30 (sulphate only)
Kiehl *et al.* (2000)			Martin *et al.* (1994); Martin *et al*. (1994) with N_d minima; Jones *et al.* (1994b); B&L (1995)	Rasch and Kristjansson (1998)	−0.68; −0.40; −0.80; −1.78
Rotstayn (1999)	Sulphate: 0.21 TgS	Sulphate: 0.30 TgS	B&L (1995); Roelofs *et al.* (1998)	Smith, (1990)	−1.2; –1.7
Iversen *et al.* (2000)	Sulphate: 0.14 TgS, BC: 0.01 TgC, Sea salt and dust included, but not quantified	Sulphate: 0.60 TgS, BC: 0.25 TgC	Similar to Chuang and Penner (1995)	Rasch and Kristjansson (1998)	–1.36

cloud base and the satellite observations of r_{eff} are weighted for cloud top, the satellite observations will tend to overestimate the overall r_{eff} compared with that determined from *in situ* studies. *In situ* data sets against which to make absolute comparisons are few in number (e.g. Boers and Kummel, 1998). However, for now model evaluations are better done using the contrasts in r_{eff} between the land and ocean and between the Southern Hemisphere and the Northern Hemisphere. Most of the models listed in Table 5.12, with the exception of Roelofs *et al.* (1998), approximate the difference between r_{eff} over the Southern Hemisphere ocean vs the Northern Hemisphere ocean. Over land, the Southern Hemisphere *vs* Northern Hemisphere difference from Roelofs *et al.* (1998) is closest to the observed difference. For r_{eff} over Southern Hemisphere land vs Southern Hemisphere ocean, several models are relatively close to the difference from the observations (Boucher and Lohmann, 1995; Chuang *et al.*, 1997; Roelofs *et al.*, 1998; Lohmann *et al.*, 1999b,c). Some models compare with observations better than others, but there is no model that is able to reproduce all the observed differences. The r_{eff} calculated with the same parametrization but using different GCM meteorologies are quite different (compare Jones and Slingo (1996) vs Boucher and Lohmann (1995)). As noted above, Jones and Slingo determined the "cloud top" r_{eff} by assuming a LWC profile that increased with height from cloud base to cloud top. Such a profile is more similar to observed profiles and might be expected to produce a better comparison with the observations. While the Jones and Slingo (1996) model does reasonably well in terms of hemispheric contrasts, their results indicate a land-ocean contrast in the opposite direction to that from the other models and the observations. We note that many factors may affect the results of this type of comparison. For example, Roelofs *et al.* (1998) estimate the sensitivity of the r_{eff} calculations to uncertainties in the sulphate concentration field, cloud cover and cloud liquid-water content to be of the order of a few micrometres. Moreover, the satellite determination of r_{eff} is probably no more accurate than a few micrometres (Han *et al.*, 1994).

Column mean N_d has been retrieved from satellite observations (Han *et al.*, 1998a), and this offers another validation

***Table 5.11b**: Comparison of indirect forcing by different models with cloud amount and liquid-water path feedback.*

Model	Pre-industrial aerosol (Tg)	Industrial aerosol (Tg)	Nucleation parametrization	Cloud cover; autoconversion parametrization	Forcing (Wm^{-2})
Lohmann and Feichter (1997)	Sulphate: 0.3 TgS (interactive)	Sulphate: 0.38 Tg S (interactive)	Boucher and Lohmann (1995)	Sundqvist *et al.* (1989); Beheng (1994)	–1.4
Lohmann and Feichter (1997)	Sulphate: 0.3 TgS (interactive)	Sulphate: 0.38 Tg S (interactive)	Boucher and Lohmann (1995)	Xu and Randall (1996); Berry (1967)	–2.2
Lohmann and Feichter (1997)	Sulphate: 0.3 TgS (interactive)	Sulphate: 0.38 Tg S (interactive)	Boucher and Lohmann (1995)	Xu and Randall (1996); Beheng (1994)	–4.8
Lohmann *et al*., (2000a)	Monthly average Sea salt: 0.79 Tg Monthly average Dust: 5.23 Tg Interactive Organic matter: 0.12 Tg Interactive sulfate	Total interactive sulphate: 1.04 Tg Interactive organic matter:1.69 Tg (tot) Interactive black carbon: 0.24 Tg	Chuang and Penner (1995)	Sundqvist *et al.* (1989); Beheng (1994)	Total forcing: –1.1 to –1.9 Carbon only: –0.9 Sulfate only: –0.4
Rotstayn (1999)	Monthly average Sulphate: 0.21 Tg S	Monthly average sulphate: 0.30 Tg S	Boucher and Lohmann (1995); Roelofs *et al.* (1998)	Cloud cover; Smith (1990)	–2.1; –3.2
Iversen *et al.,* (2000)	Sulphatee: 0.14 TgS, BC: 0.01 TgC, Sea salt and dust included, but not quantified	Sulphate: 0.60 TgS, BC: 0.25 TgC	Similar to Chuang and Penner (1995)	Rasch and Kristjansson (1998)	–1.9
Ghan *et al.,* (2001b)	Sulphate: 0.42 TgS, OC: 1.35 Tg, BC: 0.22 Tg, Sea salt: 4.3 Tg, Dust: 4.3 Tg	Sulphate: 0.68 TgS	Abdul-Razzak and Ghan (2000)	0 if unsaturated, 1 if saturated; Ziegler (1985)	–1.7 Sulphate; (2.8 °×2.8 °)
Ghan *et al.*, (2001b)	Sulphate: 0.39 TgS, OC: 1.14 Tg, BC: 0.18 Tg, Sea salt: 3.8 Tg, Dust: 4.6 Tg	Sulphate: 0.58 TgS	Abdul-Razzak and Ghan (2000)	0 or 1; Ziegler (1985)	–2.4 (4.5 °×7.5 °)
Ghan *et al.,* (2001b)	As above	As above	Abdul-Razzak and Ghan (2000)	0 or 1; modified Tripoli and Cotton (1980)	–3.2 (4.5 °×7.5 °)

parameter over the global scale, but the derivation of r_{eff} is implicit in the determination of the column N_d. Because of the inverse relationship between r_{eff} and N_d for a given optical depth, the column N_d will be lower than *in situ* observations, since r_{eff} is higher than *in situ* observations (Han *et al.*, 1998a). Lohmann *et al.* (1999b,c) were able to simulate the general pattern of column N_d found by Han *et al.*, but their absolute values were higher.

As discussed in Section 5.3.2, Han *et al.* (1998b) found an increase in cloud albedo with decreasing droplet size for all optically thick clouds (τ_c>15) and optically thin clouds (τ_c<15) over land. Such an observation is consistent with expectations associated with the first indirect effect. However, for optically thinner clouds over marine locations, they found that the albedo decreased with decreasing droplet size, which might seem to be in conflict with an indirect effect. Using the ECHAM GCM, Lohmann *et al.* (1999b,c), were able to simulate the observed pattern for optically thick clouds. In addition, optically thin clouds over the oceans conformed to the observations. The ability of this model, which predicts an indirect effect (Table 5.11b; Lohmann *et al.*, 2000), to reproduce this satellite observation shows that this observation does not necessarily negate the indirect effect. The reasons for optically thin clouds to display a reduction in albedo with decreasing r_{eff} have not been elucidated (LWP was found to increase with increasing r_{eff} for all water clouds), and this is a reminder that interpretations must be considered carefully.

Table 5.12: Cloud droplet effective radius of warm clouds (in μm).

All results for 45°S to 45°N	Ocean Southern Hemisphere	Ocean Northern Hemisphere	Land Southern Hemisphere	Land Northern Hemisphere	Total
Han *et al.* (1994)	11.9	11.1	9.0	7.4	10.7
Boucher and Lohmann (1995)	8.9 to 10.1	8.3 to 9.3	5.4 to 8.7	4.9 to 8.0	
Jones and Slingo (1996)	9.6 to 10.8	9.0 to 10.4	10.2 to 11.8	9.9 to 10.8	9.5 to 11.1
Roelofs *et al.* (1998)	12.2	10.3	8.8	6.9	10.4
Chuang *et al.* (1997)	11.6 to 12.0	10.7 to 11.4	8.8 to 9.1	8.6 to 9.0	10.7 to 11.2
Lohmann *et al.* (1999b,c)	10.7	10.2	8.3	4.9	
Rotstayn (1999)	11.2	10.9	9.8	9.5	10.7
Ghan *et al.* (2001a,b)					11.0 to 11.7

Nakajima *et al.* (2001) examined the variation of cloud albedo, droplet concentration, and effective radius with column aerosol concentration. They found that the cloud droplet column concentration increased while r_{eff} decreased over a range of values of column aerosol number concentration. They did not find a significant increase in liquid-water path as aerosol number concentration increased. This observation may indicate that the 2nd indirect effect is not important on a global scale, however, further work is needed to confirm this.

5.4.5 Assessment of the Uncertainty in Indirect Forcing of the First Kind

Estimation of the uncertainty in the complete (i.e. the first and second indirect effects) radiative forcing is not currently feasible due to a lack of analytical relationships to treat the indirect forcing of the second kind. However, the indirect forcing of the first kind can be treated if we adopt a simple box-model approach such as those used in early assessments of indirect forcing (e.g., Charlson *et al.*, 1992; Schwartz and Slingo, 1996).This evaluation of uncertainty is only illustrative both because of the box-model nature of the estimate and because our assessment of the uncertainty in the parameters is only first order. Nevertheless, it is useful to make such calculations since they can yield valuable information both on our current state of knowledge with regard to the indirect forcing and can help guide efforts to reduce uncertainty. Moreover they illustrate a rigorous method that could allow a more quantitative estimate of uncertainty than the methods followed in Chapter 6.

We adopt a functional relationship between sulphate concentrations and cloud droplet number concentration based on empirical relationships in order to render the calculations more tractable. Therefore, this analysis is only applicable to the Northern Hemisphere, since data from this region were used to derive the empirical relationship. The analysis is further restricted to the marine atmosphere and excludes any consideration of indirect forcing by biomass aerosols.

The indirect forcing of the first kind (hereafter called simply the indirect forcing) can be expressed as:

$$\Delta F = F_d T_a^2 f_c \Delta A_p \qquad (1)$$

where F_d is the average downward flux at the top of the atmosphere, T_a is the atmospheric transmission above the cloud layer, f_c is the fractional cloud cover of those clouds susceptible to aerosol modulation and ΔA_p is the change in planetary albedo (equivalent here to the above cloud albedo) associated with an increase in the cloud droplet number concentration (CDNC). To take into account multiple reflections between the cloud layer and the surface, the expression of Liou (1980) is used with an assumption of no absorption within the cloud. This assumption is very reasonable for the bulk of the incoming radiation which will be scattered by cloud drops, i.e., subject to the indirect effect, but does restrict the radiation band to a range from 0.3 to 0.7 μm. Thus:

$$A_p = A_c + R_s\left[(1-A_c)^2/(1-R_s A_c)\right] \qquad (2)$$

where A_c is the cloud albedo and R_s is the albedo of the underlying surface. ΔA_p is then calculated as the difference between this function evaluated for A_c, the background cloud albedo, and A_c', the anthropogenically perturbed albedo (note that "primed" quantities will always refer to anthropogenically perturbed values of the quantity). Cloud albedo is, in turn, evaluated using the relationship:

$$A_c = \tau_c/(\tau_c + 7.7) \qquad (3)$$

which is an approximation of the two stream evaluation of cloud albedo for conservative scattering assuming an asymmetry parameter of 0.85 (Lacis and Hansen, 1974). Here, τ_c is the cloud optical depth, given by the expression of Twomey (1977):

$$\tau_c = h\,(9\pi LWC^2 N_d/2\rho^2)^{1/3} \qquad (4)$$

where h is the cloud layer thickness, LWC is the layer mean liquid-water content, N_d is the CDNC, and ρ is the density of water. To relate the CDNC to anthropogenic emissions, we use the empirical expression of Boucher and Lohmann (1995) which has the form:

$$N_d = A(SO_4^{2-})^B \qquad (5)$$

where SO_4^{2-} is the mean concentration of sulphate aerosol at cloud base in μg m^{-3}, and A and B are empirical constants. We adopt the values of A=115 and B=0.48 which are appropriate for marine air (Boucher and Lohmann, 1995).

Using the same procedures as with the assessment of uncertainties in the direct forcing (e.g. Section 5.4.2), we first

determine the uncertainties in the most fundamental parameters. We then use Taylor expansions of the various equations given above to determine the uncertainty in the forcing associated with the central values of the parameters used in the calculations. Thus the uncertainty involves the uncertainties in the concentration of SO_4^{2-} and in the empirical coefficients used to relate the concentration of SO_4^{2-} to N_d. Moreover, the calculation of uncertainty necessarily involves an evaluation of A_c for both the background and anthropogenically perturbed values. These quantities, together with corresponding values for LWC and h, which are based on available observations, are then used to generate uncertainties in the cloud optical depth. This hierarchical evaluation proceeds "upward" from the uncertainty in the primary variables until the uncertainty in the forcing itself, together with the associated central value can be assessed. Such an uncertainty estimate is different in philosophy from that used in Chapter 6 which only assesses the range of estimates in the literature.

Several issues arise that deserve some discussion. The first such issue is the concatenation of uncertainties in the empirical relationship between the concentration of SO_4^{2-} and N_d. The uncertainty in SO_4^{2-} is straightforward and is based on the assessment of uncertainty in burden and the uncertainty in emissions as used in Section 5.4.2. The uncertainty in the relationship between SO_4^{2-} and $N_{d,}$ equation (3), requires an evaluation of the uncertainties in the coefficients A and B. Based on a comparison of the parametrization of Boucher and Lohmann (1995) with that of Jones *et al.* (1994b) (Figure 5.7), we assign an *ad hoc* contribution of the functional relationship to the uncertainty in N_d of 40% of the central value. We then further assume that the uncertainties in A and B contribute equally to the total uncertainty (i.e., 40%) and, with these constraints, derived the uncertainties in A and B. This allows us to use Taylor expansions for both the perturbed and unperturbed atmosphere. Due largely to the form of the functional relationship, this procedure yields uncertainties whose major components in both the perturbed and unperturbed cases are attributable to the uncertainty in the parametrization (61% for the unperturbed case and 64% for the perturbed case) rather than the uncertainty in burden or emissions.

In order to assess the overall uncertainty in forcing, the covariance between the base parameters N_d, LWC and h must be evaluated. But both LWC and h are assumed to be constant in the first indirect effect, and therefore the covariance is assumed to be zero. Certainly, the limited observations available (cf., Hegg *et al.*, 1996b) do not show any covariance. Nevertheless, it is important to note this potential effect and the possible impact of the second indirect effect (precipitation modulation effects by aerosols) on the uncertainty in the first.

Another covariance which cannot be neglected arises in the evaluation of the uncertainty in ΔA_p from the possible covariance between A_c and A_c'. This covariance arises because of the dependence of the perturbation in cloud albedo on both the unperturbed aerosol concentration and the unperturbed albedo. We assessed this covariance by using equations (4) and (3) to generate a set of corresponding values of the perturbed and unperturbed albedos for different values of N_d. Then a linear fit to the parameters ΔN_d and A_c' was used to derive the correlation coefficient and then the covariance. Various sample sizes and incremental values of the aerosol perturbation were generated to test the stability of the correlation. This procedure resulted in a stable correlation coefficient between A_c and A_c' of 0.74.

A final issue arises as to the choice of susceptible cloud fraction (f_c) in the basic forcing equation. Here, we follow the analysis of Charlson *et al.* (1987) and use the estimates in the cloud atlas of Warren *et al.* (1988). The total fractional cover of low and mid level clouds is not used since mid-level clouds can be mixed phase and the relationship of these clouds to anthropogenic aerosol is still unclear (Section 5.3.6). Instead, we use the estimates of Charlson *et al.* (1987) for non-overlapped low marine cloud as a lower bound (2/3 bound) for the susceptible cloud fraction and the sum (correcting for overlap) of the low and

Table 5.13: *Factors contributing to uncertainties in the estimates of the first indirect forcing over Northern Hemisphere marine locations by aerosols associated with fossil fuels and other industrial processes and their estimated range.*

Quantity	**Central Value**	**2/3 Uncertainty Range**
Background N_d for Northern Hemisphere marine locations (cm^{-3})	140	66 to 214
Perturbed N_d for Northern Hemisphere marine location (cm^{-3})	217	124 to 310
Cloud mean liquid-water content (LWC) ($g\ m^{-3}$)	0.225	0.125 to 0.325
Background sulphate concentration ($\mu g\ m^{-3}$)[a]	1.5	0.85 to 2.15
Cloud layer thickness (m)	200	100 to 300
Perturbed sulphate concentration ($\mu g\ m^{-3}$)[b]	3.6	2.4 to 4.8
Susceptible cloud fraction, f_c	0.24	0.19 to 0.29
Atmospheric transmission above cloud layer, T_a	0.92	0.78 to 1.00
Mean surface albedo	0.06	0.03 to 0.09
Result: If central value is $-1.4\ Wm^{-2}$ the 2/3 uncertainty range is from 0 to $-2.8\ Wm^{-2}$		

[a] Calculated from a central value for the Northern Hemisphere marine burden of 0.12 TgS with an uncertainty range from 0.07 to 0.17 TgS. The central estimate for sulphur emissions in the Northern Hemisphere was 12 TgS/yr with an uncertainty range from 9 to 17 TgS/yr.

[b] Calculated from a central value for the Northern Hemisphere marine perturbed burden of 0.28 TgS with an uncertainty range from 0.15 to 0.41 TgS. The central value for the Northern Hemisphere emissions of natural and anthropogenic sulphur was 74 TgS/yr with a 2/3 uncertainty range of 57 to 91 Tg S/yr.

middle marine stratiform cloud as an upper limit for f_c. The central value is taken as midway between these extremes.

The above assumptions, together with the parameter values given in Table 5.13, yield a central value for the indirect forcing over marine areas of -1.4 Wm^{-2} together with an uncertainty of ± 1.4 Wm^{-2}. Hence, the forcing lies in the range between zero and -2.8 Wm^{-2}. This range is in reasonable agreement with that given in Chapter 6, based on GCM assessments. Nearly all of the uncertainty in the forcing is associated with that in the planetary albedo which, in turn, is dominated by the uncertainties in the perturbed and unperturbed cloud albedos, and thus in the cloud optical depths. However, it is interesting to note that most of the uncertainty in the optical depths for both perturbed and unperturbed clouds arises from the uncertainties in the cloud LWC and cloud thickness, and not from the uncertainties in the CDNC. This is not actually particularly surprising and is simply due to the stronger functional dependence of the optical depth on the LWC and thickness, h. This allocation of uncertainty may be slightly misleading because the 1st indirect effect depends on an assumption of fixed h and LWC. Yet here we are concerned with evaluating both the central estimate as well as its uncertainty. Hence, knowledge of h and LWC are needed. Indeed, consideration of these parameters and the accuracy of their representation in GCMs must certainly contribute to any uncertainty in the estimates of forcing from GCMs. Thus, it seems clear that progress in reducing the uncertainty in the indirect forcing of the first kind will be at least as dependent on acquiring better data on cloud LWC and thickness as on better quantifying anthropogenic aerosol concentrations and their effects on N_d. At a somewhat lower priority, it is clearly quite important to better understand the relationship between cloud drop number concentration and sulphate concentration. The total uncertainty is clearly dependent on this relationship. If it were significantly different in form, a somewhat different order of contribution to total uncertainty might have arisen. On the other hand, the uncertainty in the magnitude of the emissions of sulphur gases as well as the uncertainty in the burden of sulphate played only a minor role in the determination of the overall uncertainty.

5.5 Aerosol Effects in Future Scenarios

5.5.1 Introduction

Aerosol concentrations and forcing will change in the future, both as a result of changing emissions and as a result of changing climate. The uncertainties associated with our knowledge of the present day distribution of aerosols noted in previous sections will carry over into uncertainties in analysis of future scenarios. Nonetheless, models are the best available tool for making an assessment of what changes might follow. To estimate these future changes, we specified a set of emissions for the IPCC model intercomparison workshop (Section 5.4.1) based on the draft scenarios developed for the IPCC Special Report on Emissions Scenarios (SRES) (Nakićenović *et al.*, 2000). The results from the workshop form the basis of the future aerosol forcing reported in Chapter 6 and contribute to the climate change scenarios reported in Chapter 9.

Separate estimates for the amount of biomass-burning activity were not available for the SRES scenarios (though growth in biomass burning was included in the SRES analysis). Also, estimates of emissions of organic carbon and black carbon aerosols from fossil fuels and industrial activity were not available. Therefore, these were constructed using the ratio of source strengths for CO in 2030 and 2100 to that in 2000, respectively. This ratio was then used to scale the emissions for organic carbon and black carbon from fossil fuel and biomass burning. Because the scenarios do not provide a breakdown of emissions for CO by source category, this scaling implicitly assumes that as a given region develops, the ratio of emissions of CO by biomass burning and by fossil fuel burning remains roughly constant. We note that our projected carbon particle emissions may be too large if countries choose to target particle emissions for reduction to a greater extent than they target emissions of CO.

In addition to the emissions of carbon particles, we constructed emissions for NH_3 in order to examine possible changes in the emissions of NH_3 and HNO_3 to aerosol abundance and forcing. Only the A2 scenario in 2100 was considered. For this simulation, the growth in anthropogenic NH_3 emissions was assumed to follow the growth in anthropogenic N_2O emissions. Anthropogenic emissions grew from 46.9 TgN/yr in 2000 to 111.5 TgN/yr in 2100. The anthropogenic NO_x emissions were 39.5 TgN/yr in 2000 and grew to 109.7 TgN/yr in 2100.

The emissions for 2030 and 2100 from the draft A2 and B1 scenarios that were considered in the IPCC workshop are shown in Table 5.7 (see the Appendix to this volume for the final SRES emissions). As noted there, SO_2 emissions in 2030 are about a factor of 1.6 higher than those in 2000 in the draft A2 scenario, but decrease thereafter to global average levels that are less than the present-day estimates in 2100. Carbon aerosol emissions grow by a factor of 1.3 in 2030 in the A2 scenario and continue to grow to 2100 by an additional factor of 1.8. In the B1 scenario, both SO_2 and carbon aerosol emissions are controlled by 2100, falling by 60 and 3%, respectively, compared to 2000. For comparison, the table also shows emissions for the IS92a scenario, with carbon aerosol emissions constructed as above for the SRES scenarios. In the IS92a scenario, growth continues throughout the time period for both SO_2 and carbon emissions: SO_2 and CO emissions are a factor of 1.8 and 1.6 larger in 2100, respectively, than the same emissions in 2000.

5.5.2 Climate Change and Natural Aerosol Emissions

Aerosols that originate from natural emissions may also be expected to change in future scenarios. For example, terpene emissions depend on temperature, precipitation and light levels, and sea salt emissions depend on wind speed and temperature. DMS emissions depend on wind speed and temperature, and dust emissions depend on soil moisture and wind speed. Changes to natural emissions associated with changes to these factors were considered in scenarios SC5 and SC8.

To construct future changes in natural emissions, the NCAR CSM simulations (Dai *et al.*, 2001) were used to estimate possible changes in climate. This climate simulation was one formulated to treat a "business as usual" (IS92a) scenario and

resulted in a global average surface temperature change for the decade prior to 2100 relative to that for the decade prior to 2000 of 1.76°K. While methods are available to estimate the effect of changes in climate on natural emissions, given current vegetation cover, tools to define the impact of future changes in land use and land cover on spatially disagreggated emissions are not well developed. Thus, even though changes in land use would be expected to affect vegetation cover and this is responsible for emissions of terpenes and determines which areas are subject to dust uplift, these effects could not be included. Furthermore, the understanding of how phytoplankton populations that produce DMS may change with changes in climate is poor. Therefore, in the following, only the effects of changes in temperature, precipitation, light levels, and wind speeds on future emissions were considered. The changes in wind speed were estimated from the ratio of monthly average wind speeds for the years 2090 to 2100 to that for the years 1990 to 2000 associated with the IS92a scenario (Dai *et al.*, 2001). This ratio was used to adjust the wind speeds that were used to generate current (2000) emissions to obtain future (2100) emissions of both DMS and dust. This method gives only a first-order estimate of possible changes, since it assumes that the distribution of wind speeds within a month remains constant with time. For wind speeds associated with sea salt, a somewhat different method was used (see below). The terpene fluxes were estimated directly from the daily data that were projected by the CSM simulation for 2100.

5.5.2.1 Projection of DMS emissions in 2100

Emissions of DMS were projected using the procedures described in Kettle *et al.* (1999). Since the atmospheric concentration of DMS is negligible in relation to what it would be if the atmospheric and oceanic concentrations were in equilibrium, the DMS flux is assumed to depend only on the sea surface concentrations and the wind speed. The projected DMS flux (as well as that for 2000) used the average of the parametrizations of Liss and Merlivat (1986) and Wanninkhof (1992). A correction of the piston velocity for sea surface temperature was made using the Schmidt number dependence of Saltzman *et al.* (1993).

The DMS flux for 2000 was calculated from the monthly average sea surface temperature data of Levitus and Boyer (1994) and the sea surface DMS concentration data of Kettle *et al.* (1999). In addition, climatological wind speeds from Trenberth *et al.* (1989) and climatological sea ice cover fields from Chapman and Walsh (1993) were used. The global flux for the year 2100 was calculated as the product of this initial field and the ratio of the piston velocity field in 2100 to that in 2000 using the sea surface temperature and wind speed information from the NCAR CSM.

There are several possible sources of error in these calculations. The most serious assumption is that the DMS concentration fields do not change between the years 2000 to 2100. DMS is produced as part of phytoplankton bloom cycles, especially in high latitude areas. It is likely that the mean distribution of phytoplankton blooms in the upper ocean would change between 2000 and 2100 given any perturbation of the sea surface temperature, wind speed, and sunlight. The other major assumption is that the monthly climatological ice cover does not change between 2000 and 2100. Ice acts as a lid on the ocean in upper latitudes through which DMS cannot pass.

Overall, the calculations suggest a small increase in global DMS flux between the year 2000 (with a global DMS flux of 26.0 TgS/yr) and the year 2100 (with a global DMS flux of 27.7 TgS/yr). The most noticeable features in the 2100 fields are the predicted increases in DMS fluxes in some areas of the North Atlantic, North Pacific, and some areas of the Southern Ocean immediately adjacent to the Antarctic continent. There are some localised increases predicted in the tropical and sub-tropical Pacific Ocean.

5.5.2.2 Projection of VOC emissions in 2100

Emissions of isoprene, monoterpenes, and other VOC were calculated using the GLOBEIS model (Guenther *et al.,* 1999) which estimates biogenic VOC emissions as a function of foliar density, an emission capacity (the emission at specified environmental conditions), and an emission activity factor that accounts for variations due to environmental conditions. The foliar densities, emission capacities, and algorithms used to determine emissions activities for both 2000 and 2100 are the same as those described by Guenther *et al.* (1995). One difference between this work and that of Guenther *et al.* (1995) is that here we used hourly temperatures for each hour of a month to determine the monthly average emission rate whereas Guenther *et al.* (1995) used monthly average temperatures to drive emission algorithms. This results in about a 20% increase in isoprene emissions in 2000 and 10% increase in emissions of other biogenic VOC.

Global annual emissions of monoterpenes for 2000 were 146 Tg (compared to the estimate of 127 Tg in Guenther *et al.* (1995) which was used for the workshop 2000 emissions). These increase by 23% for 2100 relative to the 2000 scenario. The changes are much higher at certain seasons and locations. The spatial distribution of changes in total monoterpene emissions range from a 17% decrease to a 200% increase.

The simple model used for this analysis does not consider a number of other factors that could significantly influence long-term trends in biogenic VOC emissions. For example, we did not consider changes in soil moisture which could significantly impact emission rates. In addition, we did not consider changes in future concentrations of OH, O_3, and NO_3 in determining the yield of aerosol products. Instead, a constant yield of 11% of the terpene emissions was assumed for all future emissions.

5.5.2.3 Projection of dust emissions in 2100

The meteorological variables used to compute the dust emission for 2000 corresponded to those computed for daily meteorological data from the Data Assimilation Office analysis for 1990 (the GEOS-1 DAS, see Schubert *et al.*, 1993) using algorithms outlined by P. Ginoux. For this computation, the total dust flux was scaled to yield a total emission of about 2000 Tg/yr. Emissions in four size categories were specified (diameter 0.2 to 12.0 μm).

In order to calculate dust flux in 2100, the monthly mean variables were computed by averaging the wind speed at the lowest level (100 m) and the soil moisture content over the ten years ending in 1999 and 2099. The fluxes for the 21st century were calculated using the same meteorological variables, corresponding

to 1990, scaled by the monthly mean ratio of the equivalent variables computed by the NCAR CSM model.

Overall, predicted dust emissions increase by approximately 10%. There are substantial increases in some seasons and locations (e.g. increases in Australia (85%) in winter and in Europe (86%) and East Asia (42%) in summer). Because dust may be especially important as an ice-nucleating agent in clouds, these possible changes add substantial uncertainty to the projected future indirect forcing.

5.5.2.4 Projection of sea salt emissions in 2100

The production of sea salt aerosol is also a strong function of wind speed. The semi-empirical formulation of Monahan *et al.* (1986) was used to produce global monthly sea salt fluxes for eight size intervals (dry diameter of 0.06 to 16 μm) using procedures discussed in Gong *et al.* (1997a,b). In order to project sea salt emissions for the workshop, the ratio of daily average wind speed in the ten years prior to 2100 and 2000 was used to scale the 2000 daily average sea salt flux to the one in 2100. Because this method may overestimate emissions if the product of the daily average ratio with the daily average winds in 2000 produces high wind speeds with a high frequency, the calculation was checked using the ratio of the monthly average wind speeds. This produced a total sea salt flux that was 13% smaller than the projections given in the workshop specifications.

Predicted sea salt emissions were 3,340 Tg in 2000 and increased to 5,880 Tg in 2100. These increases point to a potentially important negative climate feedback. For example, the present day direct radiative impact of sea salt is estimated to be between –0.75 and –2.5 Wm^{-2} using the clear-sky estimates from Haywood *et al.* (1999) or –0.34 Wm^{-2} using the whole-sky estimates from Jacobson (2001). Assuming the ratio of whole-sky to clear-sky forcing from Jacobson (2000b), we project that these changes in sea salt emissions might lead to a radiative feedback in 2100 of up to –0.8 Wm^{-2}. If we assume that the near-doubling of the sea salt mass flux would result in a proportional increase in the number flux, a significant increase in reflected radiation may also result from the indirect effect. The LLNL/Umich model was used to evaluate the possible impact of these emissions. It was found that the changes in natural emissions in 2100 result in a radiative feedback of –1.16 Wm^{-2} in the 2100 A2 scenario. These projected climate changes rely on the projected wind speed changes from the NCAR CSM model. Because projections from other models may not be as large, we also calculated the projected sea salt emissions from three other climate models using the ratio of monthly average winds for the time period from 2090 to 2100 to that for the time period 1990 to 2000 to scale the 2000 sea salt fluxes. Compared to the projections from the NCAR CSM, these models resulted in annual average fluxes that were 37% higher (GFDL model), 13% smaller (Max Planck model), and 9% smaller (Hadley Centre UK Met Office model). The monthly average temperature change associated with these wind speed and sea salt projections was 2.8°K (GFDL model; Knutson *et al.* 1999), 2.8°K (Max Planck model; Roeckner *et al.* 1999) and 2.15°K (Hadley Centre UK Met Office model; Gordon *et al.*, 2000) compared to the temperature projection of 1.8°K from the NCAR CSM model (Dai *et al.*, 2001).

5.5.3 Simulation of Future Aerosol Concentrations

In order to project future aerosol concentrations, we formed the average burdens from the models that gave reasonable agreement with observations for the 2000 scenario. As noted above, the differences in the burdens calculated by the different models point to substantial uncertainties in the prediction of current burdens and these translate into similar uncertainties in projecting future burdens. Except for sulphate and black carbon, however, the future projected global average burdens scaled approximately linearly with emissions. Thus, we may assume that the projected uncertainty in future burdens is mainly determined by the uncertainty in the emissions themselves together with the uncertainty in the burdens associated with different model treatments. For SO_4^{2-}, future anthropogenic concentrations were not linear in the emissions. For example, some models projected increases in burden relative to emissions while others projected decreases. The range of projected changes in anthropogenic burden relative to emissions was −14% to +25% depending on the scenario. Use of the average of the models for the projection of anthropogenic SO_4^{2-} and total SO_4^{2-} may therefore bias the results somewhat, but the uncertainties in the projected SO_4^{2-} concentrations are smaller than those introduced from the range of estimates for the 2000 scenario itself. Table 5.14 gives our projected average burdens for each draft SRES scenario. Results for the burdens associated with the final SRES scenarios are reproduced in Appendix II and are shown in Figure 5.13 (see Chapter 9 and Nakićenović *et al.* (2000) for scenario definitions).

One issue of importance for future scenarios concerns the treatment of black carbon removal rates. Whereas most models projected changes for BC to be approximately linear, the ULAQ and GISS models had somewhat different treatments. In the ULAQ model, the reaction of O_3 with BC leads to additional losses for BC. This caused a change of −30% for BC in the A2 2100 scenario in the simulation that included consideration of chemistry feedbacks (SC6) relative to the scenario without changes in chemistry (SC3). The GISS model, on the other hand, did not consider any heterogeneous loss, but did assume that the loss of BC associated with wet scavenging depended on the interaction of BC with SO_4^{2-}. In this model, as SO_2 emissions decrease, the lifetime of BC increased. This model projects a 50% increase in BC lifetime (and thus in the concentrations relative to emissions) in 2100 associated with the A2 scenario. Thus, the uncertainty associated with the projection of BC concentrations is larger than that for the other aerosol types.

In addition to the studies outlined above, one additional study was performed. In this study, the A2 2100 emission scenario was used to simulate HNO_3 concentrations in 2100 using the Harvard University model (see Chapter 4) and the present day anthropogenic NH_3 emissions were scaled by the increase in N_2O emissions in 2100 from the draft SRES A2 scenario. Then the model described by Adams *et al.* (1999) was used to estimate direct forcing after condensation of the additional HNO_3 and NH_3 onto the calculated sulphate aerosol. The nitrate and ammonium burdens increased by about a factor of 4.7 and a factor of 1.9, respectively, in the A2 2100 scenario. The estimated forcing associated with anthropogenic SO_4^{2-},

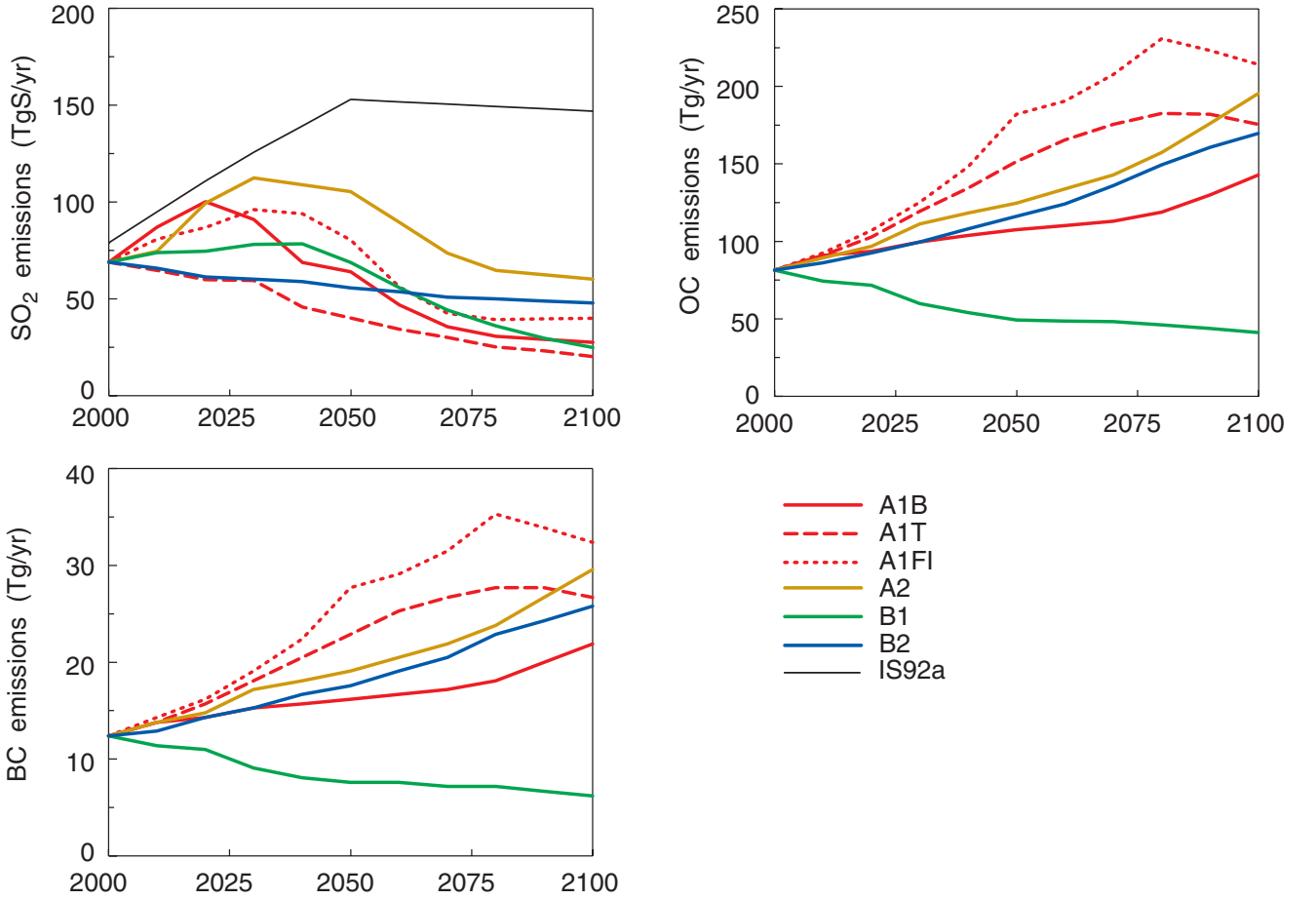

Figure 5.13: *Anthropogenic aerosol emissions projected for the SRES scenarios (Nakicenovic et al., 2000).*

Table 5.14: *Projected future aerosol burden for draft SRES scenarios. The range predicted from the models that participated in the workshop are given for 2000.*

	2000 (SC1)	**A2 2030 (SC2)**	**A2 2100 (SC3)**	**B1 2100 (SC4)**	**A2 2100 with natural aerosols (SC5)**	**B1 2100 with natural aerosols (SC8)**
Sulphate Natural (TgS)	0.26 0.15 - 0.36	0.26	0.26	0.26	0.28	0.28
Sulphate Anthr. (TgS)	0.52 0.35 - 0.75	0.90	0.55	0.28	0.54	0.26
Nitrate Natural (TgN)	0.02		0.02			
Nitrate Anthr. (TgN)	0.07		0.38			
Ammonium Nat. (TgN)	0.09		0.09			
Ammonium Anthr. (TgN)	0.33		0.72			
BC (Tg)	0.26 0.22 - 0.32	0.33	0.61	0.25	0.61	0.25
OC Natural (Tg)	0.15 0.08 - 0.28	0.15	0.15	0.15	0.22	0.22
OC Anthr. (Tg)	1.52 1.05 - 2.21	1.95	2.30	0.90	2.30	0.90
Dust (D<2 µm) (Tg)	12.98 6.24 - 17.73	13.52	13.52	13.52	13.54	13.54
Dust (D>2 µm) (Tg)	19.58 7.39 - 33.15	19.58	19.58	19.58	20.91	20.91
Sea salt (D<2 µm) (Tg-Na)	2.74 1.29 - 7.81	2.74	2.74	2.74	4.77	4.77
Sea salt (D>2 µm) (Tg-Na)	3.86 1.22 - 6.51	3.86	3.86	3.86	6.68	6.68

nitrate, and ammonium aerosols increased from −1.78 Wm^{-2} to −2.77 Wm^{-2}. Thus, the control of sulphate aerosol in future scenarios may not necessarily lead to decreases in forcing, if the levels of ammonium nitrate in aerosol increase.

Two final considerations include the possible impact of chemistry and climate changes on future concentrations. These were examined by the ULAQ model for the A2 2100 scenario. Future concentration changes were small for the simulation that included changes in chemistry only (scenario SC6). Climate feedbacks, however, were significant. Aerosol concentrations changed by as much as −20% relative to the model simulations that did not include climate change.

5.5.4 Linkage to Other Issues and Summary

As we have seen, anthropogenic aerosols may have a substantial effect on the present day aerosol abundance, optical depth and thus forcing of climate. While we have made substantial progress in defining the role of anthropogenic aerosols on direct forcing, significant uncertainties remain, particularly with the role of anthropogenic organic and black carbon aerosols in detemining this forcing. Our ability to assess the indirect forcing by aerosols has a much larger uncertainty associated with it. The largest estimates of negative forcing due to the warm-cloud indirect effect may approach or exceed the positive forcing due to long-lived greenhouse gases. On the other hand, there is sufficient uncertainty in the calculation of indirect forcing to allow values that are substantially smaller than the positive forcing by greenhouse gases. Other factors which have not been assessed include possible anthropogenic perturbations to high level cirrus clouds as well as to clouds in the reservoir between 0°C and −35°C. As we have discussed, significant positive forcing is possible from aerosol-induced increased formation of cirrus and/or from increased glaciation of clouds in the region between 0°C and −35°C.

Concerns about aerosols derive from a number of other considerations. These include visibility, toxic effects and human health, interactions of aerosols with chemical processes in the troposphere and stratosphere, acid deposition, and air pollution. Of these concerns, those associated with toxic effects and visibility have led the industrialised countries to promulgate standards to reduce the concentrations of aerosols in urban and also more pristine locations. Also, concerns about the effects of acid rain have led to increased controls over the emissions of SO_2. As shown above, the SRES scenarios for the future (Nakićenović *et al.*, 2000) have all assumed that emissions of SO_2 will eventually decrease, and the A1T and B2 scenarios predict that sulphur emissions start to decrease on a global average basis almost immediately.

Emissions of carbon aerosols in the future may not necessarily follow the scenarios outlined for SO_2 within the SRES scenarios. Furthermore, older scenarios, developed by IPCC (1992), do not presume that SO_2 emissions would necessarily decrease. We have evaluated a set of scenarios for future aerosols that account for a range of possible future emissions. We noted that one of the future effects that need to be evaluated includes the perturbation to the cycles of natural aerosols. Another includes the interaction of chemical cycles with aerosols and the prediction of how changes in other gas-phase emissions may be perturbing aerosols. We must also consider how changes in aerosols may perturb gas phase cycles. Our evaluation of these interactions has been necessarily limited. Both the interaction of atmospheric chemical cycles with aerosols and the perturbation to natural aerosol components through changing climate patterns need to be better understood.

5.6 Investigations Needed to Improve Confidence in Estimates of Aerosol Forcing and the Role of Aerosols in Climate Processes

Atmospheric measurements have lagged behind awareness of the importance of aerosols in climate. There is a great challenge in adequately characterising the nature and occurrence of atmospheric aerosols and in including their effects in models to reduce uncertainties in climate prediction. Because aerosols: (i) originate from a variety of sources, (ii) are distributed across a wide spectrum of particle sizes and (iii) have atmospheric lifetimes that are much shorter than those of most greenhouse gases, their concentrations and composition have great spatial and temporal variability. Satellite-based measurements of aerosols are a necessary but not sufficient component of an approach needed to acquire an adequate information base upon which progress in understanding the role of aerosols in climate can be built. Below we outline measurements and process level studies that are necessary to reduce uncertainties in both direct and indirect forcing. These studies and observations are needed both to improve the models on which climate forcing rely and to check our understanding of this forcing as aerosol concentrations change in the future.

I. Systematic Ground-Based Measurements

There is a need for countries of the world to develop and support a network of systematic ground-based observations of aerosol properties in the atmosphere that include a variety of physical and chemical measurements ranging from local *in situ* to remotely sensed total column or vertical profile properties. The Global Atmospheric Watch programme of the World Meterological Organization is but one player in organising routine aerosols measurements on a stage that includes other international organisations (e.g. International Atmoic Energy Agency, IAEA) as well as national research programmes (e.g. national environmental agencies, national atmospheric research agencies).

It is recommended that, at all levels, emphasis be placed in developing a *common strategy* for aerosol and gas measurements at a selected set of regionally representative sites. One possible model is to develop a set of primary, secondary and tertiary aerosol networks around the world. At the primary stations, a comprehensive suite of aerosol and gas measurements should be taken that are long-term in scope (gaseous precursors are an essential part of the aerosol story since much aerosol mass is formed in the atmosphere from gas-to-particle conversion). At secondary stations, a less comprehensive set of observations would be taken that would provide background information for intensive shorter term process-oriented studies. It would be

desirable to co-locate vertical profiling networks that involve complex instrumentation such as lidars with these baseline stations. Tertiary stations may include stations operated by national research programmes that are related to urban aerosol issues and human health.

These measurements should be closely co-ordinated with satellite observations of aerosols. The types of measurements should include *in situ* size-segregated concentrations of aerosol physical properties such as number and mass but also chemical properties such as composition and optical properties. Total column properties such as aerosol optical depth, Angstrom coefficient, CO and O_3 add value to these data sets in evaluating the simulation of aerosols as active constitutents in climate models.

II. Systematic Vertical Profile Measurements

There is a paucity of systematic vertical profile measurements of size-segregated or even total atmospheric aerosol physical, chemical and optical properties. For these parameters, no climatological database exists that can be used to evaluate the performance of climate models that include aerosols as active constituents. The COSAM model comparison (Barrie *et al.*, 2001) had to use vertical profile observations from a few intensive aircraft campaigns of only a few months duration to evaluate climate model aerosol predictions. Such measurments would be best co-located with the ground-based network stations. Since they involve routine aircraft surveillance missions and are costly, the development of robust, sensitive lightweight instrument packages for deployment in small aircraft or on commercial airliners is a high priority. Both continuous real time measurements and collection of aerosols for post-flight analysis are needed.

The network design needs to be systematically developed and implemented. One possible model is to conduct observations at pairs of stations around – and downwind of – major aerosol sources types such as industrial (Europe, North America, Asia), soil dust (Sahara or Asian), biomass burning (Amazon or southern Africa) and sea salt (roaring forties of the southern Pacific Ocean region).

III. Characterisation of Aerosol Processes in Selected Regions

There is a need for integrated measurements to be undertaken in a number of situations to enhance the capability to quantitatively simulate the processes that influence the size-segregated concentration and composition of aerosols and their gaseous precursors. The situations need to be carefully selected and the observations sufficiently comprehensive that they constrain models of aerosol dynamics and chemistry. The International Global Atmospheric Chemistry (IGAC) programme in its series of Atmospheric Chemistry Experiments in the roaring forties of the southern Pacific (ACE-1), the outflow from North Africa and Europe to the eastern North Atlantic and the 2001 study in Southeast Asia and downwind in the Pacific (ACE-Asia) are examples of attempts to do this that require support and continued adjustment of experimental design to match outstanding questions. Such studies need to be conducted in industrial continental and neighboring marine, upper-tropospheric, Arctic, remote oceanic and dust-dominated air masses. Closure of aerosol transport and transportation models as well as direct forcing closure studies should be an integral part of these studies.

IV. Indirect Forcing Studies

There is a need for several carefully designed multi-platform (surface-based boat, aircraft and satellite) closure studies that elucidate the processes that determine cloud microphysical (e.g., size-distributed droplet number concentration and chemical composition, hydrometeor type) and macrophysical properties (e.g. cloud thickness, cloud liquid-water content, precipitation rate, total column cloud, albedo). A second goal would be to understand how aerosols influence the interaction of clouds with solar radiation and precipitation formation. These studies should take place in a variety of regions so that a range of aerosol types as well as cloud types can be explored. Emphasis should be placed on reducing uncertainties related to scaling-up of the processes of aerosol-cloud interactions from individual clouds (about 1 to 10 km) to the typical resolution of a climate model (about 100 to 500 km). Can sub-grid parametrizations of cloud processes accurately represent cloud-radiation interactions and the role that aerosols play in that interaction? Answering this question will require that process studies be performed in conjunction with a range of model types such as models that include a detailed microphysical representation of clouds to models that include the parametrizations in climate models.

V. Measurements of Aerosol Characteristics from Space

An integrated strategy for reducing uncertainties should include high quality measurements of aerosols from space. At the time of this report, only measurements from AVHRR and POLDER were available. The latter instrument may yield measurements of aerosol optical depth over land, but it was operational for less than a year. High quality satellite measurements together with systematic comparisons with models and the process-level studies noted above should allow us to reduce the uncertainties in current aerosol models. Systematic comparison of models that include an analysis of the indirect effect with satellite measurements of clouds and with data gathered from process-level studies will also reduce uncertainties in indirect effects and in projected climate change.

References

Abdou, W.A., J.V. Martonchik, R.A. Kahn, R.A. West, and D.J. Diner, 1997: A modified linear-mixing method for calculating atmospheric path radiances of aerosol mixtures. *J. Geophys. Res*., **102**, 16883-16888.

Abdul-Razzak, H. and S. Ghan, 2000: A parametrization of aerosol activation 2. Multiple aerosol types. *J. Geophys. Res*., **105**, 6837-6844.

Abdul-Razzak, H., S. Ghan and C. Rivera-Carpio, 1998: A parametrization of aerosol activation 1. Single aerosol type. *J. Geophys. Res*., **103**, 6123-6131.

Ackerman, T.P, and O.B. Toon, 1981: Absorption of visible radiation in atmosphere containing mixtures of absorbing and nonabsorbing particles. *Appl. Opt*., **20**, 3661-3668.

Ackerman, A.S., O.B. Toon, J.P. Taylor, D.W. Johnson, P.V. Hobbs and R.J. Ferek, 2000: Effects of aerosols on cloud albedo: Evaluation of Twomey's parametrization of cloud susceptibility using measurements of ship tracks. *J. Atmos. Sci.*, **57** 2684-2695.

Adams, P.J., J.H. Seinfeld and D.M. Koch, 1999: Global concentrations of tropospheric sulphate, nitrate and ammonium aerosol simulated in a general circulation model. *J. Geophys. Res*., **104**, 13791–13823.

Adams, P.J. J.H. Seinfeld, D. Koch, L. Mickley, and D. Jacob, 2001: General circulation model assessment of direct radiative forcing by the sulphate-nitrat-ammonium-water inorganic aerosol system. *J. Geophys. Res*., **106**, 1097-1111.

Albrecht, B., 1989: Aerosols, cloud microphysics and fractional cloudiness. *Science*, **245**, 1227–1230.

Al-Naime, R. and C.P.R. Saunders, 1985: Ice nucleus measurements: Effects of site location and weather. *Tellus*, **37B**, 296–303.

Anderson, B.E., W.B. Grant, G.L. Gregory, E.V. Browell, J.E. Collins Jr., D.W. Sachse, D.R. Bagwell, C.H. Hudgins, D.R. Blake and N.J. Blake, 1996: Aerosols from biomass burning over the tropical South Atlantic region: Distributions and impacts. *J. Geophys. Res*., **101**, 24,117-24,137.

Andreae M.O. and W.A. Jaeschke, 1992: Exchange of Sulphur between biosphere and atmosphere over temperate and tropical regions, in: Sulphur cycling on the continents: *Wetlands, Terrestrial Ecosystems, and Associated Water Bodies. SCOPE* **48**, R.W. Howarth, J.W.B. Stewart and M.V. Ivanov (eds), Wiley, Chichester, 27-61.

Andreae, M.O. 1995: Climatic effects of changing atmospheric aerosol levels. In: *World Survey of Climatology. Vol. 16: Future Climates of the World*, A. Henderson-Sellers (ed). Elsevier, Amsterdam, pp. 341–392.

Andreae, M.O. and P.J. Crutzen, 1997: Atmospheric aerosols: Biogeochemical sources and role in atmospheric chemistry. *Science*, **276**, 1052–1056.

Andreae, M.O., E.V. Browell, M. Garstang, G.L. Gregory, R.C. Harriss, G.F. Hill, D.J. Jacob, M.C. Pereira, G.W. Sachse, A.W. Setzer, P.L.S. Dias, R.W. Talbot, A.L. Torres and S.C. Wofsy, 1988: Biomass-burning emissions and associated haze layers over Amazonia. *J. Geophys. Res*., **93**, 1509–1527.

Andreae, M.O., W. Elbert, R. Gabriel, D.W. Johnson, S. Osborne and R. Wood, 2000: Soluble ion chemistry of the atmospheric aerosol and SO_2 concentrations over the eastern North Atlantic during ACE-2. *Tellus*, **52**, 1066-1087.

Andreae, M.O., W. Elbert, Y. Cai, T.W. Andreae and J. Gras, 1999: Non-seasalt sulphate, methanesulfonate, and nitrate aerosol concentrations and size distributions at Cape Grim, Tasmania. *J. Geophys. Res*., **104**, 21,695-21,706.

Andres, R.J. and A.D. Kasgnoc, 1998: A time-averaged inventory of subaerial volcanic sulphur emissions. *J. Geophys. Res*. Atmos., **103**, 25251–25261.

Appel, B.R., Y. Tokiwa, and E.L. Kothny, 1983: Sampling of carbonaceous particles in the atmosphere. *Atmos. Env*., **17**, 1787-1796.

Artaxo, P., E.T. Fernandes, J.V. Martins, M.A. Yamasoe, P.V. Hobbs, W. Maenhaut, K.M. Longo and A. Castanho, 1998a: Large-scale aerosol source apportionment in Amazonia. *J. Geophys. Res*., **103**, 31837–31847.

Artaxo, P., E. Swietlicki, J. Zhou, H.-C. Hansson, W. Maenhaut, M. Claeys, M.O. Andreae, J. Ström, J.V. Martins, M.A. Yamasoe and R. van Grieken, 1998b: Aerosol properties in the central Amazon Basin during the wet season during the LBA/CLAIRE experiment. *Eos Trans. AGU*, **79**, F155.

Atherton, C.A., 1996: Biomass burning sources of nitrogen oxides, carbon monoxide, and non-methane hydrocarbons, *Lawrence Livermore National Laboratory Report* UCRL-ID-122583, 1996.

Atlas, R.M., R.N. Hoffman, S.C. Bloom, J.C. Jusem, and J. Ardizzone, 1996: A multiyear global surface wind velocity dataset using SSM/I wind obsevations, *Bull. Am. Meteorol. Soc*., **77**, 869-882.

Austin, P., Y. Wang,R. Pincus and V. Kujala, 1995: Precipitation in stratocumulus clouds: observational and modeling results, *J. Atmos. Sci*., **52**, 2329-2352.

Barrie, L.A., Y. Yi, W.R. Leaitch, U. Lohmann, P. Kasibhatla, G.-J. Roelofs, J. Wilson, F. McGovern *et al.*, 2001: A comparison of large scale atmospheric sulphate aerosol models (COSAM): Overview and highlights. *Tellus B*, in press.

Barth, M.C., P.J. Rasch, J.T. Kiehl, C.M. Benkowitz, and S.E. Schwartz, 2000: Sulphur chemistry in the NCAR CCM: description, evaluation, features and sensitivity to aqueous chemistry. *J. Geophys. Res*., **105**, 1387-1416.

Bassett, M., and J.H. Seinfeld, 1984: Atmospheric equilibrium model of sulphate and nitrate aerosols. II. Particle size analysis. *Atmos. Env*., **18**, 1163.

Bates, T.S., B.K. Lamb, A. Guenther, J. Dignon, and R.E. Stoiber, 1992: Sulphur emissions to the atmosphere from natural sources. *J. Atmos. Chem*., **14**, 315-337.

Bates, T.S., V.N. Kapustin, P.K. Quinn, D.S. Covert, D.J. Coffman, C. Mari, P.A. Durkee, W.J. De Bruyn, and E.S. Saltman, 1998: Processes controlling the distribution of aerosol particles in the lower marine boundary layer during the First Aerosol Characterization Experiment (ACE 1). *J. Geophys. Res*., **103**, 16369-16383.

Beard, K.V., 1992: Ice nucleation in warm-base convective clouds: An assessment of micro-physical mechanisms. *Atmos. Res*., 28, 125-152.

Beheng, K.D., 1994: A parametrization of warm cloud microphysical conversion processes. *Atmos. Res*., **33**, 193-206.

Benkovitz, C.M., C.M. Berkowitz, R.C. Easter, S. Nemesure, R. Wagner, and S.E. Schwartz, 1994: Sulphate over the North Atlantic and adjacent regions: Evaluation for October and November 1986 using a three-dimensional model driven by observation-derived meteorology. *J. Geophys. Res*., **99**, 20,725-20,756.

Benkovitz, C.M., M.T. Scholtz, J. Pacyna, L. Tarrason, J. Dignon, E.C.Voldner, P.A.Spiro, J.A. Logan, T.E. Graedel, 1996: Global gridded inventories of anthropogenic emissions of sulphur and nitrogen. *J. Geophys. Res*., **101**, 29,239-29,253.

Benkovitz, C.M., S.E. Schwartz, 1997: Evaluation of modelled sulphate and SO2 over North America and Europe for four seasonal months in 1986-1987. *J. Geophys. Res*., **102**, 25,305-25,338.

Berry, E.X., 1967: Cloud drop growth by collection. *J. Atmos. Sci*., **24**, 688-701.

Bigg, E.K., 1990: Long-term trends in ice nucleus concentrations. *Atmos. Res*., **25**, 409–425.

Blanchard, D.C., 1983: The production, distribution and bacterial enrichment of the sea-salt aerosol. In: *Air-Sea Exchange of Gases and Particles*, P.S. Liss and W.G.N. Slinn (eds), Reidel, Boston, USA, pp. 407–454.

Blanchet J.-P. and E. Girard, 1995: Water vapor and temperature feedback in the formation of continental Arctic air: Its implications for climate, *Sci. Total Environ*., 160-161, 793-802.

Bodhaine, B.A., 1995: Aerosol absorption measurements at Barrow,

Mauna Loa and the South Pole. *J. Geophys. Res*., **100**, 8967-8975.

Boers, R. and R.M. Mitchell, 1994: Absorption feedback in stratocumulus clouds – influence on cloud top albedo. *Tellus*, **46**, 229–241.

Boers, R., 1995: Influence of seasonal variation in cloud condensation nuclei, drizzle, and solar radiation, on marine stratocumulus optical depth. *Tellus*, **47B**, 578–586.

Boers, R. and P. Krummel, 1998: Microphysical properties of boundary layer clouds over the Southern Ocean during ACE I. *J. Geophys. Res*., **103**, 16651-16663.

Boers, R., J. B. Jensen, P. B. Krummel 1998: Microphysical and radiative structure of marine stratocumulus clouds over the Southern Ocean: Summer results and seasonal differences. *Quart. J. Royal Meteor. Soc*., **124**, 151-168.

Bond, T.C., R.J. Charlson and J. Heintzenberg, 1998: Quantifying the emission of light-absorbing particles: Measurements tailored to climate studies. *Geophys. Res. Lett*., **25**, 337–340, 1998.

Borys, R. D., 1989: Studies of ice nucleation by arctic aerosol on AGASP-II. *J. Atmos. Chem*., **9**, 169–185.

Boucher, O. and U. Lohmann, 1995: The sulphate-CCN-cloud albedo effect - A sensitivity study with two general circulation models. *Tellus*, **47B**, 281–300.

Boucher, O., and D. Tanré, 2000: Estimation of the aerosol perturbation to the Earth's radiative budget over oceans using POLDER satellite aerosol retrievals, *Geophys. Res. Lett*., **27**, 1103-1106.

Boucher, O., S.E. Schwartz, T.P. Ackerman, T.L Anderson, B. Bergstrom, B. Bonnel, P. Chylek, A. Dahlback, Y. Fouquart, Q. Fu, R.N. Halthore, J.M. Haywood, T. Iversen, S. Kato, S. Kinne, A. Kirkevag, K.R. Knapp, A. Lacis, I. Laszlo, M.I. Mishchenko, S. Nemesure, V. Ramaswamy, D.L. Roberts, P. Russell, M.E. Schlesinger, G.L. Stephens, R. Wagener, M. Wang, J. Wong, F. Yang, 1998: Intercomparison of models representing direct shortwave radiative forcing by sulphate aerosols, *Geophys. Res*, **103**, 16,979-16,998.

Bouwman, A.F., D.S. Lee, W.A.H. Asman, F.J. Dentener, K.W. Van Der Hoek, and J.G.J. Olivier, 1997: A global high-resolution emission inventory for ammonia. *Global Biochem. Cycles*, **11**, 561-588.

Braham, R. R. Jr. and P. Spyers-Duran, 1974: Ice nuclei measurements in an urban atmosphere. *J. Appl. Meteor*., **13**, 940–945.

Brasseur, G. P., D. A. Hauglustaine, S. Walters, P. J. Rasch, J.-F. Muller, C. Granier, X. Tie, 1998: MOZART, a global chemical transport model for ozone and related chemical tracers. Part 1: Model description . *J. Geophys. Res*., **103**, 28,265-28,289.

Brenguier, J.-L., H. Pawlowska, L. Schuller, R. Preusker, J. Fischer and Y. Fouquart, 2000: Radiative properties of boundary layer clouds: droplet effective radius versus number concentration. *J. Atmos. Sci*., **57**, 803-821.

Cachier, H., C. Liousse, P. Buat-Menard and A. Gaudichet, 1995: Particulate content of savanna fire emissions. *J. Atmos. Chem*., **22**, 123–148.

Carrico, C.M., M.J. Rood and J.A. Ogren, 1998: Aerosol light scattering properties at Cape Grim, Tasmania during the First Aerosol Characterization Experiment (ACE-1). *J. Geophys. Res*., **103**, 16,565-16,574.

Carrico, C.M., M.J. Rood, J.A. Ogren, C. Neuses, A. Wiedensolhler and J. Heintzenberg, 2000: Aerosol light scattering properties at Sagres, Portugal, during ACE-2, *Tellus*, **52**, 694-715.

Chapman, W. L. and J. E.,Walsh, 1993: Recent variations of sea ice and air temperature in high latitudes, *Bull. Am. Met. Soc*., **74**, 33-47.

Charlson, R. J., D. S. Covert and T. V. Larson, 1984: Observation of the effect of humidity on light scattering by aerosols. In *Hygroscopic Aerosols*, ed. T. H. Rukube and A. Deepak, pp. 35-44, A. Deepak, Hampton, VA.

Charlson, R. J., J. E. Lovelock, M. O. Andreae, and S. G. Warren, 1987: Ocean phytoplankton, atmospheric sulphur, cloud albedo and climate. *Nature*, **326**, 655-661.

Charlson, R.J., S.E. Schwartz, J.M. Hales, R.D. Cess, J.A. Coakley, J.E. Hansen and D.J. Hofmann, 1992: Climate forcing by anthropogenic aerosols. *Science*, **255**, 423–430.

Chen, Y., S. M. Kreidenweis, L. M. McInnes, D. C. Rogers, and P. J. DeMott, 1998, Single particle analyses of ice nucleating aerosols in the upper troposphere and lower stratosphere. *Geophys. Res. Lett*., **25**, 1391-1394.

Chin, M., R.B. Rood, S.-J. Lin, J.-F. Muller, and A. M. Thompson, 2000: Atmospheric sulphur cycle simulated in the global model GOCART: Model description and global properties. *J. Geophys. Res*., **105**, 24671-24687.

Chuang, C.C. and J.E. Penner, 1995: Effects of anthropogenic sulphate on cloud drop nucleation and optical properties. *Tellus*, **47**, 566–577.

Chuang, C.C., J.E. Penner, K.E. Taylor, A.S. Grossman, and J.J. Walton, 1997: An assessment of the radiative effects of anthropogenic sulphate. *J. Geophys. Res*., **102**, 3761-3778.

Chuang, C. C., J. E. Penner, K. E. Grant, J. M. Prospero, G. H. Rau and K. Kawamoto, 2000: Cloud susceptibility and the first aerosol indirect forcing: sensitivity to black carbon and aerosol concentrations. *J. Geophys. Res.* Submitted. Also: Lawrence Livermore National Laboratory Report, UCRL-JC-139097 Rev 1.

Chylek, P. and J. Wong, 1995: Effects of absorbing aerosols on the global radiation budget. *J. Geophys. Res. Lett.,* **22**, 929-931.

Claquin, T., M. Schulz, Y. Balkanski and O. Boucher, 1998: Uncertainties in assessing radiative forcing by mineral dust. *Tellus*, **50B**, 491–505.

Claquin, T., M. Schulz, and Y. J. Balkanski, 1999: Modeling the mineralogy of atmospheric dust sources. *J. Geophys. Res*., **104**, 22,243-22,256.

Clarke, A. D. J. N. Porter, F. P. J. Valero, and P. Pilewskie, 1996: Vertical profiles, aerosol microphysics, and optical closure during the Atlantic Stratocumulus Transition Experiment: measured and modelled column optical properties. *J. Geophys. Res*., **101**, 4443-4453.

Clarke, A. P., J. Eisele, V. N. Kapustin, K. Moore, D. Tanner, L. Mauldin, M. Litchy, B. Lienert, M. A. Carroll and G. Albercook, 1999: Nucleation in the equatorial free troposphere: Favorable environments during PEM-Tropics. *J. Geophys. Res*., **104**, 5735-5744.

Coakley, J. A., Jr., R. L. Bernstein and P. A. Durkee, 1987, Effect of shipstack effluents on cloud reflectivity. *Science*, **237**, 1020–1022.

Collins, D. R., H. H. Jonsson, R. C. Flagan, J. H. Seinfeld, K. J. Noone, E. Ostrom, D. A. Hegg, S. Gasso, P. B. Russell, J. M. Livingston, B. Schmid and L. M. Russell, 2000: In situ aerosol size distributions and clear column radiative closure during ACE-2. *Tellus*, **52B**, 498 525.

Cooke, W.F. and J.J.N. Wilson, 1996: A global black carbon aerosol model. *J. Geophys. Res. Atmos*., **101**, 19395–19409.

Cooke, W.F., C. Liousse, H. Cachier, and J. Feichter, 1999: Construction of a 1° × 1° degree fossil fuel emission data set for carbonaceous aerosol and implementation and radiative impact in the ECHAM4 model. *J. Geophys. Res*, **104**, 22,137-22,162.

Cooper, W. A., 1980: A method of detecting contact ice nuclei using filter samples. Preprints Cloud Phys. Conf., Clermont-Ferrand, France, pp. 605–669.

Corrigan, C.E., and T. Novakov, 1999: Cloud condensation nucleus activity of organic compounds: A laboratory study. *Atmos. Env*., **33**, 2661-2668.

Covert, D. S., V. N. Kapustin, T. S. Bates and P. K. Quinn, 1996: Physical properties of marine boundary layer aerosol particles of the mid-Pacific in relation to sources and meteorological transport. *J. Geophys. Res*., **101**, 6919-6930.

Cruz, C.N. and S.N. Pandis, 1997: A study of the ability of secondary organic aerosol to act as cloud condensation nuclei. *Atmos. Environ*., **31**, 2205–2214.

Cruz, C.N. and S.N. Pandis, 1998: The effect of organic coatings on the cloud condensation nuclei activation of inorganic atmospheric aerosol. *J. Geophys. Res. Atmos*., **103**, 13111–13123.

Curry, J. A., F. G. Meyer, L. F. Radke, C. A. Brock and E. E. Ebert, 1990: The occurrence and characteristics of lower tropospheric ice crystals in the Arctic. *Int. J. Climate*, **10**, 749–764.

Cusack, S., A. Slingo, J. M. Edwards, and M. Wild, 1998: The radiative impact of a simple aerosol climatology on the Hadley Centre atmospheric GCM. *Q. J. R. Met. Soc*, **124**, 2517-2526.

Daggett, D. L., D. J. Sutkus Jr., D. P. DuPois, and S. L. Baughcum, 1999: An evaluation of aircraft emissions inventory methodology by comparisons with reported airline data. NASA/CR-1999-209480, 75 pp.

Dai, A., T.M.L. Wigley, B.A. Boville, J.T. Kiehl, and L.E. Buja, 2001: Climates of the 20th and 21st centuries simulated by the NCAR Climate System Model. *J. Climate*, in press.

Dai, J. C., L. G. Thompson, and E. Mosley-Thompson, 1995: A 485 year record of atmospheric chloride, nitrate and sulphate: results of chemical analysis of ice cores from Dyer Plateau, Antarctic Peninsula. *Annals of Glaciology*, **21**, 182-188.

D'Almeida, G.A., 1991: Atmospheric aerosols : Global climatology and radiative characteristics. A. Deepak Pub., Hampton, Va., USA.

DeMott, P.J., J.L. Stith, R.J. Zen and D.C. Rogers, 1996: Relations between aerosol and cloud properties in North Dakota cumulus clouds. Preprints, 12th Int. Conf. on Clouds and Precipitation, Zurich, Switzerland, 19-23 August, pp. 320–323.

DeMott, P. J., D.C. Rogers and S.M. Kreidenweis, 1997: The susceptibility of ice formation in upper tropospheric clouds to insoluble aerosol components. *J. Geophys. Res*., **102**, 19575–19584.

DeMott, P.J., D.C. Rogers and S.M. Kreidenweis, Y. Chen, C.H. Twohy, D. Baumgardner, A.J. Heymsfield and K.R. Chan, 1998: The role of heterogeneous freezing nucleation in upper tropospheric clouds: inferences from SUCCESS. *J. Geophys. Res. Lett.,* **25**, 1387–1390.

Deuzé, J.L., M. Herman, P. Goloub, D. Tanré, and A. Marchand, 1999: Characterization of aerosols over ocean from POLDER/ADEOS-1. *Geophys. Res. Lett*., **26**, 1421-1424.

Döscher, A., H., W. Gäggeler, U. Schotterer, and M. Schwikowski, 1995: A 130 years deposition record of sulphate, nitrate, and chloride from a high-alpine glacier. *Water Air Soil Pollut*., **85**, 603-609.

Dubovik, O., B.N. Holben, Y.J. Kaufman, M. Yamasoe, A. Smirnov, D. Tanré and I. Slutsker, 1998: Single-scattering albedo of smoke retrieved from the sky radiance and solar transmittance measured from ground. *J. Geophys. Res*., **103**, 31,903–31,923.

Duce, R., 1995: Distributions and fluxes of mineral aerosol. In *Aerosol Forcing of Climate*, R.J. Charlson and J. Heintzenberg (eds), John Wiley, Chichester, UK, pp. 43–72.

Eagen, R. C., P.V. Hobbs and L.F. Radke, 1974: Particle emissions from a large craft paper mill and their effects on the microstructure of warm clouds,, *J. Applied Meteorl*., **13**, 535-557.

Eatough, D.J., D.A. Eatough, L. Lewis and E.A. Lewis, 1996: Fine particulate chemical composition and light extinction at Canyonlands National Park using organic particulate material concentrations obtained with a multi-system, multichannel diffusion denuder sampler. *J. Geophys. Res*., **101**, 19515–19531.

Eccleston, A. J., N. K. King and D. R. Packham, 1974: The scattering coefficient and mass concentration of smoke from some Australian forest fires. J. Air. Poll. Cont. Assoc., **24**, 1047-1050.

Echalar, F., P. Artaxo, J.V. Martins, M.A. Yamasoe, F. Gerab, W. Maenhaut and B. Holben, 1998: Long-term monitoring of atmospheric aerosols in the Amazon Basin: Source identification and apportionment. *J. Geophys. Res*., **103**, 31,849-31,864.

Eck, T. J., B. N. Holben, J. S. Reid, O. Duborik, S. Kinne, A. Smirnov, N. T. O'Neill and I. Slutsken, 1999: The wavelength dependence of the optical depth of biomass burning, urban, and desert dust aerosols. *J. Geophys. Res*., **104**, 31,333-31,349.

Eichel, C., M. Kramer, L. Schutz, and S. Wurzler, 1996: The water-soluble fraction of atmospheric aerosol particles and its influence on cloud microphysics. *J. Geophys. Res*. Atmos., **101**, 29499–29510.

Einfeld, W., D. E. Ward and C. Hardy, 1991: Effects of fire behavior on prescribed fire smoke characteristics: A case study. In Global Biomass Burning: Atmospheric, Climate, and Biospheric Implications, ed. J. S. Levine, pp. 209-224, MIT Press, Cambridge, MA.

Eisele, F.L. and P.H. McMurry, 1997: Recent progress in understanding particle nucleation and growth, *Phil. Trans. R. Soc. Lond.* B, **352**, 191-201.

Erickson, D.J. III and R.A. Duce, 1988: On the global flux of atmospheric sea salt. *J. Geophys. Res*., **93**, 14079–14088.

Facchini, M.C., M. Mircea, S. Fuzzi, and R.J. Charlson, , 1999: Cloud albedo enhancement by surface-active organic solutes in growing droplets. *Nature*, **401**, 257-259.

Fahey, D. W., U. Schumann, S. Ackerman, P. Artaxo, O. Boucher, M.Y. Danilin, B. Kärcher, P. Minnis, T. Nakajima, and O.B. Toon, 1999: Aviation-produced aerosols and cloudiness. In Aviation and the Global Atmosphere, J.E. Penner, D.H. Lister, D.J. Griggs, D.J. Dokken, and M. McFarland (Eds.), Cambridge University Press, Cambridge, U.K., 65-120.

Fassi-Fihri, A., K. Suhre, R. Rosset, 1997: Internal and external mixing in atmospheric aerosols by coagulation: impact on the optical and hygroscopic properties of the sulphate-soot system. *Atmos. Env*., **31**, 1393-1402.

Feichter, J., E. Kjellstrom, H. Rodhe, F. Dentener, J. Lelieveld and G.-J. Roelofs. 1996: Simulation of the tropospheric sulphur cycle in a global climate model. *Atmos. Env*., **30**, 1693–1707.

Feichter, J., U. Lohmann and I. Schult, 1997: The atmospheric sulphur cycle in ECHAM-4 and its impact on the shortwave radiation. *Climate Dynamics*, **13**, 235–246.

Feingold, G., R. Boers, B. Stevens and W.R. Cotton, 1997: A modelling study of the effect of drizzle on cloud optical depth and susceptibility. *J. Geophys. Res*., **102**, 13527-13534.

Feingold, G., S.M. Kreidenweis, and Y. Zhang, 1998: Stratocumulus processing of gases and cloud condensation nuclei: Part I: trajectory ensemble model. *J. Geophys. Res*., **103**, 19527-19542.

Feingold, G., W. R. Cotton, S. M. Kreidenweis, and J. T. Davis, 1999a: Impact of giant cloud condensation nuclei on drizzle formation in marine stratocumulus: Implications for cloud radiative properties. *J. Atmos. Sci.*, **56**, 4100-4117.

Feingold, G., A.S. Frisch, B. Stevens, and W.R. Cotton, 1999b: The stratocumulus boundary layer as viewed by K-band radar, microwave radiometer and lidar. *J. Geophys. Res*., **104**, 22195-22203.

Ferek, R. J., D. A. Hegg, P. V. Hobbs, P. Durkee and K. Nielson, 1998: Measurements of ship-induced tracks in clouds off the Washington Coast. *J. Geophys. Res*. Atmos., **103**, 23199–23206.

Ferrare, R. A., Melfi, S. H. Whiteman, D. N., Evans, K. D., Leifer, R., 1998: Raman lidar measurements of aerosol extinction and backscattering, 1, Methods and comparisons. *J. Geophys. Res*., **103**, 19,663-19,672.

Ferrare, R., S. Ismail, E. Browell, V. Brakett, . Clayton, S. Kooi, S. H. Melfi, D. Whiteman, G. Schwemmer, K. Evans, P. Russell, J. Livingston, B. Schmid, B. Holben, L. Remer, A. Smirnov, and P. V. Hobbs, 2000: Comparison of aerosol optical properties and water vapor among ground and airborne lidars and Sun photometers during TARFOX. *J. Geophys. Res*., **105**, 9917-9933.

Fischer, H., D. Wagenbach, and J. Kipfstuhl, 1998: Sulphate and nitrate firn concentrations on the Greenland ice sheet 2. Temporal anthropogenic deposition changes. *J. Geophys. Res*., **103**, 21935-21942.

Fitzgerald, J. W., 1991: Marine aerosols: A review. *Atmos. Environ*., **25A**, 533-545.

Fitzgerald, J. W. and W. A. Hoppel, 1982: The size and scattering coefficient of urban aerosol particles at Washington D.C. as a function of relative humidity. *J. Atmos. Sci*., **39**, 1838-1852.

Flamant, C., J. Pelon, P. Chazette, V. Trouillet, K. Quinn, R. Frouin, D. Bruneau, J. F. Leon, T. S. Bates, J. Johnson, and J. Livingston, 2000:

Airborne lidar measurements of aerosol spatial distribution and optical properties over the Atlantic Ocean during a European pollution outbreak of ACE-2, *Tellus*, **52B**, 662-677.

Flowerdew, R. J., and J. D. Haigh, 1996: Retrieval of aerosol optical thickness over land using the ATSR-2 dual-look satellite radiometer. *Geophys. Res. Lett*., **23**, 351-354.

Fowler, L. D. and D. A. Randall, 1996: Liquid and ice cloud microphysics in the CSU general circulation model. Part III: Sensitivity to model assumption. *J. Climate*, **9**, 561–586.

Fraser, R.S. and Y.J. Kaufman, 1985: The relative importance of aerosol scattering and absorption in remote sensing. IEEE Trans Geoscience and Remote Sensing, **23**, 625–633.

Frick, G. M. and W. A. Hoppel, 1993: Airship measurements of aerosol size distributions, cloud droplet spectra, and trace gas concentrations in the marine boundary layer. *Bull. Amer. Met. Soc*., **74**, 2195-2202.

Fuller, K.A., W.C. Malm, and S.M. Kreidenweis, 1999: Effects of mixing on extinction by carbonaceous particles. *J. Geophys. Res*., **104**, 15,941-15,954.

Gard, E. E., M. J. Kleeman, D. S. Gross, L. S. Hughes, J. O. Allen, B. D. Morrical, D. P. Fergenson, T. Dienes, M. E. Galli, R. J. Johnson, G. R. Cass, Glen R, and K. A. Prather, 1998: Direct observation of heterogeneous chemistry in the atmosphere. *Science*, **279**, 1184-1187.

Garrett, T. J. and P. V. Hobbs, 1995: Long-range transport of continental aerosols over the Atlantic Ocean and their effects on cloud structures. *J. Atmos. Sci*., **52**, 2977–2984.

Gasso, S., D.A. Hegg, D.S. Covert, D. Collins, K.J. Noone, E. Ostrom, B. Schmid, P.B. Russell, J.M. Livingston, P.A. Durkee and H. Jonsson, 2000: Influence of humidity on the aerosol scattering coefficient and its effect on the upwelling radiance during ACE-2. *Tellus*, **52B**, 546-567.

Ghan, S.J., C. Chuang and J.E. Penner, 1993: A parametrization of cloud droplet nucleation part I: single aerosol type. *Atmos. Res*., **30**, 197–211.

Ghan, S.J., C.C. Chuang, R.C. Easter, and J.E. Penner, 1995: A parametrization of cloud droplet nucleation. 2. Multiple aerosol types. *Atmos. Res*., **36**, 39-54.

Ghan, S., L.R. Leung, R.C. Easter, and H.Abdul-Razzak, 1997: Prediction of cloud droplet number in a general circulation model. *J. Geophys. Res. Atmos.*, **102**, 21777–21794.

Ghan, S.J., G. Guzman and H. Abdul-Razzak, 1998: Competition between sea salt and sulphate particles as cloud condensation nuclei. *J. Atmos. Sci*., **55**, 3340–3347.

Ghan, S., R. Easter, J. Hudson, and F.-M. Bréon, 2001a: Evaluation of aerosol indirect radiative forcing in MIRAGE. *J. Geophysical Research*, in press.

Ghan, S., R. Easter, E. Chapman, H. Abdul-Razzak, Y. Zhang, R. Leung, N. Laulainen, R. D. Saylor, and R. Zaveri, 2001b: A physically-based estimate of radiative forcing by anthropogenic sulphate aerosol. *J. Geophysical Research*, in press.

Ghan, S., N. Laulainen, R. Easter, R. Wagener, S. Nemesure, E. Chapman, Y. Zhang, and R. Leung, 2001c: Evaluation of aerosol direct radiative forcing in MIRAGE, *J. Geophys. Res*., in press.

Gillani, N., S.E. Schwartz, W.R. Leaitch, J.W. Strapp and G.A. Isaac, 1995: Field observations in continental stratiform clouds: partitioning of cloud droplets between droplets and unactivated interstitial aerosols. *J. Geophys. Res. Atmos.*, **100**, 18687–18706.

Gillette, D., 1978: Wind-tunnel simulation of erosion of soil: Effect of soil texture, sandblasting, wind speed and soil consolidation on dust production. *Atmos. Environ*., **12**, 1735–1743.

Glantz, P. and K.J. Noone, 2000: A physically-based algorithm for estimating the relationship between aerosol mass to cloud droplet number. *Tellus*, **52**, 1216-1231.

Goloub, P., D. Tanré, J.-L. Deuzé, M. German, A. Marchand, and F.-M. Bréon, 1999: Valication of the first algorithm applied for deriving the aerosol properties over the ocean using the POLER/ADEOS measurements. IEEE.*Trans. Geosc. Rem. Sens*., **27**, 1586-1596.

Gong, S.L., L.A. Barrie, and J.-P. Blanchet, 1997a: Modeling sea-salt aerosols in the atmosphere. Part 1: Model development, *J. Geophys. Res*., **102**, 3805-3818.

Gong, S. L., L. A. Barrie, J. Prospero, D. L. Savoie, G. P. Ayers, J.-P. Blanchet, and L. Spacek, 1997b: Modeling sea-salt aerosols in the atmosphere, Part 2: Atmospheric concentrations and fluxes. *J. Geophys. Res*. **102**, 3819-3830.

Gong, S.L., L.A. Barrie, J.-P. Blanchet and L. Spacek, 1998: Modeling size-distributed sea salt aerosols in the atmosphere: An application using Canadian climate models. In: Air Pollution Modeling and Its Applications XII, S.-E. Gryning and N. Chaumerliac (eds), Plenum Press, New York.

Gordon, C., C. Cooper, C. A. Senior, H. Banks, J. M. Gregory, T. C. Johns, J. F. B. Mitchell, and R. A. Wood, 2000: The simulation of SST, sea-ice extents and ocean heat transport in a version of the Hadley Centre coupled model without fluxx adjustments. *Climate Dynamics*, **16**, 147-168.

Goudie, A.S. and N.J. Middleton, 1992: The changing frequency of dust storms through time. *Clim. Change*, **20**, 197-225.

Graf, H.-F., J. Feichter and B. Langmann, 1997: Volcanic sulphur emissions: Estimates of source strength and its contribution to the global sulphate distribution. *J. Geophys. Res*., **102**, 10727–10738.

Graf, H.-F., B. Langmann and J. Feichter, 1998: The contribution of Earth degassing to the atmospheric sulphur budget. Chem. Geol., **147**, 131–145.

Gras, J. L., 1995: CN, CCN, and.particle size in Southern Ocean air at Cape Grim, *Atmos. Res*., **35**, 233-251.

Greenwald, T. J., G. L. Stephens, T. H. Vonder Haar, and D. L. Jackson, 1993: A physical retrieval of cloud liquid water over the global oceans using special sensor microwave/imager (SSM/I) observations. *J. Geophys. Res*., **98**, 18,471-18,488.

Griffin, R.J., D.R. Cocker, III, R.C. Flagan and J.H. Seinfeld, 1999a: Organic aerosol formation from the oxidation of biogenic hydrocarbons. *J. Geophys. Res*., **104**, 3555–3567.

Griffin, R.J., D.R. Cocker, III, J.H. Seinfeld and D. Dabdub 1999b: Estimate of global atmospheric organic aerosols from oxidation of biogenic hydrocarbons. *Geophys. Res. Lett*., **26**, 2721–2724.

Gschwandtner, G., K. Gschwandtner, K. Eldridge, C. Mann, and D. Mobley, 1986: Historic emissions of sulphur and nitrogen oxides in the United States from 1900 to 1980. *J. Air Pollut. Control Assoc*., **36**, 139-149.

Guenther, A., C. Hewitt, D. Erickson, R. Fall, C. Geron, T. Graedel, P. Harley, L. Klinger, M. Lerdau, W. McKay, T. Pierce, B. Scholes, R. Steinbrecher, R. Tallamraju, J. Taylor and P. Zimmerman, 1995: A global model of natural volatile organic compound emissions. *J. Geophys. Res. Atmos*., **100**, 8873–8892.

Guenther, A., B. Baugh, G. Brasseur, J. Greenberg, P. Harley, L. Klinger, D. Serca, and L. Vierling, 1999: Isoprene emission estimates and uncertainties for the Central African EXPRESSO study domain, *J. Geophys. Res*., **104**, 30,625-30,639.

Gultepe, I. and G.A. Isaac, 1998: Scale effects on averaging of cloud droplet and aerosol number concentrations: observations and models. *J. Climate*, **12**, 1268-1279.

Hagen, D. E., J. Podzinsek and M. B. Trueblood, 1995: Upper-tropospheric aerosol sampled during FIRE IFO II. *J. Atmos. Sci*., **52**, 4196–4209.

Han, Q., W. B. Rossow, and A. A. Lacis, 1994: Near-global survey of effective droplet radii in liquid water clouds using ISCCP data. *J. Climate,* **7**, 465-497.

Han, Q, W.B. Rossow, J. Chou and R.M. Welch 1998a: Global variation of column droplet concentration in low-level clouds, *Geophys. Res. Lett*, **25**, 1419-1422.

Han, Q., Rossow, W.B., Chou, J. and Welch, R.M., 1998b: Global survey

of the relationships of cloud albedo and liquid water path with droplet size using ISCCP. *J. Climate*, **11**, 1516–1528.

Hansen, J.E., M. Sato and R. Ruedy, 1997: Radiative forcing and climate response. *J. Geophys. Res*., **102**, 6831–6864.

Hansson, H.-C., M.J. Rood, S. Koloutsou-vakakis, K. Hameri, D. Orsini, and A. Wiedensohler, 1998: NaCl aerosol particle hygroscopicity dependence on mixing with organic compounds. *J. Atmos. Chem*., **31**, 321–346.

Havers, N., Burba, P., Lambert, J. and Klockow, D., 1998: Spectroscopic characterization of humic-like substances in airborne particulate matter. *J. Atmos. Chem*., **29**, 45-54.

Haywood, J.M. and K.P. Shine, 1995: The effect of anthropogenic sulphate and soot aerosol on the clear sky planetary radiation budget. *Geophys. Res. Lett*., **22**, 603–606.

Haywood, J., and V. Ramaswamy, 1998: Global sensitivity studies of the direct radiative forcing due to anthropogenic sulphate and black carbon aerosols. *J. Geophys. Res*., **103**, 6043-6058.

Haywood, J., V. Ramaswamy, and B. Soden, 1999: Tropospheric aerosol climate forcing in clear-sky satellite observations over the oceans, *Science*, **283**, 1299-1303.

Hegg, D. A., L. F. Radke and P. V. Hobbs, 1993: Aerosol size distributions in the cloudy atmospheric boundary layer of the North Atlantic Ocean. *J. Geophys. Res*., **98**, 8841-8846.

Hegg, D.A., 1994: Cloud condensation nucleus-sulphate mass relationship and cloud albedo. *J. Geophys. Res*., **99**, 25,903-25,907.

Hegg, D. A., D. S. Covert, M. J. Rood and P. V. Hobbs, 1996a: Measurement of the aerosol optical properties in marine air. *J. Geophys. Res*., **96**, 12893-12903.

Hegg, D.A., P.V. Hobbs, S. Gasso, J.D. Nance and A.L. Rango, 1996b: Aerosol measurements in the Arctic relevant to direct and indirect radiative forcing. *J. Geophys. Res*., **101**, 23349–23363.

Hegg, D.A., J. Livingston, P.V. Hobbs, T. Novakov and P. Russell, 1997: Chemical apportionment and aerosol column optical depths off the mid-Atlantic coast of the United States. *J. Geophys. Res*., **102**, 25,293–25,303.

Heintzenberg, J., K. Okada and J. Strom, 1996: On the composition of non-volatile material in upper tropospheric aerosols and cirrus crystals. *Atmos. Res*., **41**, 81–88.

Heintzenberg, J., R.J. Charlson, A.D. Clarke, C. Liousse, V. Ramaswamy, K.P. Shine, M. Wendisch and G. Helas, 1997: Measurements and modelling of aerosol single-scattering albedo: Progress, problems and prospects. *Contr. Atmosph. Phys.*, **70**, 249–263.

Herman, M., J. L. Deuzé, P. Goloub, F. M. Bréon, and D. Tanré, 1997: Remote sensing of aerosols over land surfaces including polarization measurements and application to POLDER measurements. *J. Geophys. Res*., **102**, 17039-17049.

Herzog, M., J. E. Penner, J. J. Walton, S. M. Kreidenweis, D. Y. Harrington, and D. K. Weisenstein, 2000: Modeling of global sulphate aerosol number concentrations. In Nucleation and Atmospheric aerosols 2000: 15th International Conference, B. N. Hale and M. Kulmala, Eds., AIP Conference Proceedings, **534**, 677-679.

Heymsfield, A. J. and L. M. Miloshevich, 1993: Homogeneous ice nucleation and supercooled liquid water in orographic wave clouds. *J. Atmos. Sci*., **50**, 2335–2353.

Heymsfield A,J,, and L.M. Miloshevich 1995: Relative humidity and temperature influences on cirrus formation and evolution -observations from wave clouds and FIRE II. *J. Atmos. Sci*., **52**, 4302-4326.

Hignett, P., 1991: Observations of diurnal variation in a cloud-capped marine boundary layer. *J. Atmos. Sci*., **48**, 1474-1482.

Hignett, P., J. T. Taylor, P. N. Francis, and M. D. Glew, 1999: Comparison of observed and modelled direct forcing during TARFOX, *J. Geophys. Res*., **104**, 2279-2287.

Higurashi, A., and T. Nakajima, 1999: Development of a two channel aerosol algorithm on a global scale using NOAA/AVHRR. *J. Atmos. Sci*, **56**, 924-941.

Hobbs, P. V. and J. D. Locatelli, 1970: Ice nucleus measurements at three sites in western Washington. *J. Atmos. Sci*., **27**, 90–100.

Hobbs, P. V., J. S. Reid, J. D. Herring, J. D. Nance, R. E. Weiss, J. L. Ross, D. A. Hegg, R. D. Ottmar and C. A. Liousse, 1997: Particle and trace-gas measurements in the smoke from prescribed burns of forest products in the Pacific Northwest. In Biomass Burning and Global Change, ed., J. S. Levine, pp. 697-715, MIT Press, Cambridge, MA.

Hoffmann, T., J.R. Odum, F. Bowman, D. Collins, D. Klockow, R.C. Flagan and J.H. Seinfeld, 1997: Formation of organic aerosols from the oxidation of biogenic hydrocarbons. *J. Atmos. Chem*., **26**, 189–222.

Hofmann, D. J., 1993: Twenty years of balloon-borne tropospheric aerosol measurements at Laramie, Wyoming. *J. Geophys. Res*., **98**, 12753-12766.

Hogan, A. W., 1967: Ice nuclei from direct reaction of iodine vapor with vapors from leaded gasoline. *Science*, **158**, 158.

Holben, B. N., T. F. Eck, I. Slutsker, D. Tanré, J. P. Buis, A. Stezer, E. Vermote, J. A. reagan, U. J. Kaufman, T. Nakajima, F. Lavenu, I. Jankowiak, and A. Smirnov, 1998: AERONET–A federated instrument network and data archive for aerosol characterization. *Remote Sens. Environ.*, **66**, 1-16.

Horvath, H., 1993: Atmospheric light absorption-a review. *Atmos. Env*., **27A**, 293-317.

Houweling, S., F. Dentener, and J. Lelieveld, 1998: The impact of non-methane hydrocarbon compounds on tropospheric chemistry. *J. Geophys. Res*., **103**, 10,673-106,96.

Howell, S.G. and B.J. Huebert, 1998: Determining marine aerosol scattering characteristics at ambient humidity from size-resolved chemical composition. *J. Geophys. Res. Atmos.*, **103**, 1391–1404.

Hsu, N. C., J. R. Herman, O. Torres, B. N. Holben, D. Tanré, T. F. Eck, A. Smirnov, B. Chatenet, and F. Lavenu, 1999: Comparisons of the TOMS aerosol index with Sun-photometer aerosol optical thickness: Results and applications. *J. Geophys. Res*., **104**, 6269-6279.

Hudson, J. G. and S. S. Yum, 1997: Droplet spectral broadening in marine stratus. *J. Atmos. Sci*., **54**, 2642–2654.

Hudson, J., and X. Da, 1996: Volatility and size of cloud condensation nuclei. *J. Geophys. Res*., **101**, 4435–4442.

Husar, R. B., and W. E. Wilson, 1993: Haze and sulphur emission trends in the Eastern United States. *Envir. Sci. Tech*. **27**, 12-16.

Husar, R. B., J. M. Prospero, and L. L. Stowe, 1997: Characterization of tropospheric aerosols over the oceans with the NOAA advanced very high resolution radiometer optical thickness operational product, *J. Geophys. Res*., **102**, 16889-16909.

IPCC, 1992: Climate Change 1992: The Supplementary Report to the IPCC Scientific Assessment. Houghton, J.T., B.A. Callander, and S.K.Varney (eds.). Cambridge University Press, Cambridge, UK, 200 pp.

IPCC, 1996: Climate Change 1995: The Science of Climate Change. Contribution of Working Group I to the Second Assessment Report of the Intergovernmental Panel on Climate Change. Houghton, J.T., L.G. Meira Filho, B.A. Callander, N. Harris, A. Kattenberg, and K. Maskell (eds.). Cambridge University Press, Cambridge, United Kingdom and New York, NY, USA, 572 pp.

Isaac, G.A., W.R. Leaitch and J.W. Strapp, 1990: The vertical distribution of aerosols and acid related compounds in air and cloudwater. *Atmos. Environ*., **24A**, 3033–3046.

Iversen, T., A. Kirkevåg, J. E. Kristjansson, and Ø. Seland, 2000: Climate effects of sulphate and black carbon estimated in a global climate model. In Air Pollution Modeling and its Application XIV, S.-E. Gryning and F.A. Schiermeier, Eds. Kluwer/Plenum Publishers, New York, 335-342.

Jacob, D.J., M.J. Prather, P.J. Rasch, R.-L. Shia, Y.J. Balkanski, S.R. Beagley, D.J. Bergmann, W.T. Blackshear, M. Brown, M. Chiba,

M.P. Chipperfield, J. de Grandpré, J.E. Dignon, J. Feichter, C. Genthon, W.L. Grose, P.S. Kasibhatla, I. Köhler, M.A. Kritz, K. Law, J.E. Penner, M. Ramonet, C.E. Reeves, D.A. Rotman, D.Z. Stockwell, P.F.J. Van Velthoven, G. Verver, O. Wild, H. Yang, and P. Zimmermann, 1997: Evaluation and intercomparison of global atmospheric transport models using 222Rn and other short-lived tracers. *J. Geophys. Res*., **102**, 5953-5970.

Jacobson, M. Z., 2000: A physically-based treatment of elemental carbon optics: Implications for global direct forcing of aerosols, *Geophys. Res. Lett*., **27**, 217-220.

Jacobson, M.Z., 2001: Global direct radiative forcing due to multicomponent anthropogenic and natural aerosols. *J. Geophys. Res*., in press.

Jaenicke, R., 1993: Tropospheric aerosols. In Aerosol-Cloud-Climate Interactions, ed. P. V. Hobbs, Academic Press, San Diego, CA, pp. 1-31.

Jankowiak, I., and D. Tanré, 1992: Satellite climatology of Saharan dust outbreaks: Method and preliminary results. *J. Clim*., **4**, 646-656.

Jennings, S. G., C. D. O'Dowd, T. C. O'Conner and J. M. McGovern, 1991: Physical characteristics of the ambient aerosol at Mace Head. *Atmos. Environ*., **25A**, 557-562.

Jensen, E.J., and O.B. Toon, 1992: The potential effects of volcanic aerosols on cirrus cloud microphysics. *Geophys. Res. Lett*., **19**, 1759-1762.

Jensen, E.J., and O.B. Toon, 1994: Ice nucleation in the upper troposphere - sensitivity to aerosol number density, temperature, and cooling rate. *Geophys. Res. Lett*., **21**, 2019-2022.

Jensen, E.J. and O.B. Toon, 1997: The potential impact of soot particles from aircraft exhaust on cirrus clouds. *Geophys. Res. Lett*., **24**, 249–252.

Jeuken, A., P. Veefkind, F. Dentener, S. Metzger, 2001: Simulation of the aerosol optical depth over Europe for August 1997 and a comparison with observations. *J. Geophys. Res*., in press.

Johnson, D.W., S. Osborne, R. Wood, K. Suhre, R. Johnson, S. Businger, P.K. Quinn, A. Weidensohler, P.A. Durkee, L.M. Russell, M.O. Andreae, C. O'Dowd, K.J. Noone, B.Bandy, J. Rudolph and S. Rapsomanikis, 2000: An overview of the Langrangian experiments undetaken during the North Atlantic regional Aerosol Characterisation Experiment (ACE-2), *Tellus*, **52B**, 290-320.

Jones, P.R., R.J. Charlson and H. Rodhe, 1994a: Aerosols. In: Climate Change 1994: Radiative Forcing of Climate Change and an evaluation of the IPCC IS92a Emission Scenarios. A special Report of IPCC Working Groups I and III. Houghton J.T., L.G. Meira Filho, J. Bruce, Hoesung Lee, B.A. Callander, E. Haites, N. Harris, and K. Maskell (eds.), Cambridge University Press, Cambridge, UK, pp. 131–162.

Jones, A., D.L. Roberts, and A. Slingo, 1994b: A climate model study of indirect radiative forcing by anthropogenic aerosols. *Nature*, **370**, 450–453.

Jones, A. and A. Slingo, 1996: Predicting cloud-droplet effective radius and indirect sulphate aerosol forcing using a general circulation model. *Quart. J. R. Met. Soc*., **122**, 1573–1595.

Kahn, R. A., West, D. McDonald, B. Rheingans, and M. I. Mishchenko, 1997: Sensitivity of multiangle remote sensing observations to aerosol sphericity. *J. Geophys. Res*., **102**, 16861-16870.

Kanakidou, M., K. Tsigaridis, F. J. Dentener, and P. J. Crutzen, 2000: Human activity enhances the formation of organic aerosols by biogenic hydrocarbon oxidation. *J. Geophys. Res*., **1-5**, 9243-9254.

Kärcher, B., Th. Peter, U. M. Biermann, and U. Schumann, 1996: The initial composition of jet condensation trails, *J. Atmos. Sci*., **53**, 3066-3083.

Kärcher, B., R. Busen, A. Petzold, F.P. Schröder, U. Schumann, and E.J. Jensen, 1998: Physicochemistry of aircraft-generated liquid aerosols, soot, and ice particles, 2, Comparison with observations and sensitivity studies. *J. Geophys. Res.,* **103***,* 17129-17148.

Kaufman, Y. J. , 1987: Satellite sensing of aerosol absorption. *J. Geophys. Res*., **92**, 4307-4317.

Kaufman, Y.J., D. Tanré, H.R. Gordon, T. Nakajima, J. Lenoble, R. Frouin, H. Grassl, B.M. Herman, M.D. King and P.M. Teillet, 1997: Passive remote sensing of tropospheric aerosol and atmospheric correction for the aerosol effect. *J. Geophys. Res*., **102**, 16,815–16,830.

Kent, G.S., and M.P. McCormick, 1984: SAGE and SAM II measurements of global stratospheric aerosol optical depth and mass loading. *J. Geophys. Res*., **89**, 5303-5314.

Kettle, A.J., M.O. Andreae, D. Amouroux, T.W. Andreae, T.S. Bates, V. Berrresheim, H. Bingemer, R. Boniforti, M.A.J. Curran, G.R. DiTullio, G. Helas, G.B. Jones, M.D. Keller, R.P. Kiene, C. Leck, M. Levasseur, G. Malin, M. Maspero, P. Matrai, A.R. McTaggart, N. Mihalopoulos, B.C. Nguyen, A. Novo, J.P. Putaud, S. Rapsomanikis, G. Roberts, G. Schebeske, S. Sharma, R. Simo, R. Staubes, S. Turner and G. Uher, 1999: A global database of sea surface dimethylsulfide (DMS) measurements and a procedure to predict sea surface DMS as a function of latitude, longitude and month. *Global Biogeochemical Cycles*, **13**, pp. 399–444.

Kettle, A.J., and M.O. Andreae, 2000: Flux of dimethylsulfide from the oceans: A comparison of updated data sets and flux models. *J. Geophys. Res*., **105**, 26793-26808.

Kiehl, J.T., T.L. Schneider, P.J. Rasch, M.C. Barth and J. Wong, 2000: Radiative forcing due to sulphate aerosols from simulations with the NCAR community model (CCM3). *J. Geophys. Res*., **105**, 1441-1458.

King, M.D., Y.J. Kaufman, D. Tanré, and T. Nakajima, 1999: Remote sensing of tropospheric aerosols from space: Past, present and future. *Bull.Amer. Meteor. Soc*., 2222-2259.

Knutson, T.R., T.L. Delworth, K.W. Dixon and R.J. Stouffer, 1999: Model assessment of regional surface temperature trends (1949-97). *J. Geophys. Res*., **104**, 30,981-30,996.

Koch, D., D. Jacob, I. Tegen, D. Rind and M. Chin, 1999: Tropospheric sulphur simulation and sulphate direct radiative forcing in the Goddard Institute for Space Studies general circulation model. *J. Geophys. Res*., **104**, 23,799–23,822.

Koop, T., A.K. Bertram, L.T. Molina and M.J. Molina, 1999: Phase transitions in aqueous NH_4HSO_4 solutions. *J. Phys. Chem*., **103,** 9042-9048.

Kotchenruther, R. A. and P. V. Hobbs, 1998: Humidification factors of aerosols from biomass burning in Brazil. *J. Geophys. Res*., **103,** 32081-32090.

Kotchenruther, R. A., P. V. Hobbs and D. A. Hegg, 1999: Humidification factors for atmospheric aerosols off the mid-Atlantic coast of the United States. *J. Geophys. Res*., **104**, 2239-2251.

Krekov, G.M., 1993: Models of atmospheric aerosols. In Aerosol Effects on Climate, S.G. Jennings, ed., U. of Arizona Press, Tucson, Ariz.

Kriedenweis, S.M., Y. Chen, D.C. Rogers and P.J. DeMott, 1998: Isolating and identifying atmospheric ice-nucleating aerosols: A new technique. *Atmos. Res*., **46**, 263–279.

Kuang, Z. and Y.L. Yung, 2000: Reflectivity variations off the Peru coast: Evidence for indirect effect of anthropogenic sulphate aerosols on clouds. *Geophys. Res. Lett*., **16**, 2501-2504.

Kulmula, M., A. Laaksonen, P. Korhonen, T. Vesala and T. Ahonen, 1993: The effect of atmospheric nitric acid vapor on cloud condensation nucleus activation. *J. Geophys. Res*., **98**, 22949–22958.

Kulmala, M., P. Korhonen, T. Vesala, H.-C. Hansson, K. Noone and B. Svenningsson, 1996: The effect of hygroscopicity on cloud droplet formation. *Tellus*, **48B**, 347–360.

Kumai, M., 1976: Identification of nuclei and concentrations of chemical species in snow crystals sampled at the South Pole. *J. Atmos. Sci*., **33**, 833–841.

Laaksonen, A., P. Korhonen, M. Kulmala and R.J. Charlson, 1998: Modification of the Kohler equation to include soluble trace gases and slightly soluble substances, *J. Atmos. Sci*., **55**, 853-862.

Lacis, A. A. and J. E. Hansen, 1974: A parametrization for the absorption of solar radiation in the Earth's atmosphere. *J. Atmos. Sci*., **31**, 118-133.

Langer, G., J. Posenski and C. P. Edwards, 1967: A continuous ice nucleus counter and its application to tracking in the troposphere. *J. Appl. Meteor*., **6**, 114–125.

Langner, J. and H. Rodhe, 1991: A global three-dimensional model of the tropospheric sulphur cycle. *J. Atmos. Chem*., **13**, 225–263.

Lavanchy, V. M. H., H. W. Gäggeler, U. Schotterer, M. Schwikowski, and U. Baltensperger, 1999: Historical record of carbonaceous particle concentrations from a European high-alpine glacier (Colle Gnifetti, Switzerland). *J. Geophys. Res*., **104**, 21227-21236.

Lawrence, M.G., W.L. Chameides, P.S. Kasibhatla, H. Levy II, and W. Moxim, 1995: Lightning and atmospheric chemistry: The rate of atmospheric NO production, in Handbook of Atmospheric Electrodynamics, 1, H. Volland, Editor, 189-202, CRC Press, Boca Raton, Florida.

Leaitch, W. R. and G. A. Isaac, 1991: Tropospheric aerosol size distribution from 1982 to 1988 over Eastern North America. *Atmos. Environ*., **25A**, 601-619.

Leaitch, W.R., S.-M., Li, P.S.K. Liu, C.M. Banic, A.M. Macdonald, G.A. Isaac, M.D. Couture, and J.W. Strapp, 1996a: Relationships among CCN, aerosol size distribution and ion chemistry from airborne measurements over the Bay of Fundy in August-September, 1995. In: Nucleation and Atmospheric Aerosols, M. Kulmala and P. Wagner (eds). Elsevier Science Inc., pp. 840–843.

Leaitch, W.R., C.M. Banic, G.A. Isaac, M.D. Couture, P.S.K. Liu, I. Gultepe, S.-M. Li, L.I. Kleinman, P.H. Daum and J.I. MacPherson, 1996b: Physical and chemical observations in marine stratus during 1993 NARE: Factors controlling cloud droplet number concentrations. *J. Geophys. Res. Atmos.*, **101**, 29123–29135.

Leaitch, W.R., J.W. Bottenheim, T.A. Biesenthal, S.-M. Li, P.S.K. Liu, K. Asalian, H. Dryfhout-Clark, F. Hopper and F.J. Brechtel, 1999: A case study of gas-to-particle conversion in an eastern Canadian forest. *J. Geophys. Res. Atmos*., **104**, 8095–8111.

Le Canut, P., M. O. Andreae, G. W. Harris, J. G. Wienhold and T. Zenker, 1996: Airborne studies of emissions from savanna fires in southern Africa. 1. Aerosol emissions measured with a laser optical particle counter. *J. Geophys. Res*., **101**, 23615-23630.

Le Canut, P., M. O. Andreae, G. W. Harris, J. G. Wienhold and T. Zenker, 1992: Aerosol optical properties over southern Africa during SAFARI-92. In Biomass Burning and Global Change, ed. J. S. Levine, pp. 441-459, MIT Press, Cambridge, MA.

Le Treut, H., and Z.X. Li, 1991: Sensitivity of an atmospheric general circulation model to prescribed SST changes: Feedback effects associated with the simulation of cloud optical properties, *Climate Dynam.*, **5**, 175-187.

Lelieveld, J., G.J. Roelofs, L. Ganzeveld, J. Feichter, and H. Rodhe, 1997: Terrestrial sources and distribution of atmospheric sulphur, *Phil. Trans. R. Soc. Lond. B.*, **352**, 149-158.

Leroy, M., J. -L. Deuzé, F. -M. Bréon, O. Hautecoeur, M. Herman, J.-C. Buriez, D. Tanré, S. Bouffiés, P. Chazette, and J.-L. Roujean, 1997: Retrieval of atmospheric properties and surface bidirectional reflectances over land from POLDER/ADEOS. *J. Geophys. Res*., **102**, 17023-17037.

Levin, Z. and S. A. Yankofsky, 1983: Contact versus immersion freezing of freely suspended droplets by bacterial ice nuclei. *J. Climate* Appl. Meteor., **22**, 1964–1966.

Levitus, S. and T.P. Boyer, 1994: NOAA Atlas NESDIS 4, World Ocean Atlas 1994, vol. 4: Temperature. Nat. Environ. Satellite, Data, and Inf. Serv., Nat. Oceanic and Atmos. Admin., U.S. Dep. Of Comm. Washington, D.C.

Li, S.-M., C.M. Banic, W.R. Leaitch, P.S.K. Liu, G.A. Isaac, X.-L. Zhou, and Y.-N. Lee 1996: Water-soluble fractions of aerosol and the relation to size distributions based on aircraft measurements from the North Atlantic Regional Experiment. *J. Geophys. Res. Atmos.*, **101**, 29,111-29,121.

Li, F, and K. Okada, Diffusion and modification of marine aerosol particles over the coastal areas in China, A case study using a single particle analysis, 1999: *J. Atmos. Sci.*, **56**, 241-248.

Li-Jones, X. and J.M. Prospero, 1998: Variations in the size distribution of non-sea-salt sulphate aerosol in the marine boundary layer at Barbados: Impact of African dust. *J. Geophys. Res*., **103**, 16073–16084.

Lin, H., K.J. Noone, J. Strom, and A.J. Heymsfield, 1998: Small ice crystals in cirrus clouds: A model study and comparison with in-situ observations. *J. Atmos. Sci*., **55**, 1928-1939.

Liou, K.-N., 1980: An Introduction to Atmospheric Radiation, Academic Press, New York.

Liou, K.-N. and S.-C. Cheng, 1989: Role of cloud microphysical processes in climate: an assessment from a one-dimensional prespective. *J. Geophy. Res*., **94**, 8599-9607.

Liousse, C., H. Cachier and S.G. Jennings, 1993: Optical and thermal measurements of black carbon aerosol content in different environments: Variation of the specific attenuation cross-section, sigma (s). *Atmos. Environ*., **27A**, 1203–1211.

Liousse, C., J.E. Penner, C. Chuang, J.J. Walton, H. Eddleman and H. Cachier, 1996: A global three-dimensional model study of carbonaceous aerosols. *J. Geophys. Res. Atmos*., **101**, 19411–19432.

Lippman, M. , 1980: Size distribution in urban aerosols. Am. N. Y. Acad. Sci., **328**, 1-12.

Liss, P.S. and L. Merlivat, 1986: Air-sea gas exchange rates: Introduction and synthesis. In: The Role of Air-Sea Exchange in Geochemical Cycling. P. Buat Menard (ed), D. Reidel Publishing, Berlin, 113–127.

Lohmann, U. and J. Feichter, 1997: Impact of sulphate aerosols on albedo and lifetime of clouds: A sensitivity study with the ECHAM4 GCM. *J. Geophys. Res. Atmos*., **102**, 13685–13700.

Lohmann, U., K. Von Salzen, and N. McFarlane, H.G. Leighton, and J. Feichter, 1999a: The tropospheric sulphur cycle in the Canadian general circulation model. *J. Geophys. Res*., 26,833-26,858.

Lohmann, U., J. Feichter, C.C. Chuang and J.E. Penner, 1999b: Prediction of the number of cloud droplets in the ECHAM GCM. *J. Geophys. Res*., **104**, 9169–9198.

Lohmann, U., J. Feichter, C.C. Chuang, and J.E. Penner, 1999c: Erratum, *J. Geophys. Res*., **104**, 24,557-24,563.

Lohmann, U., J. Feichter, J.E. Penner, and R. Leaitch, 2000: Indirect effect of sulphate and carbonaceous aerosols: A mechanistic treatment, *J. Geophys. Res*., **105**. 12,193-12,206.

Lohmann, U., R. Leaitch, K. Law, L. Barrie, Y. Yi, D. Bergmann, M. Chin, R. Easter, J. Feichter, A. Jeukin, E. Kjellstroem, D. Koch, C. Land, P. Rasch, G.-J. Roelofs, 2001: Comparison of the vertical distributions of sulphur species from models which participated in the COSAM excercise with observations. *Tellus*, in press.

Lovett, R.F., 1978: Quantitative measurement of airborne sea salt in the North Atlantic. *Tellus*, **30**, 358-364.

Ludwig, J., L.T. Marufu, B. Huber, M.O. Andreae and G. Helas, 2001: Combustion of biomass fuels in developing countries - A major source of atmospheric pollutants. *Environmental Pollution*, in press.

Marticorena, B., G. Bergametti, B. Aumont, Y. Callot, C. Ndoume and M. Legrand, 1997: Modeling the atmospheric dust cycle. 2. Simulation of Saharan dust sources. *J. Geophys. Res. Atmos.*, **102**, 4387–4404.

Martin, S.T., 1998: Phase transformations of the ternary system (NH4)2SO4-H2SO4-H2O and the implications for cirrus cloud formation. *Geophys. Res. Lett*., **25**, 1657–1660.

Martin, G.M., D.W. Johnson, and A. Spice, 1994: The measurement and parametrization of effective radius of droplets in warm stratocumulus clouds, *J. Atmos. Sci*. **51**, 1823-1842.

Martins, J.V., P. Artaxo, C. Liousse, J.S. Reid, P.V. Hobbs and Y.J. Kaufman, 1998: Effects of black carbon content, particle size, and

mixing on light absorption by aerosols from biomass burning in Brazil. *J. Geophys. Res. Atmos*., **103**, 32041–32050.

Matthias-Maser, S. and R. Jaenicke, 1995: The size distribution of primary biological aerosol particles with radii >0.2 µm in an urban-rural influenced region. *Atmospheric Research*, **39**, 279–286.

McCormick, M.P., and R.E. Veiga, 1992: SAGE II measurements of early Pinatubo aerosols. *Geophys. Res. Lett*., **19**, 155-158.

McCormick, M.P., L.W. Thomason and C.R. Trepte, 1995: Atmospheric effects of the Mt. Pinatubo eruption. *Nature*, **373**, 399–404.

McInnes, L.,D. Covert and B. Baker, 1997: The number of sea-salt , sulphate, and carbonaaceous particles in the marine atmosphere: EM measurements consistent with the ambient size distribution, *Tellus*, **49B**, 300-313.

McInnes, L., M. Bergin, J. Ogren and S. Schwartz, 1998: Apportionment of light scattering and hydroscopic growth to aerosol composition. *Geophys. Res. Lett*., **25**, 513-516.

McMurry, P.H., X.Q. Zhang and C.T. Lee, 1996: Issues in aerosol measurement for optics assessments. *J. Geophys. Res. Atmos*., **101**, 19189–19197.

Menon, S., and V.K. Saxena, 1998: Role of sulphates in regional cloud-climate interactions. *Atmos. Res*., **47-48**, 299–315.

Meszaros, E., 1981: Atmospheric Chemistry. Elsevier, New York, pp. 1-201.

Miller, R.L. and I. Tegen, 1998: Climate response to soil dust aerosols. *J. Climate*, **11**, 3247–3267.

Minnis, P., E. F. Harrison, L. L. Stowe, G. G. Gibson, F. M. Denn, D. R. Doelling, W. L. Smith, Jr., 1993: Radiative climate forcing by the Mt. Pinatubo eruption. *Science*, **259**, 1411-1415.

Mishchenko, M.K., I.V. Geogdzhayev, B. Cairns, W.B. Rossow, and A.A. Lacis, 1999: Aerosol retrievals over the ocean using channel 1 and 2 AVHRR data: A sensitivity analysis and preliminary results, *Applied Optics*, **38**, 7325-7341.

Monahan, E.C., D.E. Spiel and K.L. Davidson, 1986: A model of marine aerosol generation via whitecaps and wave disruption in oceanic whitecaps. In: Oceanic whitecaps and their role in air-sea exchange processes, E.C. Monahan and G.M. Niocaill (eds), D. Reidel Publishing, Dordrecht, Holland, pp. 167–174.

Moosmüller, H., W.P. Arnott, C.F. Rogers, J.C. Chow, C.A. Frazier, L.E. Sherman and D.L. Dietrich, 1998: Photo-acoustic and filter measurements related to aerosol light absorption during the Northern Front Range Air Quality Study (Colorado 1996/1997). *J. Geophys. Res. Atmos*., **103**, 28149–28157.

Moulin, C., C.E. Lambert, F. Dulac and U. Dayan, 1997: Control of atmospheric export of dust from North Africa by the North Atlantic oscillation. *Nature*, **387**, 691–694.

Murphy, D. M., and D. S. Thomson, 1997: Chemical composition of single aerosol particles at Idaho Hill: Negative ion measurements. *J. Geophys. Res*. **102**, 6353-6368.

Murphy, D.M., J.R. Anderson, P.K. Quinn, L.M. McInnes, F.J. Brechtel, S.M. Kreidenweis, A.M. Middlebrook, M. Posfai, D.S. Thomson and P.R. Buseck, 1998a: Influence of sea-salt on aerosol radiative properties in the Southern Ocean marine boundary layer. *Nature*, **392**, 62–65.

Murphy, D.M., D.S. Thomson and T.M.J. Mahoney, 1998b: In situ measurements of organics, meteoritic material, mercury, and other elements in aerosols at 5 to 19 kilometers. *Science*, **282**, 1664–1669.

Myhre, G., F. Stordal, K. Restad and I.S.A. Isaksen, 1998: Estimation of the direct radiative forcing due to sulphate and soot aerosols. *Tellus*, **50B**, 463–477.

Mylona, S., 1996: Sulphur dioxide emissions in Europe 1980-1991 and their effect on sulphur concentrations and depositions. *Tellus*, **48B**, 662-689.

Nakajima, T. and A. Higurashi, 1997: AVHRR remote sensing of aerosol optical properties in the Persian Gulf region, summer 1991. *J. Geophys. Res*., **102**, 16,935–16,946.

Nakajima, T., A. Higurashi, K. Aoki, T. Endoh, H. Fukushima, M. Toratani, Y. Mitomi, B. G. Mitchell, and R. Frouin, 1999: Early phase analysis of OCTS radiance data for aerosol remote sensing, IEEE Trans. Geo. Remote Sens., **37**, 1575-1585.

Nakajima, T., A. Higurashi , K. Kawamoto, and J. E. Penner, 2001: A possible correlation between satellite-derived cloud and aerosol microphysical parameters. *Geophys. Res. Lett*., in press.

Nakićenović, N., J. Alcamo, G. Davis, B. de Vries, J. Fenhann, S. Gaffin, K. Gregory, A. Grubler, T.Y. Jung, T. Kram, E.L. La Rovere, L. Michaelis, S. Mori, T. Morita, W. Pepper, H. Pitcher, L. Price, K. Raihi, A. Roehrl, H.-H. Rogner, A. Sankovski, M. Schlesinger, P. Shukla, S. Smith, R. Swart, S. van Rooijen, N. Victor, and Z. Dadi, 2000: Emissions Scenarios. A Special Report of Working Group III of the Intergovernmental Panel on Climate Change. Cambridge University Press, Cambridge, United Kingdom and New York, NY, USA, 599 pp.

NASA, 1992: The atmospheric effects of stratospheric aircraft: A first program report, M.J. Prather *et al.* (eds.), NASA Ref. Publ. 1272, pp. 64–91.

Neusüß , C., D. Weise, W. Birmili, H. Wex, A. Wiedenshohler, and D. S. Covert, 2000: Size segregated chemical, gravimetric and number distribution-derived mass closure of the aerosol in Sagres, Portugal during ACE-2. *Tellus*, **52B**, 169-184.

Norman, A. L., L. A. Barrie, D. Toom-Sauntry, A. Sirois, H. R. Krouse, S. M. Li, and S. Sharma, 1999: Sources of aerosol sulphate at Alert: Apportionment using stable isotopes. *J. Geophys. Res*., **104**, 11,619-11,631.

Novakov, T. and J.E. Penner, 1993: Large contribution of organic aerosols to cloud-condensation-nuclei concentrations. *Nature*, **365**, 823–826.

Novakov, T. and C. E. Corrigan, 1996: Cloud condensation nucleus activity of the organic component of biomass smoke particles. *Geophys. Res. Lett*., **23**, 2141–2144.

Novakov, T., D.A. Hegg and P.V. Hobbs, 1997: Airborne measurements of carbonaceous aerosols on the East Coast of the United States. *J. Geophys. Res. Atmos*., **102**, 30023–30030.

Nyeki, S., F. Li, E. Weingartner, N. Streit, L. Colbeck, H. W. Gaggeler and U. Boltensperger, 1998: The background aerosol size distribution in the free troposphere: An analysis of the annual cycle at a high-alpine site. *J. Geophys. Res*., **103**, 31749-31761.

O'Dowd, C.D. and M.H. Smith, 1993: Physico-chemical properties of aerosols over the Northeast Atlantic: Evidence for wind-speed-related sub-micron sea-salt aerosol production. *J.Geophys. Res*., **98**, 1137–1149.

O'Dowd,C., M.H.Smith, I.E.Consterdine, and J. A. Lowe, 1997: Marine aerosol, sea-salt, and the marine sulphur cycle: A short review. *Atmos. Environ*., **31**, 73-80.

O'Dowd, C.D., J.A. Lowe, M.H. Smith, and A.D. Kaye, 1999: The relative importance of Nss-sulphate and sea-salt aerosol to the marine CCN population: an improved multi-component aerosol-cloud droplet parametrization. *Quart. J. Roy. Meteorol. Soc.*, **125**, 1295-1313.

Odum, J.R., T. Hoffmann, F. Bowman, D. Collins, R.C. Flagan and J.H. Seinfeld, 1996: Gas/particle partitioning and secondary organic aerosol yields. *Environ. Sci. Tech*., **30**, 2580–2585.

Osborn, M. T., G. S. Kent, and C. R. Trepte, 1998: Stratospheric aerosol measurements by the Lidar in Space Technology Experiment. *J. Geophys. Res*., **103**, 11447-11453.

Pan, W., M.A. Tatang, G.J. McRae and R.G. Prinn, 1997: Uncertainty analysis of direct radiative forcing by anthropogenic sulphate aerosols, *J. Geophys. Res*., **102**, 21915–21924.

Penner, J.E., R.E. Dickinson and C.A. O'Neill, 1992: Effects of aerosol from biomass burning on the global radiation budget. *Science*, **256**, 1432–1434.

Penner, J.E., H. Eddleman and T. Novakov, 1993: Towards the develop-

ment of a global inventory of black carbon emissions, *Atmos. Environ*., **27A**, 1277–1295.

Penner, J.E., R.J. Charlson, J.M. Hales, N. Laulainen, R. Leifer, T. Novakov, J. Ogren, L.F. Radke, S.E. Schwartz, and L. Travis, 1994a: Quantifying and minimizing uncertainty of climate forcing by anthropogenic aerosols, *Bull. Am. Met. Soc.*, **75**, 375–400.

Penner, J.E., C.A. Atherton, and T.E. Graedel, 1994b: Global emissions and models of photochemically active compounds. In Global Atmospheric-Biospheric Chemistry, ed. R. Prinn, Plenum Publishing, N.Y., 223-248.

Penner, J.E., 1995: Carbonaceous aerosols influencing atmospheric radiation: black and organic carbon, in Aerosol Forcing of Climate, ed. R.J. Charlson and J. Heintzenberg, John Wiley and Sons, Chichester, 91-108.

Penner, J.E., C.C. Chuang, and C. Liousse, 1996: The contribution of carbonaceous aerosols to climate change. In Nucleation and Atmospheric Aerosols 1996, M. Kulmala and P.E. Wagner, eds., Elsevier Science, Ltd., 759-769.

Penner, J.E., D. Bergmann, J.J. Walton, D. Kinnison, M.J. Prather, D. Rotman, C. Price, K.E. Pickering, S.L. Baughcum, 1998a: An evaluation of upper tropospheric NOx with two models. *J. Geophys. Res*., **103**, 22,097-22,114.

Penner, J.E., C.C. Chuang and K. Grant, 1998b: Climate forcing by carbonaceous and sulphate aerosols. *Clim. Dyn*., **14**, 839–851.

Penner, J.E., C.C. Chuang and K. Grant, 1999a: Climate change and radiative forcing by anthropogenic aerosols: A review of research during the last five years. Paper presented at the La Jolla International School of Science, The Institute for Advanced Physics Studies, La Jolla, CA, U.S.A.

Penner, J.E., D. Lister, D. Griggs, D. Docken M. MacFarland (Eds.), 1999b: Aviation and the Global Atmosphere, Intergovernmental Panel on Climate Change Special Report, Cambridge University Press, Cambridge, U.K., 373 pp.

Perez, P. J., J. A. Garcia, and J. Casanova, 1985: Ice nuclei concentrations in Vallodolid, Spain and their relationship to meteorological parameters. *J. Res. Atmos*., **19**, 153–158.

Petzold, A., J. Ström, S. Ohlsson, and F.P. Schröder, 1998: Elemental composition and morphology of ice-crystal residual particles in cirrus clouds and contrails. *Atmos. Res*. **49**, 21-34.

Pham, M., J.-F. Müller, G. P. Brasseur, C. Granier, and G. Mägie, 1996: A 3D model study of the global sulphur cycle: Contributions of anthropogenic and biogenic sources. *Atmos. Env*., **30**, 1815-1822.

Piccot, S.D., J.J. Watson and J.W. Jones, 1992: A global inventory of volatile organic compound emissions from anthropogenic sources. *J. Geophys. Res*., **97**, 9897–9912.

Pincus, R. and M.A. Baker, 1994: Effect of precipitation on the albedo susceptibility of clouds in the marine boundary layer. *Nature*, **372**, 250–252.

Pincus, R., M.A. Baker and C.S. Bretherton, 1997: What controls stratocumulus radiation properties? Lagrangian observations of cloud evolution. *J. Atmos. Sci*., **54**, 2215–2236.

Pitari, G., E. Mancini, A. Bregman, H.L. Rogers, J.K. Sundet, V. Grewe, and O. Dessens, 2001: Sulphate particles from subsonic aviation: Impact on upper tropospheric and lower stratospheric ozone, Physics and Chemistry of the Earth, European Geophysical Society, in press.

Pitari, G., and E. Mancini, 2001: Climatic impact of future supersonic aircraft: Role of water vapour and ozone feedback on circulation, Physics and Chemistry of the Earth, European Geophysical Society, in press.

Podgorny, I.A., W. Conant, V. Ramanathan, and S. K. Sateesh, 2000: Aerosol modulation of atmospheric and surface solar heating over the tropical Indian Ocean. *Tellus* B., **52**, 947-958.

Posfai, M., H. Xu, J.R. Anderson, and P.R. Buseck, 1998: Wet and dry sizes of atmopsheric aerosol particles: an AFM-TEM study. *Geophys. Res. Lett*., **25**, 1907–1910.

Price, C., J.E. Penner, and M.J. Prather, 1997: NOx from lightning, Part I: Global distribution based on lightning physics. *J. Geophys. Res*., **102**, 5929-2941, 1997.

Prospero, J.M., M. Uematsu, and D.L. Savoie, 1989: Mineral aerosol transport to the Pacific Ocean. In Chemical Oceanography, J.P. Riley, and R. Chester, Eds., Academic, London, 188-218.

Prospero, J.M. and R.T. Nees, 1986: Impact of the North African drought and El Nino on mineral dust in the Barbados trade winds. *Nature*, **320**, 735–738.

Prospero, J.M., 1999: Long-term measurements of the transport of African mineral dust to the southeastern United States: Implications for regional air quality. *J. Geophys. Res*., **104**, 15,917–15,928.

Pruppacher, H.R. and J.D. Klett, 1997: Microphysics of Clouds and Precipitation. Reidel, Dordrecht, 954 pp.

Putaud, J.-P., R. Van Digenen, M. Mangoni, A. Virkkula, F. Raes, H. Maring, J.M. Prospero, E. Swietlicki, O.H. Berg, R. Hillami, and T. Mäkelä, 2000: Chemical mass closure and assessment of the origin of the submicron aersol in the marine boundary layer and the free troposphere at Tenerife during ACE-2. *Tellus*, **52B**, 141-168.

Quinn, P.K., T.S. Bates, J.E. Johnson, D.S. Covert and R.J. Charlson, 1990: Interactions between the sulphur and reduced nitrogen cycles over the central Pacific Ocean. *J. Geophys. Res*., **95**, 16405-16416.

Quinn, P.K., D.S. Covert, T.S. Bates, V.N. Kapustin, D.C. Ramsey-Bell and L.M. McInnes, 1993: Dimethylsulfide/cloud condensation nuclei/climate system: Relevant size-resolved measurements of the chemical and physical properties of atmospheric aerosol particles. *J. Geophys. Res*., **98**, 10411-10427.

Quinn, P.K., V.N. Kapustin, T.S. Bates and D.S. Covert, 1996: Chemical and optical properties of marine boundary layer aerosol particles of the mid-Pacific in relation to sources and meteorological transport. *J. Geophys. Res*., **101**, 6931-6951.

Quinn, P.K. and D.J. Coffman, 1998: Local closure during the First Aerosol Characterization Experiment (ACE 1): Aerosol mass concentration and scattering and backscattering coefficients. *J. Geophys. Res*., **103**, 15575-15596.

Quinn, P.K., D.J. Coffman, V.N. Kapustin, T.S. Bates and D.S. Covert, 1998: Aerosol optical properties in the marine boundary layer during the First Aerosol Characterization Experiment (ACE 1) and the underlying chemical and physical aerosol properties. *J. Geophys. Res*., **103**, 16,547–16,563.

Radke, L. F., D. A. Hegg, P. V. Hobbs, J. D. Nance, J. H. Lyons, K. K. Laursen, R. E. Weiss, P. J. Riggan and D. E. Ward, 1991: Particulate and trace gas emissions from large biomass fires in North America. In Global Biomass Burning: Atmospheric, Climate and Biospheric Implications, ed. J. S. Levine, pp. 209-224, MIT Press, Cambridge, MA.

Raes, F., R. Van Dingenen, E. Cuevas, P.F.J. Van Velthoven and J.M. Prospero, 1997: Observations of aerosols in the free troposphere and marine boundary layer of the subtropical Northeast Atlantic: Discussion of processes determining their size distribution. *J. Geophys. Res*., **102**, 21,315-21,328.

Raes, F., T.F. Bates, F.M. McGovern and M. van Liedekerke, 2000: The second Aerosol Characterization Experiment: General overview and main results. *Tellus*, 52, 111-125.

Rangno, A. and P. V. Hobbs, 1994: Ice particle concentrations and precipitation development in small continental cumuliform clouds. Q. J. Roy. Met. Soc., **120**, 573–601.

Rasch, P.J. and J.E. Kristjansson, 1998: A comparison of the CCM3 model climate using diagnosed and predicted condensate parametrizations. *J. Climate*, **11**, 1587-1614.

Rasch, P.J, M.C. Barth, J.T. Kiehl, S.E. Schwartz and C.M. Benkowitz, 2000a: A description of the global sulphur cycle and its controlling processes in the NCAR CCM3. *J. Geophys. Res*., **105**, 1367-1386.

Rasch, P.J., H. Feichter, K. Law, N. Mahowald, J. Penner, C. Benkovitz, C. Genthon, C. Giannakopoulos, P. Kasibhatla, D. Koch, H. Levy, T.

Maki, M. Prather, D.L. Roberts, G.-J. Roelofs, D. Stevenson, Z. Stockwell, S. Taguchi, M. Kritz, M. Chipperfield, D. Baldocchi, P. McMurry, L. Barrie, Y. Balkanski, R. Chatfield, E. Kjellstrom, M. Lawrence, H.N. Lee, J. Lelieveld, K.J. Noone, J. Seinfeld, G. Stenchikov, S. Schwarz, C. Walcek, D. Williamson, 2000b: A comparison of scavenging and deposition processes in global models: Results from the WCRP Cambridge Workshop of 1995. *Tellus*, **52B**, 1025-1056.

Rea, D. K., 1994: The paleoclimatic record provided by eolian deposition in the deep sea: The geologic history of wind. *Rev. Geophys*., **i32**, 159-195.

Reid, J. S. and P. V. Hobbs, 1998: Physical and optical properties of smoke from individual biomass fires in Brazil. *J. Geophys. Res*., **103**, 32013-32031.

Reid, J.S., P.V. Hobbs, C. Liousse, J. V. Martins, R.E. Weiss, and T.F. Eck, 1998a: Comparisons of techniques for measuring shortwave absorption and black carbon content of aerosols from biomass burning in Brazil. *J. Geophys. Res*., **103**, 32,031-32,040.

Reid, J.S., P.V. Hobbs, R.J. Ferek, D.R. Blake, J.V. Martins, M.R. Dunlap and C. Liousse, 1998b: Physical, chemical, and optical properties of regional hazes dominated by smoke in Brazil. *J. Geophys. Res*., **103**, 32,059–32,080.

Remer, L. A., S. Gasso, D. A. Hegg, Y.J. Kaufman and B. N. Holben, 1997: Urban/industrial aerosol: Ground-based sun/sky radiometer and airborne in situ measurements. *J. Geophys. Res*., **10**2, 16849-16859.

Rivera-Carpio, C.A., C.E. Corrigan, T. Novakov, J.E. Penner, C.F. Rogers and J.C. Chow, 1996: Derivation of contributions of sulphate and carbonaceous aerosols to cloud condensation nuclei from mass size distributions. *J. Geophys. Res. Atmos*., **101**, 19483–19493.

Roberts, G., M.O. Andreae, W. Maenhaut, P. Artaxo, J.V. Martins, J. Zhou and E. Swietlicki, 1998: Relationships of cloud condensation nuclei to size distribution and aerosol composition in the Amazon Basin. *Eos Trans. AGU*, **79**, F159.

Robertson, A.D., J.T. Overpeck, D. Rind, E. Mosley-Thompson, G.A. Zielinski, J.L. Lean, D. Koch, J.E. Penner, I. Tegen and R. Healy, 2001: Hypothesized climate forcing time series for the last 500 years. *J. Geophys. Res*., in press.

Roeckner, E., Rieland, M. and Keup, E., 1991: Modelling of clouds and radiation in the ECHAM model. ECMWF/WCRP Workshop on Clouds, Radiative Transfer and the Hydrological Cycle, 199-222. ECMWF, Reading, U.K.

Roeckner, E., L. Bengtsson, J. Feichter, J. Lelieveld and H. Rodhe, 1999: Transient climate change simulations with a coupled atmosphere-ocean GCM including the tropospheric sulphur cycle. *J. Climate*, **12**, 3004–3032.

Roelofs, G.-J., J. Lelieveld and L. Ganzeveld, 1998: Simulation of global sulphate distribution and the influence on effective cloud drop radii with a coupled photochemistry-sulphur cycle model. *Tellus*, **50B**, 224–242.

Roelofs, G.J. , P. Kasibhatla, L. Barrie, D. Bergmann, C, Bridgeman, M. Chin, J. Christensen, R. Easter, J. Feichter, A. Jeuken, E. Kjellström, D. Koch, C. Land, U. Lohmann, P. Rasch, 2001: Analysis of regional budgets of sulphur species modelled for the COSAM exercise. *Tellus* B, in press.

Rogers, D., 1993: Measurements of natural ice nuclei with a continuous flow diffusion chamber. *Atmos. Res*., **29**, 209–228.

Rosenfeld, D. 1999: TRMM observed first direct evidence of smoke from forest fires inhibiting rainfall. *Geophys. Res. Lett*., **26**, 3105-3108.

Rosenfeld, D. 2000: Suppression of rain and snow by urban and industrial air pollution. *Science*. **287**, 1793-1796.

Rosinski, J. and G. Morgan, 1991: Cloud condensation nuclei as sources of ice-forming nuclei in clouds. *J. Aerosol Sci*., **22**, 123–133.

Ross, J. I., P. V. Hobbs, and B. Holden, 1998: Radiative characteristics of regional hazes dominated by smoke from biomass burning in Brazil: Closure tests and direct radiative forcing, *J. Geophys. Res*., **103**, 31925-31941.

Rotstayn, L. D., 1999: Indirect forcing by anthropogenic aerosols: A global climate model calculation of effective-radius and cloud-lifetime effects. *J. Geophys. Res. Atmos*., **104**, 9369–9380.

Rotstayn, L. D. and J.E. Penner, 2001: Forcing, quasi-forcing and climate response. *J. Climate*, in press.

Russell, P. B., J. M. Livingston, P. Hignett, S. Kinne, J. Wong, A. Chien, R. Bergstrom, P. Durkee, and P. V. Hobbs, 1999: Aerosol-induced radiative flux changes off the United States mid-Atlantic coast: Comparison of values calculated from sunphotometer and in situ data with those measured by airborne pyranometer. *J. Geophys. Res*., **104**, 2289-2307.

Russell, P. B., and J. Heintzenberg, 2000: An overview of the ACE-2 clear sky column closure experiment (CLEARCOLUMN). *Tellus*, **52B**, 463-483.

Saltzman, E. S., King, D. B., Holmen, K. and Leck, C., 1993: Experimental determination of the diffusion coefficient of dimethylsulfide in water. *J. Geophys. Res*., **98**, 16481-16486.

SAR, see IPCC, 1996.

Sassen, K. and G. C. Dodd, 1988: Homogeneous nucleation rate for highly supercooled cirrus cloud droplets. *J. Atmos. Sci*., **45**, 1357–1369.

Sassen, K., 1992: Evidence for liquid-phase cirrus cloud formation from volcanic aerosols: Climatic implications. *Science*, **257**, 516–519.

Sassen, K., D.O.C. Starr, G.G. Mace, M.R. Poellot, and others, 1995: The 5-6 December 1991 FIRE IFO II jet stream cirrus case study: Possible influences of volcanic aerosols. *J. Atmos. Sci*., **52**, 97–123.

Satheesh, S. K., V. Ramanathon, X. Li-Jnes, J. M. Lobert, I. A. Podgorny, J. M. Prosper, B. N. Holben, and N. G. Loev, 1999: A model for the natural and anthropogenic aerosols over the tropical Indian Ocean derived from INDOEX data. *J. Geophys. Res*., **104**, 27,421-27,440.

Saxena, P., L.M. Hildemann, P.H. McMurry and J.H. Seinfeld, 1995: Organics alter hygroscopic behavior of atmospheric particles. *J. Geophys. Res. Atmos*., **100**, 18755–18770.

Saxena, P. and L.M. Hildemann, 1996: Water soluble organics in atmospheric particles: A critical review of the literature and application of thermodynamics to identify candidate compounds. *J. Atmos. Chem*., **24**, 57–109.

Schnell, R. C. and G. Vali, 1976: Biogenic ice nuclei: Part I. Terrestrial and marine sources. *J. Atmos. Sci*., **33**, 1554–1564.

Schmid, B. J. M. Livingston, P. B. Russell, P. A. Durkee, H. H. Jonsson, D. R. Collins, R. D. Flagan, J. H. Seinfeld, S. Gassó, D. A. Hegg, E. Öström, K. J. Noone, E. J. Welton, K. J. Voss, H. R. Gordon, P. Formenti, and M. O. Andreae, 2000: Clear-sky closure studies of lower tropospheric aerosol and water vapor during ACE-2 using airborne sunphotometer, airborne in situ, space-borne, and ground-based measurements. *Tellus*, **52B**, 568-593.

Scholes, M. and M.O. Andreae, 2000: Biogenic and pyrogenic emissions from Africa and their impact on the global atmosphere. *Ambio*, **29**, 23-29.

Scholes, R.J., D. Ward and C.O. Justice, 1996: Emissions of trace gases and aerosol particles due to vegetation burning in southern-hemisphere Africa. *J. Geophys. Res. Atmos*., **101**, 23677–23682.

Schubert, S.D., R.B. Rood, and J. Pfaendtner, 1993: An assimilated data set for Earth science applications, *Bull. Amer. Met. Soc*., **24**, 2331-2342.

Schult, I., J. Feichter and W.F. Cooke, 1997: Effect of black carbon and sulphate aerosols on the Global Radiation Budget. *J. Geophys. Res. Atmos*., **102**, 30107–30117.

Schulz, M., Y.J. Balkanski, W. Guelle and F. Dulac, 1998: Role of aerosol size distribution and source location in a three-dimensional simulation of a Saharan dust episode tested against satellite-derived optical thickness. *J. Geophys. Res. Atmos*., **103**, 10579–10592.

Schwartz, S. E., 1996: The whitehouse effect - Shortwave radiative forcing of climate by anthropogenic aerosols: An overview, *J. Aer. Sci*., **27**, 359-383.

Schwartz, S.E., and A. Slingo, 1996: Enhanced shortwave cloud radiative forcing due to anthropogenic aerosols. In Clouds, Chemistry and Climate, P. J. Crutzen and V. Ramanathan, Eds., NATO ASI Series, Vol. I 35, Springer-Verlag, Berlin, 191-236.

Seinfeld, J. H. and S. N. Pandis, 1998: Atmospheric Chemistry and Physics From Air Pollution to Climate Change. Wiley Interscience, New York, 1326 pp.

Seinfeld, J.H. and S.N. Pandis, 1998: Atmospheric Chemistry and Physics: From Air Pollution to Climate Change, John Wiley and Sons, New York, 1326pp.

Sempéré, R. and K. Kawamura, 1996: Low molecular weight dicarboxylic acids and related polar compounds in the remote marine rain samples collected from western Pacific. *Atmos. Environ*., **30**, 1609–1619.

Senior, C. A. and J.L.B. Mitchell, 1993: Carbon dioxide and climate: The impact of cloud parametrization. *J. Climate*, **6**, 393–418.

Shantz, N., R. Leaitch, S.-M. Li, W. Hoppel, G. Frick, P. Caffrey, D. Hegg, S. Gao, T. Albrechcinski, 1999: Controlled studies and field measurements of organic cloud condensation nuclei. Paper Number A22B-11, American Geophysical Union Fall Meeting, San Francisco.

Shettle, E.P. and R. Fenn, 1976: Models of the atmospheric aerosols and their optical properties, AGARD Conference Proceedings, No. 183, AGARD-CP-183.

Shulman, M.L., M.C. Jacobson, R.J. Charlson, R.E. Synovec and T.E. Young, 1996: Dissolution behaviour and surface tension effects of organic compounds in nucleating droplets. *Geophy. Res. Lett*., **23**, 277–280.

Sievering, H., J. Boatman, E. Gorman, Y. Kim, L. Anderson, G. Ennis, M. Luria and S. Pandis, 1992: Removal of sulphur from the marine boundary layer by ozone oxidation in sea- salt aerosols. *Nature*, **360**, 571–573.

Simoneit, B.R.T., J.N. Cardoso and N. Robinson, 1990: An assessment of the origin and composition of higher molecular weight organic matter in aerosols over Amazonia. *Chemosphere*, **21**, 1285–1301.

Slanina, J., H.M. ten Brink and A. Khlystov, 1999: Fate of products of degradation processes: Consequences for climatic change. *Chemosphere*, **38**, 1429–1444.

Smith, R.N.B., 1990: A scheme for predicting layer clouds and their water content in a general circulation model. *Q.J.R. Meteorol. Soc*., **116**, 435-460.

Sokolik, I. and G. Golitsyn, 1993: Investigation of optical and radiative properties of atmospheric dust aerosols. *Atmos. Environ*., **27A**, 2509-2517.

Sokolik, I.N. and O.B. Toon, 1996: Direct radiative forcing by anthropogenic airborne mineral aerosols. *Nature*, **381**, 681–683.

Sokolik, I.N. and O.B. Toon, 1999: Incorporation of mineralogical composition into models of the radiative properties of mineral aerosol from UV to IR wavelengths. *J. Geophys. Res. Atmos*., **104**, 9423–9444.

Song, N., D.O'C. Starr, D.J. Wuebbles, A. Williams and S.M. Larson, 1996: Volcanic aerosols and inter-annual variation of high clouds. *Geophys. Res. Lett*., **23**, 2657–2660.

Soufflet, V., D. Tanré, A. Royer, and N. T. O'Neill, 1997: Remote sensing of aerosols over boreal forest and lake water from AVHRR data. *Rem. Sensing Env*., **60**, 22-34.

Spiro, P.A., D.J. Jacob and J.A. Logan, 1992: Global inventory of sulphur emissions with 1x1 resolution. *J. Geophys. Res*., **97**, 6023–6036.

Stenchikov, G.L., I. Kirchner, A. Robock, H.-F. Graf, J.C. Antuna, R. Grainger, A. Lambert, and L. Thomason, 1998: Radiative forcing from the 1991 Mt. Pinatubovolcanic eruption. *J. Geophys. Res*., 103, 13837-13858.

Stevens, B., W.R. Cotton, G. Feingold, and C.-H. Moeng, 1998: Large eddy simulations of strongly precipitating, shallow, stratocumulus topped boundary layers. *J. Atmos. Sci*., **55**, 3616-3638.

Stevenson, D.S., W.J. Collins, C.E. Johnson, R.G. Derwent, 1998: Intercomparison and evaluation of atmospheric transport in a Lagrangian model (STOCHEM), and an Eulerian model (UM) using ^{222}Rn as a short-lived tracer. *Quart. J. Roy. Meteorol. Soc*., **124**, 2477-2491.

Stith, J. L., D. A. Burrows and P. J. DeMott, 1994: Initiation of ice: Comparison of numerical model results with observations of ice development in a cumulus cloud. *Atmos. Res*., **32**, 13–30.

Stoiber, R.E., S.N. Williams and B. Huebert, 1987: Annual contribution of sulphur dioxide to the atmosphere by volcanoes. *J. Volcanol. Geotherm. Res*., **33**, 1–8.

Stowe, L.L., R.M. Carey and P.P. Pellegrino, 1992: Monitoring the Mt. Pinatubo aerosol layer with NOAA/11 AVHRR data. *Geophys. Res. Lett*., **19**, 159–162.

Stowe, L.L., A.M. Ignatov, and R.R. Singh, 1997: Development, validation, and potential enhancements to the second-generation operational aerosol product at the National Environmental Satellite, Data, and Information Service of the National Oceanic and Atmospheric Administration. *J. Geophys. Res*., **102**, 16923-16934.

Strom, J. and S. Ohlsson, 1998: In situ measurements of enhanced crystal number densities in cirrus clouds caused by aircraft exhaust. *J. Geophys. Res. Atmos*., **103**, 11355–11361.

Strom, J., B. Strauss, T. Anderson, F. Schroder, J. Heintzenberg and R. Wiedding, 1997: In situ observations of the microphysical properties of young cirrus clouds. *J. Atmos. Sci*., **54**, 2542–2553.

Sundqvist, H., E. Berge, and J.E. Kristjansson, 1989: Condensation and cloud parametrization studies with a mesoscale numerical weather prediction model. *Mon. Weather Rev*., **117**, 1641-1657.

Swietlicki, E., J. Zhou, O.H. Berg, B.G. Martinsson, G.Frank, S.-I. Cederfelt, U. Dusek, A. Berner, W. Birmili, A. Wiedensohler, B. Yuskiewicz, and K.N. Bower, 1999: A closure study of sub-micrometer aerosol particle hygroscopic behaviour. *Atmos. Res*., 205-240.

Szczodrak, M., P.H. Austin, and P. Krummel, 2001: Variability of optical depth and effective radius in marine stratocumulus clouds. *J. Atmos. Sci*., in press.

Szyrmer, W. and I. Zawadski, 1997: Biogenic and anthropogenic sources of ice-forming nuclei: A review. *Bull. Amer. Meteor. Soc*., **78**, 209–229.

Takeda, T., P.-M. Wu and K. Okada, 1987: Dependence of light scattering coefficient of aerosols on relative humidity in the atmosphere of Nagoya. *J. Met. Soc. Japan*, **64**, 957-966.

Tang, I.N., 1996: Chemical and size effects of hygroscopic aerosols on light scattering coefficients. *J. Geophys. Res*., **101**, 19245–19250.

Tangren, C. D., 1982: Scattering coefficient and particulate matter concentration in forest fire smoke. *J. Air Poll. Control Assoc*., **32**, 729-732.

Tanré, D., J.F. Geleyn, and J. Slingo, 1984: First results of the introduction of an advanced aerosol-radiation interaction in the ECMWF low resolution global model. In: *Aerosols and their Climate Effects.* H.F. Gerber and A. Deepak (Eds.), Deepak Publishing, 133-177.

Tanré, D., M. Herman, and Y. J. Kaufman, 1996: Information on aerosol size distribution contained in solar reflected spectral radiances. *J. Geophys. Res*., **101**, 19043-19060.

Tanré, D., L. A. Remer, Y. J. Kaufman, S. Mattoo, P. V. Hobbs, J. M. Livingston, P. B. Russell, and A. Smirnov, 1999: Retrieval of aerosol optical thickness and size distribution over ocean from the MODIS airborne simulator during TARFOX. *J. Geophys. Res*., **104**, 2261-2278.

Taylor, K.E. and J.E. Penner, 1994: Response of the climate system to atmospheric aerosols and greenhouse gases. *Nature*, **369**, 734-737.

Tegen, I., and I. Fung, 1994: Modeling of mineral dust in the atmosphere: Sources, transport, and optical thickness. *J. Geophys. Res*., **99D**,

22,897-22,914.

Tegen, I., and I. Fung, 1995: Contribution to the atmospheric mineral aerosol load from land surface modification. *J. Geophys. Res*., **100**, 18,707-18,726.

Tegen, I. and A.A. Lacis, 1996: Modelling of particle size distribution and its influence on the radiative properties of mineral dust aerosol. *J. Geophys. Res. Atmos*., **101**, 19237–19244.

Tegen, I., A.A. Lacis and I. Fung, 1996: The influence on climate forcing of mineral aerosols from disturbed soils *Nature*, **380**, 419–422.

Tegen, I. and R. Miller, 1998: A general circulation model study of the inter-annual variability of soil dust aerosol. *J. Geophys. Res. Atmos*., **103**, 25975–25995.

Tegen, I., P. Hollrig, M. Chin, I. Fung, D. Jacob and J.E. Penner, 1997: Contribution of different aerosol species to the global aerosol extinction optical thickness: Estimates from model results. *J. Geophys. Res. Atmos*., **102**, 23895–23915.

ten Brink, H. M., J. P. Veefkind, A. Waijers-Ijpelaan, and J. C. van der Hage, 1996: Aerosol light-scattering in the Netherlands, *Atmos. Environ*., **30**, 4251-4261.

Torres, O., P. K. Bhartia, J. R. Herman, Z. Ahmad and J. Gleason, 1998: Derivation of aerosol properties from satellite measurements of backscattered ultraviolet radiation: Theoretical basis. *J. Geophys. Res*., **103**, 17099-17110.

Trenberth, Kevin E., Olson, Jerry G. and Large, William G., 1989: A Global Ocean Wind Stress Climatology Based on ECMWF Analysis. National Center for Atmospheric Research, Climate and Global Dynamics Division, Boulder, Colorado.

Tripoli, G.J. and W.R. Cotton, 1980: A numerical investigation of several factors contributing to the observed variable intensity of deep convection over south Florida. *J. Appl. Meteor*ol., **19**, 1037-1063.

Turpin, B.J., J.J. Huntzicker and S.V. Hering, 1994: Investigation of organic aerosol sampling artifacts in the Los Angeles basin. *Atmos. Environ*., **28**, 3061–3071.

Twohy, C. H., P. A. Durkee, B. J. Huebert and R. J. Charlson, 1995: Effects of aerosol particles on the microphysics of coastal stratiform clouds. *J. Climate*, **8**, 773–783.

Twomey, S., 1977, Influence of pollution on the short-wave albedo of clouds. *J. Atmos. Sci*., **34**, 1149–1152.

Vali, G., 1991: Nucleation of ice. In: Atmospheric Particles and Nuclei, G. Götz, E. Mészaros and G. Vali (eds), Akadémiai Kiado, 131-132.

Vali, G., 1992: Memory effect in the nucleation of ice on mercuric iodide. In: Nucleation and Atmospheric Aerosols, N. Fukuta and P. E. Wagner (eds), A. Deepak Publishing, Hampton, VA, USA, 259–262.

Van Dingenen, R.V., F. Raes and N.R. Jensen, 1995: Evidence for anthropogenic impact on number concentration and sulphate content of cloud-processed aerosol particles over the North Atlantic. *J. Geophys. Res. Atmos*., **100**, 21057–21067.

Van Dinh, P., J.-P. Lacaux, and R. Serpolay, 1994: Cloud-active particles from African savanna combustion experiments. *Atmos. Res*., **31**, 41-58.

Van Dorland, R., F.J. Dentener and J. Lelieveld, 1997: Radiative forcing due to tropospheric ozone and sulphate aerosols. *J. Geophys. Res*., **102**, 28,079–28,100.

Van Valin, C. C., R. J. Pueschel, J. P. Parungo and R. A. Proulx, 1976: Cloud and ice nuclei from human activities. *Atmos. Environ*., **10**, 27–31.

Veefkind, J. P., G. de Leeuw, and P. A. Durkee, 1998: Retrieval of aerosol optical depth over land using two-angle view satellite radiometry during TARFOX. *Geophys. Res. Lett*., **25**, 3135-3138.

Veefkind, J.P., G. de Leeuw, P.B. Russell, P.V. Hobbs, and J.M Livingston, 1999: Aerosol optical depth retrieval using ATSR-2 and AVHRR data during TARFOX. *J. Geophys. Res*., **194**, 2253-2260.

Virkkula, A., R.V. Dingenen, F. Raes and J. Hjorth, 1999: Hygroscopic properties of aerosol formed by oxidation of limonene, a-pinene, and b-pinene. *J. Geophys. Res*., **104**, 3569–3579.

Waggoner, A. P., R. E. Weiss and T. V. Larson, 1983: In-situ, rapid response measurement of H2SO4/(NH4)2SO4 aerosols in urban Houston: A comparison with rural Virginia. *Atmos. Environ*., **17**, 1723-1731.

Wanner, W., A.H. Srahler, B. Hu, P. Lewis, J.-P. Muller, X. Li, C.L. Barker Schaaf, and M.J. Barnsley, 1997: Global retrieval of bidirectional reflectance and albedo over land from EOS MODIS and MISR data: Theory and algorithm. *J. Geophys. Res*., **102**, 17143-17161.

Wanninkhof, R., 1992: Relationship between wind speed and gas exchange over the ocean. *J. Geophys. Res*., **97**, 7373–7382.

Warren, S. G., C. J. Hahn, J. London, R. M. Chervin, R. L. Jenne, 1988: Global Distribution of Total Cloud cover and Cloud Type Amounts over the Ocean, NCAR Technical Note, TN-317+STR (National Center for Atmospheric Research, Boulder, CO).

Weber, R.J., P.H. McMurry, R.L. Mauldin III, D.J. Tanner, F.L. Eisele, A.D. Clarke and V.N. Kapustin, 1999: New particle formation in the remote troposphere: A comparison of observations at various sites, *Geophys. Res. Lett*., **26**, 307-310.

Weisenstein, D.K., G.K. Yue, M.K.W. Ko, N.-D. Sze, J.M. Rodriguez and C.J. Stott, 1997: A tw0 dimensional model of sulphur species and aerosols. *J. Geophys. Res*., **102**, 13019-13035.

Weng, F. and N.C. Grody, 1994: Retrieval of cloud liquid water using the special sensor microwave imager (SSM/I). *J. Geophys. Res*., **99**, 25,535-25,551.

Wenny, B.N., J.S. Schafer, J.J. DeLuisi, V.K. Saxena, W.F. Barnard, I.V. Petropavlovskikh, and A.J. Vergamini, 1998: A study of regional aerosol radiative properties and effects on ultraviolet-B radiation. *J. Geophys. Res*., **103**, 17,083-17,097.

Wetzel, M. and L.L. Stowe, 1999: Satellite-observed patterns in the relationship of aerosol optical thickness to stratus cloud microphysics and shortwave radiative forcing. *J. Geophys. Res. Atmos*. **104**, 31,287-31,299.

Whitby, K.T., 1978: The physical characteristics of sulphur aerosols. *Atmos. Environ*., **12**, 135-159.

WMO/UNEP, 1992: Scientific assessment of ozone depletion: 1991. Global ozoneresearch and monitoring project, report # 25, Geneva.

Wolf, M.E. and G.M. Hidy, 1997: Aerosols and climate: Anthropogenic emissions and trends for 50 years. *J. Geophys. Res. Atmos*., **102**, 11113–11121.

Wyant, M.C., C.S. Bretherton, H.A. Rand and D.E. Stevens, 1997: Numerical simulations and a conceptual model of the stratocumulus to trade cumulus transition. *J. Atmos. Sci*., **54**, 168–192.

Xu, J., D. Imre, R. McGraw and I. Tang, 1998: Ammonium sulphate: Equilibrium and metastability phase diagrams from 40 to 50 degrees C. *J. Phys. Chem*., B **102**, 7462–7469.

Xu, K.M., and D.A. Randall, 1996: A semiempirical cloudiness parametrization for use in climate models. *J.Atmos. Sci*., **53**, 3084-3102.

Yang, Z., S. Young, V. Kotamarthi, and G.R. Carmichael, 1994: Photochemical oxidant processes in the presence of dust: an evaluation of the impact of dust on particulate nitrate and ozone formation. *J. Appl. Meteorol*., **33**, 813-824.

Yienger, J.J. and H. Levy, Empirical-model of global soil-biogenic NOx emissions. 1995: *J. Geophys. Res*., **100**, 11,447-11,464.

Yu, S., 2000: Role of organic acids (formic, acetic, pyruvic and oxalic) in the formation of cloud condensation nuclei (CCN): A review. *Atmos. Res*., **53**, 185-217.

Yum, S.S. and J.G. Hudson, 1998: Comparisons of cloud microphysics with cloud condensation nuclei spectra over the summertime Southern. *J. Geophys. Res. Atmos*., **103**, 16625–16636.

Zappoli, S., A. Andracchio, S. Fuzzi, M.C. Facchini, A. Geleneser, G. Kiss, Z. Krivacsy, A. Molnar, E. Mozaros, H.-C. Hansson, K. Rosman, and Y. Zebuhr, 1999: Inorganic, organic and macromolecular components of fine aerosol in different areas of Europe in

relation to their water solubility. *Atmos. Env*., **33**, 2733-2743.

Zhang, X. Q., P.H. McMurry, S.V. Herring and G.S. Casuccio, 1993: Mixing characteristics and water content of submicron aerosols measured in Los Angeles and at the Grand Canyon. *Atmos. Environ*., **27A**, 1593-1607.

Zhang, Y. and G.R. Carmichael, 1999: The role of mineral aerosol in tropospheric chemistry in East Asia-A model study, *J. App. Met.*, **38**, 353-366.

Zhang, Y., S.M. Kreidenweis and G. Feingold, 1999: Stratocumulus processing of gases and cloud condensation nuclei: Part II: chemistry sensitivity analysis. *J. Geophys. Res*., **104**, 16,061-16,080.

Ziegler, C.L., 1985: Retrieval of thermal microphysical variables in observed convective storms, 1, Model development and preliminary testing. *J. Atmos. Sci*., **42**, 1487-1509.